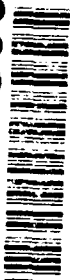# NAVAL POSTGRADUATE SCHOOL
Monterey, California

DTIC
S ELECTE
MAR 1 5 1993
C D

THESIS

AEW AIRCRAFT DESIGN

by

Michael J. Wagner

December 1992

Thesis Advisor: Conrad F. Newberry

93-05285

REPORT DOCUMENTATION PAGE

1a REPORT SECURITY CLASSIFICATION UNCLASSIFIED		1b RESTRICTIVE MARKINGS NONE			
2a SECURITY CLASSIFICATION AUTHORITY		3 DISTRIBUTION/AVAILABILITY OF REPORT Approved for public release; distribution unlimited			
2b DECLASSIFICATION/DOWNGRADING SCHEDULE					
4 PERFORMING ORGANIZATION REPORT NUMBER(S)		5 MONITORING ORGANIZATION REPORT NUMBER(S)			
6a NAME OF PERFORMING ORGANIZATION Naval Postgraduate School	6b OFFICE SYMBOL (If applicable) 31	7a NAME OF MONITORING ORGANIZATION Naval Postgraduate School			
6c ADDRESS (City, State, and ZIP Code) Monterey,CA 93943-5000		7b ADDRESS (City, State, and ZIP Code) Monterey,CA 93943-5000			
8a NAME OF FUNDING/SPONSORING ORGANIZATION	8b OFFICE SYMBOL (If applicable)	9 PROCUREMENT INSTRUMENT IDENTIFICATION NUMBER			
8c ADDRESS (City, State, and ZIP Code)		10. SOURCE OF FUNDING NUMBERS			
		PROGRAM ELEMENT NO	PROJECT NO	TASK NO	WORK UNIT ACCESSION NO

11 TITLE (Include Security Classification)

AEW Aircraft Design

12 PERSONAL AUTHOR(S)
Wagner, Michael J.

13a TYPE OF REPORT Master's Thesis	13b TIME COVERED FROM _____ TO _____	14 DATE OF REPORT (Year, Month, Day) December 1992	15 PAGE COUNT 114

16 SUPPLEMENTARY NOTATION The views expressed in this thesis are those of the author and do not reflect the official policy or position of the Department of Defense or the U.S. Government.

17	COSATI CODES		18 SUBJECT TERMS (Continue on reverse if necessary and identify by block number)
FIELD	GROUP	SUB GROUP	AEW, Design,Existing Rotodome,E2C,Proposed PEE

19 ABSTRACT (Continue on reverse if necessary and identify by block number)

The aging E-2C fleet is expected to be retired by the year 2015. In order to provide Airborne Early Warning (AEW) for the battle group during the transitional years and beyond, the design of a replacement aircraft must begin soon. In order to conform with present day economic realities, one possible configuration is a new airframe using the radar system and rotodome which currently operates on the E-2C Other likely requirements for a new AEW aircraft includes a high-speed dash (M=0.7-0.85) capability, an extended mission time (up to 7.5 hours), turbofan engines, and an aircrew ejection system

The results of this design effort includes an investigation of a possible configuration and the aerodynamics involved. Performance and Stability & Control characteristics are also discussed briefly. Finally, a qualitative analysis of the use of the E-2C's radar system on a new airframe will be presented

20 DISTRIBUTION/AVAILABILITY OF ABSTRACT ☒ UNCLASSIFIED/UNLIMITED ☐ SAME AS RPT ☐ DTIC USERS	21 ABSTRACT SECURITY CLASSIFICATION UNCLASSIFIED	
22a NAME OF RESPONSIBLE INDIVIDUAL C.F. Newberry	22b TELEPHONE (Include Area Code) (408)656-2491	22c OFFICE SYMBOL AA/NE

i

AEW Aircraft Design

by

Michael J. Wagner
Lieutenant Commander, United States Navy
B.S., La Salle College

Submitted in partial fullfillment
of the requirements for the degree of

MASTER OF SCIENCE IN AERONAUTICAL ENGINEERING

from the

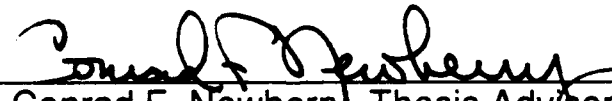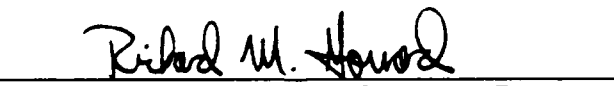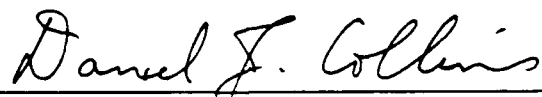NAVAL POSTGRADUATE SCHOOL
December, 1992

Author: _____
Michael J. Wagner

Approved by: _____
Conrad F. Newberry, Thesis Advisor

_____
Richard M. Howard, Second Reader

_____
Daniel J. Collins, Chairman
Department of Aeronautics and Astronautics

ii

ABSTRACT

The aging E-2C fleet is expected to be retired by the year 2015. In order to provide Airborne Early Warning (AEW) for the battle group during the transitional years and beyond, the design of a replacement aircraft must begin soon. In order to conform with present day economic realities, one possible configuration is a new airframe using the radar system and rotodome which currently operates on the E-2C. Other likely requirements for a new AEW aircraft includes a high-speed dash (M=0.7-0.85) capability, an extended mission time (up to 7.5 hours), turbofan engines, and an aircrew ejection system.

The results of this design effort includes an investigation of a possible configuration and the aerodynamics involved. Performance and Stability & Control characteristics are also discussed briefly. Finally, a qualitative analysis of the use of the E-2C's radar system on a new airframe will be presented.

iii

TABLE OF CONTENTS

I. INTRODUCTION

The purpose of this thesis is to provide an initial conceptual design for a carrier-based Airborne Early Warning (AEW) aircraft that would replace the E-2C. The AEW aircraft design is in response to a Proposed Request For Proposal (Proposed RFP), which is based on the perceived need to replace the E-2C. The Proposed RFP was prepared by C.F. Newberry after informal discussions with several individuals including students, Naval Air Systems Command (NAVAIRSYSCOM) staff, and other members of the E-2C community. It is not an official document, but rather a general guideline for an AEW design. The Proposed RFP is included as Appendix A. This chapter will provide some introductory material necessary to understanding the issues involved in designing any generic AEW aircraft. A description of a generic AEW mission profile will be discussed. Additionally, a brief description of the method of design will be presented.

A. BACKGROUND

1. Proposed Request For Proposal

With an increasingly aging E-2C fleet, the Navy has recently recognized the need for a replacement AEW aircraft. In accordance with present economic realities, the first objective is to provide a capable platform that is cost effective. A "low risk airframe configuration" is most desired. A low

risk detection system is also desired. In order to satisfy the above objectives, a Proposed RFP requirement is to include the existing 24-foot rotodome currently being used on the E-2C in the new design.

In order to detect high-speed adversary aircraft as far from the battle group as possible, and to quickly replace an aircraft with an inoperative detection system, there is a requirement that a new AEW platform possess a high speed dash (M=0.70-0.85) capability. The aircraft must also possess excellent loiter characteristics in order to provide long periods of detection for the battle group. A total unrefueled mission cycle time of 5.75 hours is required. Additionally, an in-flight refueling capability is required to extend mission cycle time.

The new AEW aircraft is required to provide direct self defense. It is expected that two AIM-7 Sparrow-sized missiles would be mounted on wing stations. Additionally, it is required that the aircraft possess chaff and flare launchers. Also, there is a requirement for a crew ejection escape system.

Carrier Suitability requirements include total compatibility with all CVN-68 (Nimitz class) carriers and subsequent, and a maximum takeoff weight of 60,000 lbs. Also, in an effort to remove the hazards of spinning propellers on the flight deck, a turbofan propulsion system is required. Table 1 outlines the significant Proposed RFP requirements for the AEW aircraft.

2. AEW Mission Profile

The Proposed RFP specified some general mission requirements the AEW aircraft must be able to accomplish. Also included is standard information

2

on essential mission parameters such as start, taxi, fuel reserves, etc. These requirements were used along with a baseline knowledge of the AEW mission to generate the mission profile shown in Figure 1. Mission parameters are summarized in Table 2.

TABLE 1. PROPOSED RFP REQUIREMENTS

PROPOSED RFP TOPIC	REQUIREMENT
High Speed Dash	Mach = 0.70-0.85
Loiter	4.5 hrs at 250 NM from Carrier
Mission Cycle Time (no refuel)	5.75 hours
Mission Cycle Time (refuel)	7.50 hours
Detection Antenna	Existing 24-Foot Rotodome
Propulsion	Turbofan
Escape System	Ejection
Maximum T/O Weight	60,000 lbs.
Carrier Suitability	Total Compatibility w/ CVN-68 and Subsequent
Carrier Launch	0 Knots Wind Over Deck (WOD)
Carrier Arrestment	0 Knots WOD
Single Engine Waveoff	500 ft./min. minimum
Weight Growth	4000 lbs. minimum
Limit Load Factor	3.0 g's
Self Defense	2 Missiles, Chaff, Flares
Cockpit	High Visibility for Ship OPS
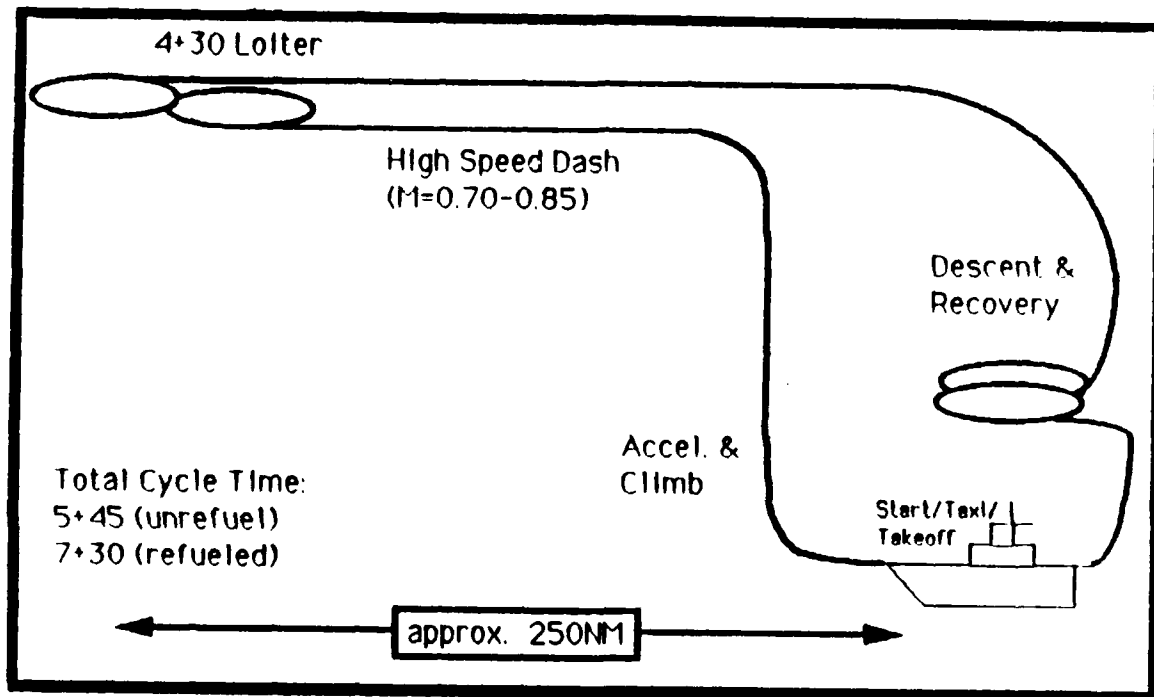
Figure 1.   AEW Mission Profile

It should be noted that some of the performance parameters presented
in the Mach number, Distance, and Time columns in Table 2, are approximated
based on historical trends and past experience.   A more detail estimation of
performance is provided in Chapter V.

4

TABLE 2. MISSION PARAMETERS

PHASE	M NO.	ALTITUDE (FT)	DIS-TANCE (NM)	TIME	TOTAL TIME	POWER
Start Taxi	0	0	-	0+20	0+20	Idle
Takeoff	0.3	0	-	-	-	Mil
Accel/Climb	0.5	0-35,000	35	0+20	0+40	Mil/Max
High Speed Dash	0.78	35,000	250	0+30	1+10	Max/Mil
Loiter	0.45	35,000	-	4+30	5+40	A/R
Descent	0.7	35,000-5,000	35	0+10	5+50	Idle
Recovery	0.7-0.2	5,000-0	-	0+15	6+05	A/R

Also note that by choosing a specific Mach number for the high speed dash phase, the first design decision was made. The Mach number range given in the Proposed RFP was too broad. The upper end of the Mach number range seemed a little too high (M=0.85), particularly from the standpoint of drag divergence. On the other hand, the lower end of the range (M=0.70) seemed a little too low from the standpoint of design technology. It was decided that a mid-range Mach number (M=0.78) was the maximum realistic speed to which this AEW aircraft could be designed.

B. DESIGN STRATEGY

As previously mentioned, the primary purpose of this research was to provide a first iteration on a conceptual design only. As such, the areas of research are directly proportional to the areas of emphasis given in the Proposed RFP. The focus of this research will be on the aircraft configuration

5

and the resulting aerodynamics. Performance and Stability & Control will also be discussed briefly. Some of the topics addressed in preliminary design books such as References (1) and (2) are outside the scope of this research. Such topics include propulsion, structures, and cost analysis. A more complete design effort is possible only after an entire design team is assembled.

The primary objective during the design process was to remain focused on what the customer (NAVAIRSYSCOM) might desire in a AEW aircraft. This design approach, known as Quality Function Deployment (QFD), seems obvious but is a new concept to most design teams. QFD will be discussed in detail in Chapter II.

In order to avoid "reinventing the wheel" and to keep costs down, characteristics of proven aircraft with similar missions (i.e., E-2C, S-3A, EA-6B) were evaluated, and integrated into this AEW aircraft design. The overall philosophy was to keep the AEW aircraft design as simple, and as conventional as possible. Design techniques and equations were used in accordance with conventional design books such as References (1) and (2). Also, computer programs such as MATLAB and EXCEL were used as much as possible to rapidly complete future iterations. The programs are included as appendices. The equations in each computer program are referenced with the appropriate book and equation number, in order to assist any follow-on work to this thesis.

II. PRE-DESIGN ANALYSIS

It is widely understood that the further along a product is in its design process, the less design freedom the engineer enjoys. Therefore before any design process begins, it is imperative that the customer's desires and parameter constraints be thoroughly analyzed. This chapter will examine the specifics of QFD, and the constraints placed on the AEW aircraft.

A. QUALITY FUNCTION DEPLOYMENT (QFD)

Because of the present realities of fierce global competition, major companies throughout the world are searching for creative ways to produce high quality products at competitive prices. For governments on tight budgets, the commitment to high quality and low cost has also become increasingly important. The results of these realities have been numerous quality-based management, engineering, and design philosophies. Some of these philosophies include Deming's Total Quality Management (TQM), Taguchi's Parameter Design Method, and Mitsubishi's Quality Function Deployment (QFD). It has been these kinds of quality-oriented philosophies that have made Japanese industries so successful. Because these strategies are complementary, the more general term of QFD will be used for the purpose of this discussion.

As noted in Reference (3), it is extremely difficult (and costly) to implement quality into a product that has already been designed. Therefore in order to design a quality product, it is imperative that before a preliminary design process begins, sufficient time must be spent on the issue of product quality. From the standpoint of QFD, the answer to the question "What is Quality?" is simple--quality is providing what the customer wants! Reference (4) provides a more formal definition--"Quality is the loss a product causes to society after being shipped, other than any losses caused by its intrinsic functions". The purpose of QFD is to investigate what the customer wants **in detail**, and then translate those desires into engineering and design decisions.

The result of implementing QFD speaks for itself. As Reference (5) points out, Toyota Auto Body reduced costs by 61% after implementing QFD. Reference (6) notes that an unspecified Japanese automaker with QFD takes 32 months from first design to finish a car, while it takes 60 months for a U.S. automaker without QFD! These results were accomplished because of a commitment to begin the design process only after extensive customer research was completed. Once the design process was underway, the need for design changes became almost non-existent, because the customer's desires were already known. Figure 2 is reproduced from Reference (5) and graphically illustrates the difference in the design philosophies between two automobile companies. The lesson to be learned is clear--if more time and money are spent investigating customer desires before the design process begins, more time and money will be saved in the long run, and product quality will be higher.
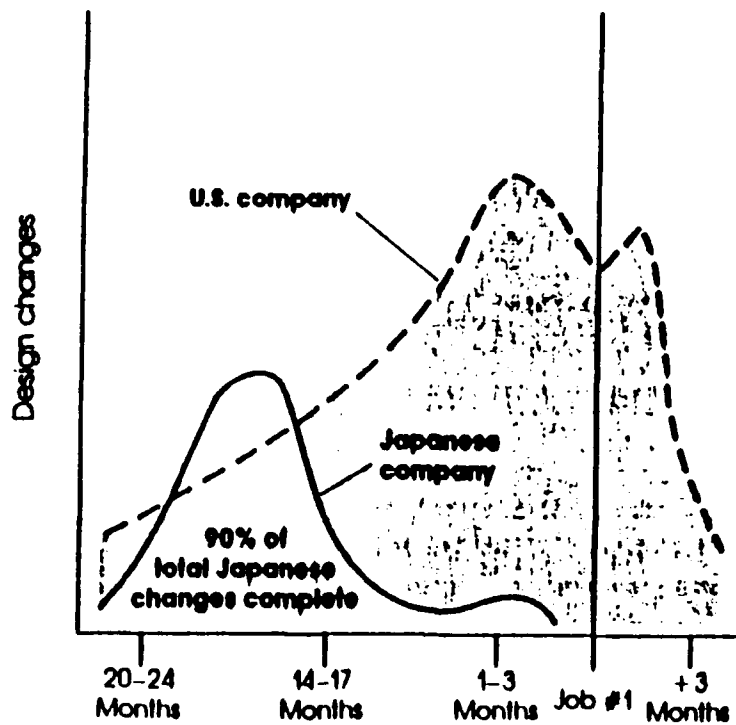
Figure 2. Results of QFD [Ref. 5]

In terms of an AEW aircraft design, a preliminary QFD analysis was performed based on the customer's (NAVAIRSYSCOM's) perceived desires expressed in the Proposed RFP. These desires, commonly referred to as Customer Attributes (CAs), were then numerically prioritized in accordance with the relative importance given them in the Proposed RFP. Based on the customer attributes and their relative importance, a House Of Quality (HOQ) was constructed. The HOQ is a matrix-type figure that puts customer attributes into a format that is usable by both engineering and management. The HOQ is shown in Figure 3.

Several items should be mentioned in the construction and use of the HOQ. As was previously mentioned, CAs were ranked according to the relative

importance given them in the Proposed RFP. The Relative Importance (RI) is an integral part of the HOQ because it is a constant reminder to both management and engineering of their priorities. The RI is a major tool for making design decisions.

RELATIONSHIPS	
++	Strongly Positive
+	Positive
--	Strongly Negative
-	Negative

Customer Attributes	Relative Importance	Weight (-)	T/W (+)	W/S (-)	Fuel Volume (+)	Cl Max. (+)	Cdo (-)	Aspect Ratio (+)	TSFC (-)	Wingfold/Sweep (+)	Technical Difficulty (-)	Avionics Technology (+)		
Life Cycle Costs	1	+	-	+	+	+	+	+	+	-	+	-		
Carrier Suitability	4	--	+	-	+	+	+	-	+	++	-	+		
Ejection Capability	7	-	-	-							--			
Existing Rotodome	6	-	-	-	-	-	--		-	-	+	-		
In-Flight Refueling	9	-	-	-	-	+	-		-		-			
Takeoff Weight	8	+	+	--	+	+	-	+	-		-			
Turbofan Engines	5	+	+	+	-		-	+	++					
Number of Crew	11	-	-	-	-		-		-		+	+		
High Speed Dash	2	+	++	+	-	+	+	-	+	-	-			
Max. Endurance Loiter	3	+	+	+	++	++	++	++	++	-	-			
Max. Sustained Load	12	+	++	+	-	++	+	-	+	-	-			
Self Defense	10	+	+	+	-	+	-	+	+	--	-			

Figure 3. House of Quality

10

Note that Figure 3 shows CAs vs. Engineering Characteristics (ECs). The CAs can be considered the "what" portion of the HOQ while the ECs can be thought of as the "how" portion. This is because the CAs communicate **what** needs to be accomplished while the ECs tell us **how** they can be accomplished. Reference (5) points out that, "Engineering Characteristics should describe the product in measurable terms and should directly affect customer perceptions". Thrust-to-Weight ratio (T/W) for example, is clearly measurable and it will directly affect how the customer perceives the product in terms of its performance characteristics. Also note that shown with each EC is a plus or minus sign. This communicates to the engineer what should ideally be accomplished with a particular EC. For example, the Weight EC is followed by a minus sign because the objective is to keep weight as low as practical.

The central matrix portion of Figure 3 is the primary vehicle in which CAs and ECs communicate. As Reference (5) notes, it is in this central matrix that ECs that affect particular CAs are identified, and relationships between them are established. For example, there is a positive relationship between low Weight (EC) and maximum Endurance loiter (CA). In other words, all other things being constant, the lower the weight the longer the loiter time. Once this matrix is completed, the engineer will have a better idea of how to proceed in terms of the design process.

Another significant part of the HOQ is the characteristic roof. The roof is used to establish relationships between various ECs. For example, there is a negative relationship between low weight and higher Fuel Volume. Like the

11

central matrix, the completed roof helps the engineer make the necessary decisions in the design process, by balancing these relationships.

The HOQ shown in Figure 3 is only the first in a series of four or more HOQs that can be used to communicate the customer's desires through to the actual manufacturing process. Figure 4 is reproduced from Reference (5) and shows an example of how these HOQs might be related and how CAs trigger a series of decisions made through to manufacturing. Note that the "how" portion of each HOQ becomes the "what" portion of the next HOQ. The subsequent HOQs in the series would necessarily be generated after future iterations in the design process. It is difficult for example, to examine the characteristics of specific parts while still in the conceptual phase.
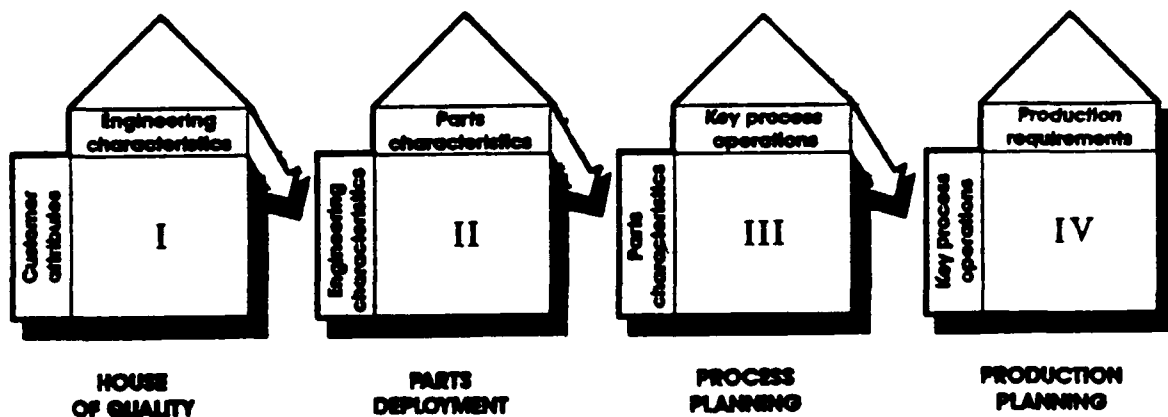
Figure 4. Linked HOQs [Ref. 5]

It should be emphasized that the HOQ shown in Figure 3 is preliminary. It is based on the preliminary requirements given in the Proposed RFP,and is primarily used for setting design priorities. Before the AEW aircraft design goes beyond the conceptual phase, detailed marketing research should be conducted to investigate what the customer wants. The research should include a survey of all the customers including NAVAIRSYSCOM, aircrew, and maintenance personnel. The research should be a study of likes and dislikes of even the smallest details of an AEW aircraft. For example, questions on the operation of the external door, or the location of a parking brake, etc., should be included when questioning customers. This research would then generate many series of HOQs.

The QFD strategy cannot be overemphasized in the aircraft design process. Although the process may seem time consuming and wasteful at first, a properly implemented QFD program will result in enormous long run benefits to both the aircraft company and the customer. Within the scope of this research, only aircraft companies with fully implemented QFD programs should be considered for development of the AEW aircraft.

B. CONSTRAINT ANALYSIS

Before the actual design process can begin, it is necessary to evaluate two of the aircraft's characteristics. These characteristics are T/W and Wing Loading (W/S). A series of performance equations may be derived in which T/W is expressed as a function of W/S.   These equations are derived in

13

Reference (7). Equation constants are obtained from performance characteristics provided in the Proposed RFP. For a range of W/S, a range of T/W may be generated for each equation. The equations are then graphed on a single constraint plot. The plot graphically depicts a solution space. Any T/W-W/S combination may be selected within that space. Obviously, some T/W-W/S combinations will be better than others. For example, suppose a constraint analysis on an aircraft reveals that lowest T/W in the solution space is 0.25. This means the aircraft can perform the required mission at a T/W = 0.25. It would be illogical to choose a T/W = 0.50 even though it is also within the solution space. It should be noted that although the constraint plot is primarily a pre-design tool, it may be used throughout the design process. As more knowledge of the design is known, more exact iterations of the constraint plot may be generated. It should also be pointed out that the constraint analysis need not be limited to performance equations only. For example, if a valid expression for maintainability in terms of T/W and W/S is found, it should also be included as part of the constraint analysis.

In order to keep future iterations simple, a computer program was written in MATLAB, based on the performance equations derived in Reference (7). The complete program is included as Appendix B. All equations in Reference (7) applicable to the AEW mission were used with the exception of takeoff and landing performance. Expressions presented in Reference (1) were used for takeoff and landing performance because of their simplicity and their more conservative results. Performance equation constants were obtained from

performance characteristics provided in the Proposed RFP and from a baseline knowledge of the AEW mission. The results of the AEW constraint analysis is shown in Figure 5.
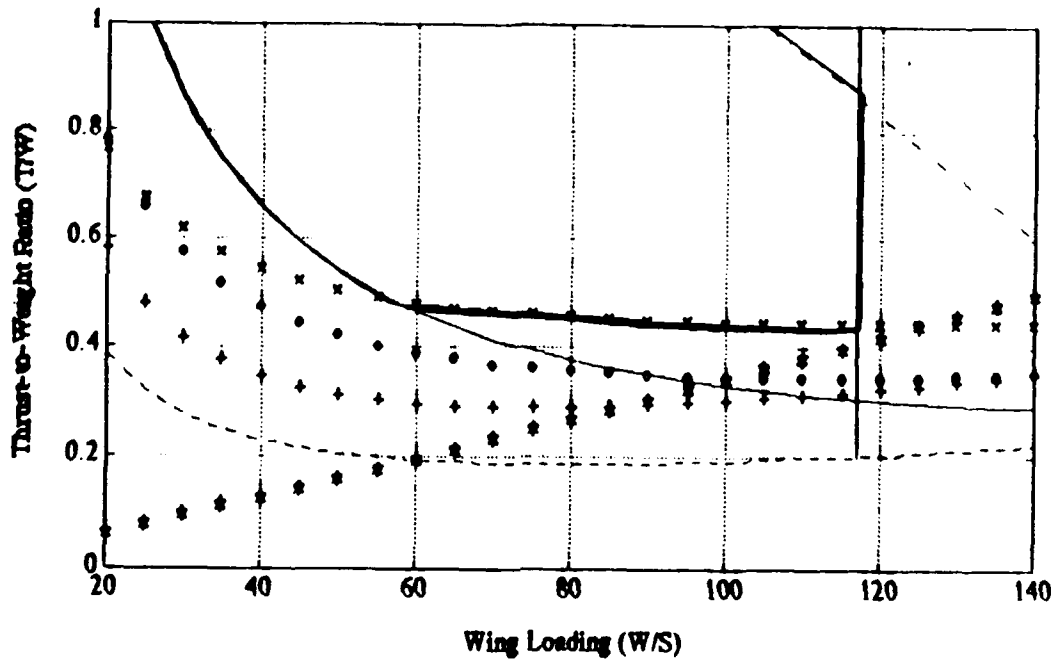
KEY: 1) High Speed Dash at M=0.78 & 35K ft. ==> '___'
2) Max Endurance at M=0.45 & 35K ft. ==> '- - -'
3) Constant Speed Climb at M=0.41 & 15K ft. ==> 'x x'
4) Sustained 'g' Turn at 2g's & 20K ft. ==> '+ +'
5) Level Accel Run at 35K ft. ==> 'o o'
6) Takeoff Performance (Nicolai) ==> '* *'
7) Landing Performance (Nicolai) ==> 'l'
8) Maintainability (MMH/FH=30) ==> '_ .'

Figure 5. AEW Constraint Analysis

The solution space is the outlined upper center portion of the graph. Note the relatively flat bottom of the solution space. This flat bottom is most fortuitous because it allows a certain degree of design freedom. For a relatively low

15

T/W of 0.46, a W/S anywhere between 55 and 116 lbs/ft2 can be chosen. Because of wing area limitations for carrier operations however, the W/S for an aircraft of this size is typically between 70 and 116 lbs/ft2.

Also note that the constraint plot includes a maintainability line. The line is the result of a equation derived in an unpublished paper by C.F. Newberry. The equation is the result of a linear curve fit of data from 25 different aircraft. It should be noted that there are limitations in the application of this equation. First, none of the aircraft for which data was supplied are Navy aircraft. Navy aircraft traditionally have different Mean Man Hours/Flight Hour (MMH/FH) rates than other aircraft. Second, a general trend should not be assumed using 25 very different aircraft. These aircraft ranged from T-38's to 747's. Although the validity of the maintainability line may be suspect, it should be investigated in greater detail, using a larger database of aircraft similar to the aircraft being designed. The current maintainability equation may be used in the constraint analysis, but only as long as its impact is integrated in a reasonable fashion.

III.   AEW CONFIGURATION

This chapter will discuss the initial conceptual design for the AEW aircraft. A description of the aircraft will be provided along with the rationale behind various design decisions. An initial weight & balance evaluation will also be discussed. Finally, an analysis of the AEW aircraft with various carrier suitability requirements will be performed.

A.   AIRCRAFT DESCRIPTION

1. Introduction

The purpose of this section is to provide a brief description of the external aircraft configuration, and to provide justification for some design choices. Not all configuration characteristics of the aircraft will be discussed in this section however. Aircraft characteristics directly related to aerodynamics will be discussed in Chapter IV. These characteristics include planform selection, airfoil selection, and high lift devices.

2. General

The AEW aircraft design is shown in Figure 6. The aircraft is designed to hold a crew of four and will be powered by twin turbofan engines. Crew seating will be arranged in a dual-tandem configuration. Large cockpit windows will allow better visibility for carrier (CV) launch and recovery operations. The rotodome antenna will be supported by the existing rotodome

17
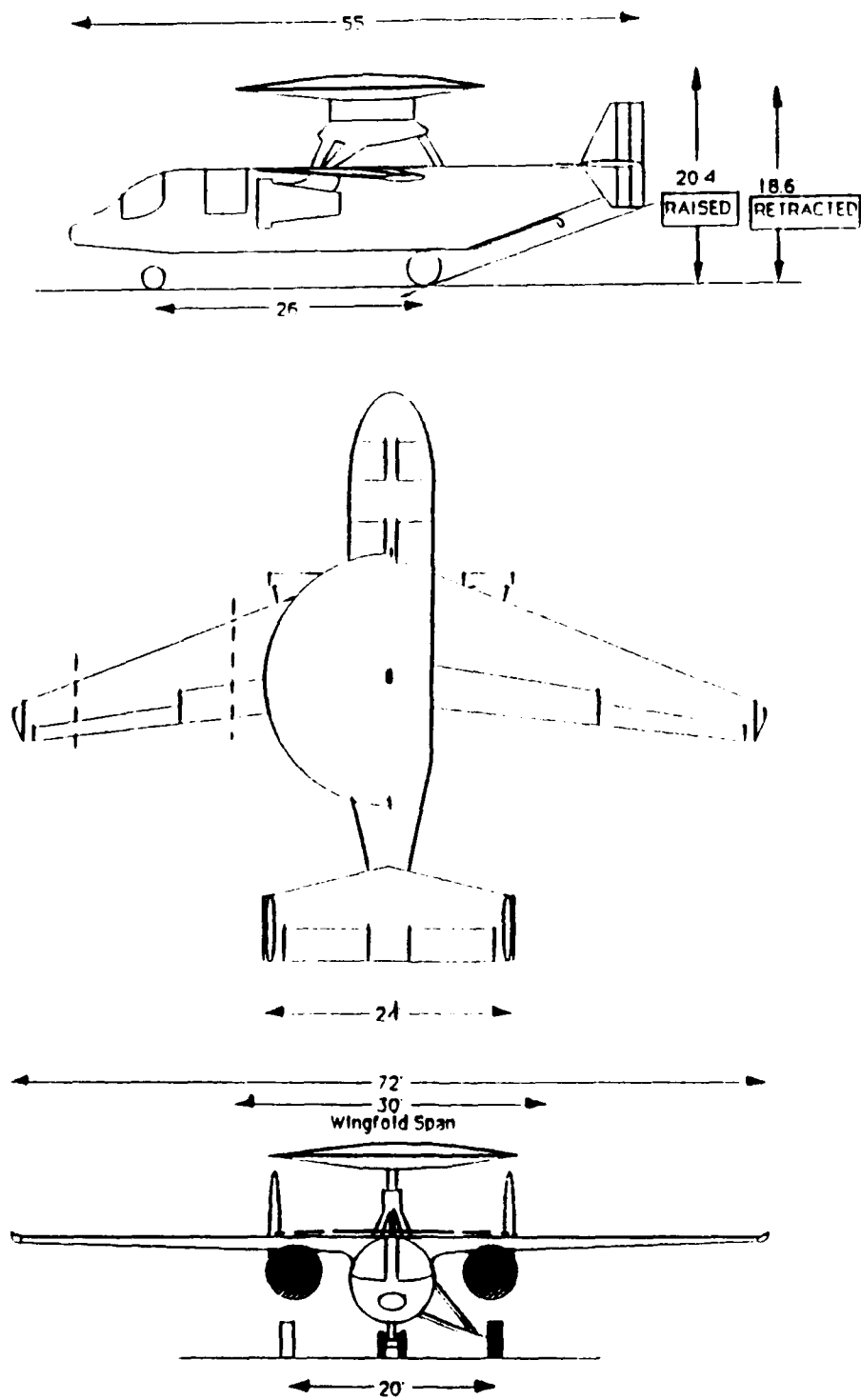
Figure 6.   AEW Aircraft Design

pylon. Also, in order to satisfy CV requirements, the rotodome retraction system that was operational on early E-2's must be used. Twin vertical stabilizers will be mid-mounted at either end of the horizontal stabilizer. A total fuel weight estimate of 14000 pounds was based on fuel volume calculation procedures set forth in Reference (8). It should be noted that this iteration of the aircraft design includes no composite materials. Significant aircraft dimensions are presented in Table 3.

3. Specific Component Description

a. Engines

Although a detailed study of the propulsion system was outside the scope of this design effort, an initial analysis of the required engine performance was made. In order to meet the mission requirements of high-speed dash and long time loiter, it is clear that a high-bypass turbofan engine with a low Thrust Specific Fuel Consumption (TSFC) is required. Assuming an initial takeoff weight of approximately 55,000 lbs. and a T/W = 0.46, the thrust per engine requirement is approximately 12,700 lbs. As shown in Reference (9), the technology for such an engine already exists. Two operational engines with characteristics similar to those required for the AEW aircraft, are presented in Table 4. Further design iterations should include an investigation into the feasibility of using an upgraded version of the General Electric (GE) TF34-GE-400A engine in the AEW aircraft.

TABLE 3. AEW AIRCRAFT DIMENSIONS

CHARACTERISTIC	DIMENSION
Body Length	55 ft.
Body Diameter	8 ft.
Body Fineness Ratio (L/D)	6.875
Wing Span	72 ft.
Wing Area	639 ft2
Wing Loading (W/S)	Approx. 85 lb/ft2
Wing Sweep (leading edge)	21 degrees
Wing Thickness Ratio (t/c)	0.12
Wing C_{mac}	9.77 ft.
Wing Aspect Ratio	8.11
Wing Taper Ratio	0.29
Horizonal Tail Area	180 ft2
Horizonal Tail Sweep	14 degrees
Elevator Area	47 ft2
Vertical Tail Area	90 ft2
Vertical Tail Sweep	26.6 degrees upper, 36.9 degrees lower
Rudder Area	60 ft2
Empennage t/c	0.10

TABLE 4. SIMILAR ENGINE CHARACTERISTICS

Engine	Maker	Type	Thrust (lbs.)	TSFC [1]	Pressure Ratio [1]	Dimensions (Dia.xL)	Weight (lbs.)
TF34-GE-400A [2]	General Electric	AFF [3]	9,275	0.363	21	52in. x 100in.	1,478
FJR-710-/600S [4]	Nat. Aero. Lab Tokyo	AFF [3]	14,330	0.340	22	57.1in. x 92.5in.	2,160

Notes: 1- At Maximum Power
2- S-3A Aircraft
3- Axial Flow Fan
4- NAL/Kawasaki Aircraft

20

The engines should be mounted closely to the wing for two reasons. First, exhaust flow through the slotted trailing edge flaps will help reattach the airflow over the wing, thereby increasing CL_{max}. Second, an engine mounted closely underneath the wing is further from the ground, and therefore less likely to ingest foreign objects. This would result in fewer engine replacements and lower life cycle costs.

b. Vertical Tail

As previously mentioned, the empennage will include two vertical stabilizers. The maximum height of the vertical stabilizers were modeled after the E-2C in an effort to keep the tails from interfering with the look-down capability of the rotodome antenna. Each vertical stabilizer will include a rudder control surface. It should be noted that if future iterations mandate higher vertical tails, maximum use of composites will be necessary to avoid antenna interference.

c. Aircraft Entry

Aircraft ingress will be accomplished through a single door in the fuselage. A walkway will allow movement between the door and the cockpits. The major advantage of this configuration is flexibility. The walkway will allow the crew to move freely throughout the aircraft to troubleshoot avionics systems, switch seats, etc. Consideration may be given to a canopy system similar to that currently operating in the EA-6B. The canopy arrangement was initially ruled out in this study due to potential engineering difficulty, increased life cycle costs, and lack of flexibility.

d. Wing Fold System

The first wing fold will be at 15 feet from the aircraft centerline. This will result in a maximum wing fold span of 30 feet. This wing fold span is within the maximum requirement of 35 feet and will allow easy storage of aircraft on the flight deck. The wings are intended to fold vertically up. At the completion of this vertical fold, the wing tip will physically interfere with the rotodome antenna. Therefore a second wing fold at 30 feet from the centerline is required. Dashed lines denote the wing fold breaks in Figure 6. The horizontal wing fold system which currently operates on the E-2C was ruled out for two reasons. First, horizontally folded wings create a large sail area. When the aircraft taxis perpendicular to the wind on the carrier deck, it tends to get blown, resulting in lose of control. Second, it is clear from the geometry of this AEW design that the wingtip of a horizontally-folded wing would not reach a wing support on the horizonal tail tip.

e. Armament

The aircraft is designed to accommodate one wing station on each wing at approximately 14 feet from the centerline. Each wing station should be capable of carrying an air-to-air missile of 500 pounds. Although use of the AIM-7 Sparrow missile was alluded to in the Proposed RFP, this is not recommended. Use of the AIM-7 would require the aircraft to possess a high-energy, target illumination capability. The new generation of "fire-and-forget" air-to-air missiles such as AMRAAM and Have-Dash are much more suitable for

the AEW aircraft. No target illumination is required for these missiles. Updated target information is provided via data link.

f. Landing Gear

A landing gear analysis was performed based on procedures set forth in Reference (2). The aircraft will use a standard tricycle system. Longitudinal placement of the main gear was determined by an estimated center of gravity location. Lateral placement of the main gear was determined by a maximum overturn angle requirement of 54 degrees. The wheelbase will be 26 feet long and the main wheel width will be 20 feet. The nose gear will have a dual-wheel configuration. The nose gear will retract aft into the fuselage. Each of the main landing gear will be a single-wheel configuration and will also retract aft into the fuselage. Approximate tire dimensions are 25 in. x 7 in. (diameter x width) for the nose and 45 in. x 17 in. for the main. These dimensions are approximately 25% greater than the statistical equation proposed by Reference (2). This dimensional increase is to account for the harsh landing environment of the aircraft carrier. The 25% dimension increase corresponds well with the tire sizes of current carrier aircraft.

g. Escape System

The Proposed RFP requires the installation of an all-crew ejection system in the AEW aircraft. This requirement has resulted in many difficulties in the design of the escape system. These difficulties are obviously the result of the rotodome. An approximate trajectory of the aircrew on ejection is shown in Figure 7 for three flight conditions. An ejection trajectory computer program was

23

written in MATLAB and is included as Appendix C. The parabolic approximation is based on an ejection analysis presented in Reference (10). The identical pair of trajectories represent the front seat and back seat ejections. The diamond figure represents the location of the rotodome antenna.

It is obvious from the Figure 7 that the ejection system will result in aircrew impact with the rotodome. A bottom or sideways ejection would require development of a new ejection system, and obviously could not provide a 0/0 ejection capability. After an examination of various aircrew and rotodome placements, it became apparent that with today's technology, there are no safe ejection alternatives with the rotodome installed.

Ejection of the rotodome prior to crew ejection also has significant problems. The rotodome antenna alone (not including the supporting pylon and shaft) weighs 2350 pounds. In order to get the crew out of the aircraft quickly, the rotodome would have to be ejected with a typical acceleration of approximately 12g's. This would require a series of rockets that would have to generate a combined force of over 28000 pounds. These rockets would most likely have to be very large in order to provide such a force. It is unlikely that the rockets would fit into a supporting pylon that is only approximately one foot wide.

Additionally, it is obvious that the rockets would have to be directly attached to the rotodome. This means they would rotate with the rotodome. This means there would be no way to direct the trajectory of the rotodome, because it must be ejectable at any time during the rotation. Therefore, the

rockets would have to be of equal propulsive force. During certain flight conditions, including a 0/0 ejection, the crew would still be in danger of ejecting into the rotodome.
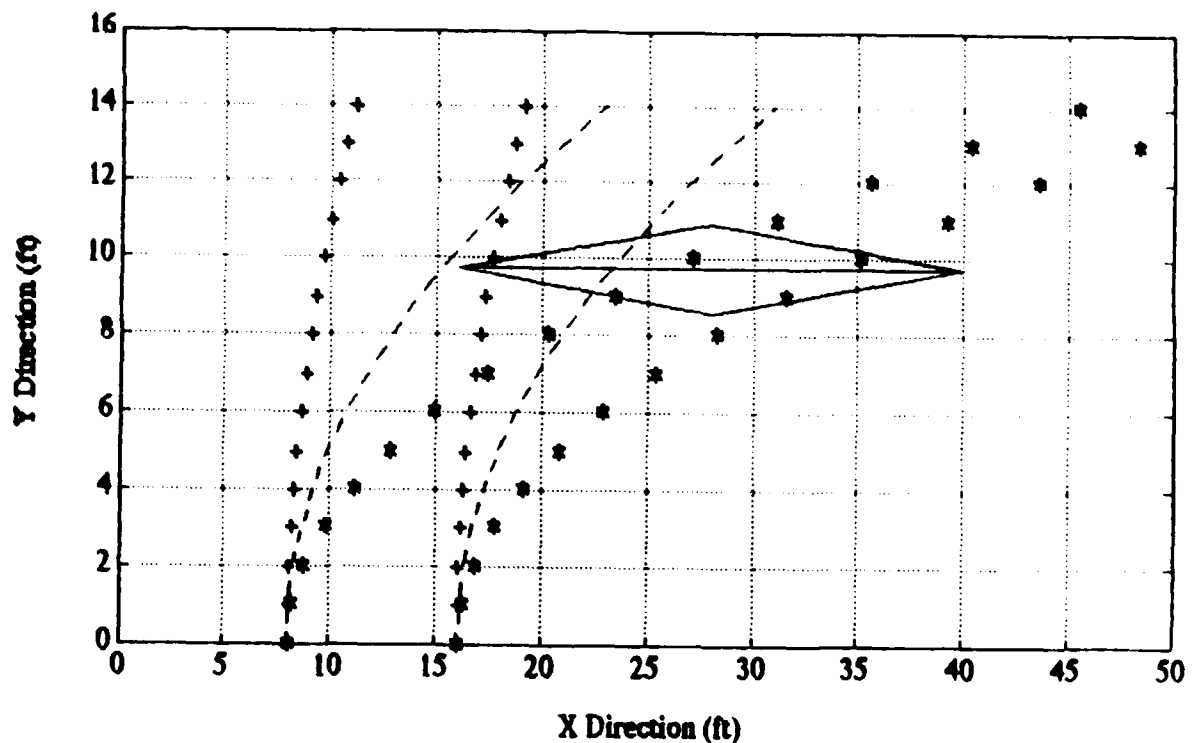
KEY· 1) M=0.76 at 5000 ft. ==> '**'
      2) M=0.48 at 5000 ft. ==> '--'
      3) M=0.20 at sea level ==> '++'

Figure 7. Aircrew Ejection Trajectory

Ejecting the entire rotodome structure would eliminate the controlled trajectory problem, but would generate other problems. Now the rockets would have to generate a combined force of over 38000 pounds. The rockets under the forward supports would most likely ignite the fuel in the fuel

cells directly below. The resulting explosion would jeopardize the lives of the aircrew during ejection.

Two final points are worth mentioning. First, the new technology and the resulting developmental costs of ejecting a rotodome will likely be enormous. Second, any further investigation into rotodome ejection should necessarily include an examination of how the pitching moments about the center of gravity are affected .

B. WEIGHTS, CENTER OF GRAVITY, AND MOMENTS OF INERTIA

1. Weights

An evaluation of the AEW aircraft weight was performed using the individual component equations given in References (1) and (8). A computer program was written on MATLAB using the applicable equations. Many of the equations represented individual weight components as a function of takeoff weight. Since the determination of the takeoff weight was the ultimate objective, the program uses a secant method iteration procedure to find the takeoff weight. The weight program is included as Appendix D. In order to assure the accuracy of the program, a weight analysis on the E-2C was performed. It was found that the program prediction came within 300 pounds of the actual E-2C weight. The program was then used to analyze the weight of the AEW aircraft. The predicted weight was found to be approximately 53000 pounds which is comparable to the E-2C weight and well within the maximum requirement of

60000 pounds. The aircraft possesses a 7000 pound weight growth potential for future avionics upgrades.

2. Center of Gravity and Moment of Inertia

Component weights calculated from the weight program were used to approximate the aircraft's Center of Gravity (CG) and Moment of Inertia. Component CG locations were approximated based on procedures set forth in References (1), (2), and (8). Component Moment of Inertia values were calculated in accordance with procedures set forth in References (2). The component characteristics were used to calculate aircraft CG and Moment of Inertia values. All calculations were performed on a computer program written on EXCEL. The computer program was acquired from Reference (11). The computer program and the results of this program are included as Appendix E. An initial approximate CG location is 32.4 feet aft from 5 forward of the nose (approximately 48.6% MAC), and 10.9 feet up from 5 feet below the fuselage. More detailed CG and Moment of Inertia calculations will obviously be necessary with future iterations of the design.

C. CARRIER SUITABILITY REQUIREMENTS

Carrier suitability dimensional requirements and the significant AEW aircraft dimensions are shown in Table 5.

TABLE 5. CARRIER SUITABILITY DIMENSIONAL COMPARISON

DIMENSION	REQUIREMENT	AEW AIRCRAFT
Max. Gross Weight	60000 lbs.	53000 lbs.
Max. Wing Span	82 ft.	72 ft.
Max. Height	18.5 ft.	18.5 ft. (rotodome retracted)
Max. Main Gear Width	22 ft.	20 ft.
Min. Tipback Angle	15 deg.	20 deg.
Max. Tipover Angle	54 deg.	52.5 deg.
Elevator Size Restriction	52 X 85 ft.	55 X 30 ft.

IV. AERODYNAMICS

In order to get maximum effectiveness from an airframe and its propulsion system, a thorough examination of the aircraft's aerodynamic characteristics during the design process is mandatory. This chapter will examine the design decisions involved in selecting the AEW aircraft's airfoil and wing planform. Additionally, the aircraft's lift curve slope and high lift devices will be discussed. Finally, an analysis of the aircraft's drag characteristics will be presented.

A. AIRFOIL SELECTION

Because of the Proposed RFP requirements, the AEW aircraft will be expected to operate under a variety of flight conditions. It must be able to cruise at high subsonic speeds, loiter for long periods of time, and possess carrier-suitable, slow flight characteristics. In order to meet these requirements, the wing's airfoil must possess several seemingly contradictory characteristics. The airfoil should have a relatively high thickness ratio in order to increase Cl_{max}, increase benefit from high lift devices, decrease weight, and increase wing fuel storage capacity. If the wing is too thick however, the drag divergent Mach number (M_{dd}) will be too low to satisfy the high speed dash requirement. An increase in M_{dd} could be accomplished through an increase in wing sweep, but this generates additional problems which will be discussed in the next section. The airfoil must also have a high Cl_{max} for the loiter and landing

29

phases of flight. Most high speed airfoils however, are not known for their high Cl_{max} values. Finally, the airfoil's thickness distribution should be investigated in terms of its skin friction drag characteristics. As Reference (12) notes, a maximum thickness that is close to the trailing edge results in a more favorable pressure gradient on the forward portion of the airfoil. This helps create more laminar flow which results in reduced skin friction drag. It should be noted however, that an aft maximum thickness can cause poor pressure recovery characteristics at high angles-of-attack.

Based on the above requirements, it became clear that a supercritical airfoil was necessary. A supercritical airfoil is characterized by a relatively flat upper surface, and a maximum thickness located near the trailing edge. It also has a relatively blunt leading edge, and it is cambered at the aft portion of the airfoil. Reference (13) notes that for a given thickness ratio, the supercritical airfoil has a higher M_{dd} than conventional airfoils. This allows a thicker wing and less wing sweep. Additionally, the supercritical airfoil has a much higher Cl_{max} than a comparable conventional airfoil. Finally, the thickness distribution and the trailing edge upper and lower surface tangency results in a more favorable pressure gradient. The aft maximum thickness of the supercritical airfoil does not result in pressure recovery problems, because the camber is accomplished primarily by the lower surface. This allows the upper surface to remain relatively flat.

It should be pointed out that use of a supercritical airfoil will not be without its difficulties. First, the very thin trailing edge could prove to be a structural and

30

manufacturing problem. Second, although the original supercritical airfoil was designed in 1965, development and testing of an entire family of supercritical airfoils has been relatively recent. Because supercritical airfoils are relatively new technology, development costs may be high. Finally, the aft camber of the airfoil will result in large negative pitching moments. Despite the potential difficulties however, the supercritical airfoil shows the most promise in terms of satisfying the requirements of the Proposed RFP.

Initially it was hoped that an airfoil with a thickness ratio of 0.14 could be used for on the aircraft. Even with some compromise in the wing sweep, it soon became evident that a lower thickness ratio would be necessary in order to reach an acceptable M_{dd}. Experimental data presented in Reference (14) shows that at a thickness ratio of 0.12 and a design Cl of 0.7, the airfoil M_{dd} is approximately 0.76. A moderate wing sweep should permit reasonably low drag characteristics at the design cruise Mach number of 0.78.

After an evaluation of the family of NASA supercritical airfoils, it became clear that the best airfoil for the required mission was the NASA SC(2)-0712. This airfoil is shown in Figure 8. The airfoil's coordinates are reproduced from Reference (14), and is included as Appendix F. An explanation of the NASA supercritical airfoil designation system is presented below.

SC(2) - 07 12

| Supercritical phase 2. There are currently 3 phases of airfoil designs. | Design lift coefficient (tenths) | Thickness Ratio (hundredths) |
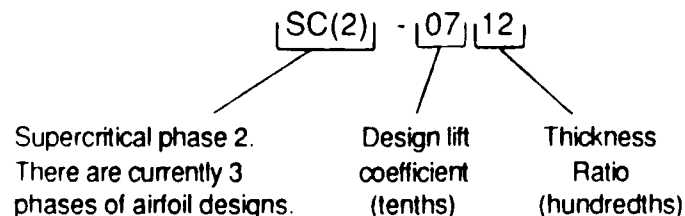
One of the biggest difficulties in selecting an airfoil was in obtaining the specific airfoil characteristics. Because of the relatively new technology, there is no compiled source of information for supercritical airfoils (such as Reference (15) for conventional airfoils). The three sources that provided most of the information on the airfoil were References (14), (16) and (17) . Airfoil characteristics are presented in Table 6.
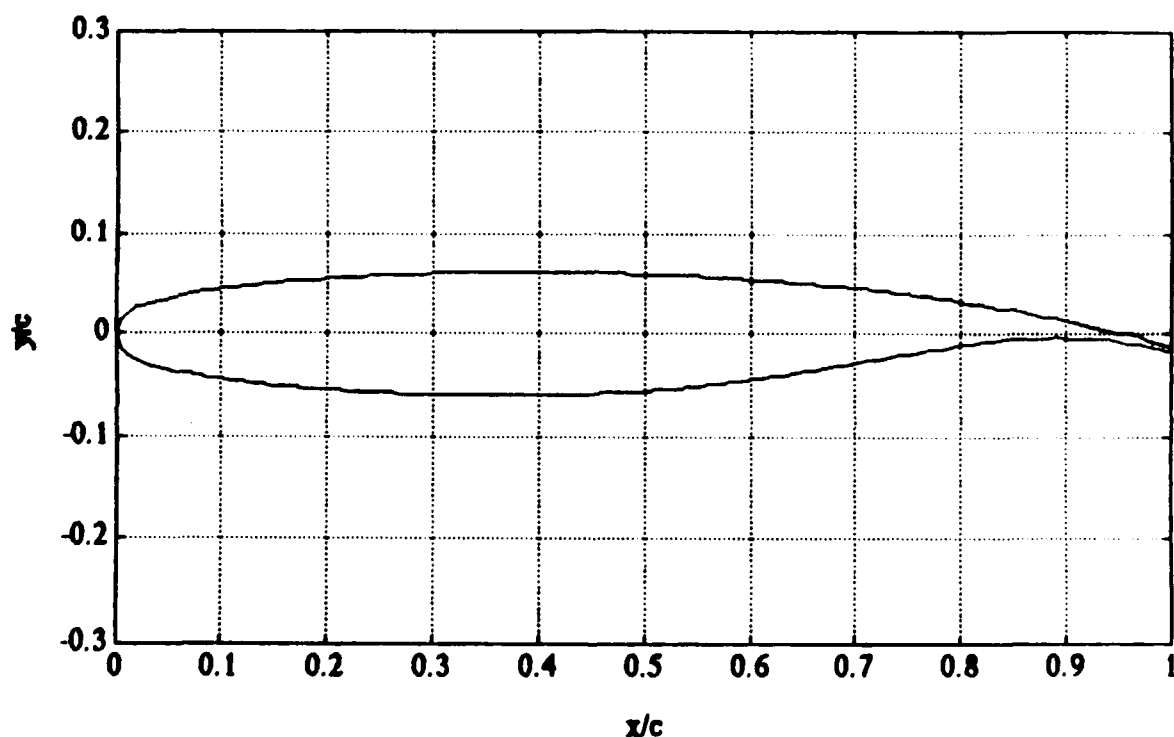
Figure 8. NASA SC(2)-0712 Airfoil

TABLE 6. NASA SC(2)-0712 CHARACTERISTICS

α_0	Cl_α	Cl_{max}	α_{max}	Cm_0
-4.37 deg.	0.08557/deg.	2.0	19 deg.	-0.14

B. PLANFORM DESIGN

Given the target cruise Mach number of 0.78 and the relatively thick airfoil, it was clear a planform with significant wing sweep would be required. Too much wing sweep however, generated numerous problems including a decrease in CL_{max} and CL_{α}, increased wing weight and decreased wing fuel volume. Selection of the previously mentioned airfoil was made only after it was determined that a relatively high M_{dd} could be attained with a modest wing sweep.

Figures 9 and 10 show the results of trade studies conducted to graphically illustrate the parameters involved in planform design and airfoil selection. Figure 9 shows M_{dd} as a function of thickness ratio with varying sweep. Figure 10 shows how thickness ratio and wing sweep affect wing weight. The results of these parametric studies were used to select the optimum planform design and airfoil thickness. With an airfoil thickness ratio of 0.12, a leading edge wing sweep of 21 degrees is the optimum choice considering all the parameters involved. This results in a wing M_{dd} of 0.81.

With the leading edge wing sweep selected, the focus of attention was then directed to the trailing edge sweep. A trailing edge sweep of 6.5 degrees was selected for a first iteration. The relatively small sweep will insure efficient use of flaps and aileron control surfaces. The flatter trailing edge sweep also allows an increase in wing area and wing fuel volume. With a wingtip chord length of four feet selected as a first iteration, and the above planform characteristics, a wing area of 639 ft2 was calculated.
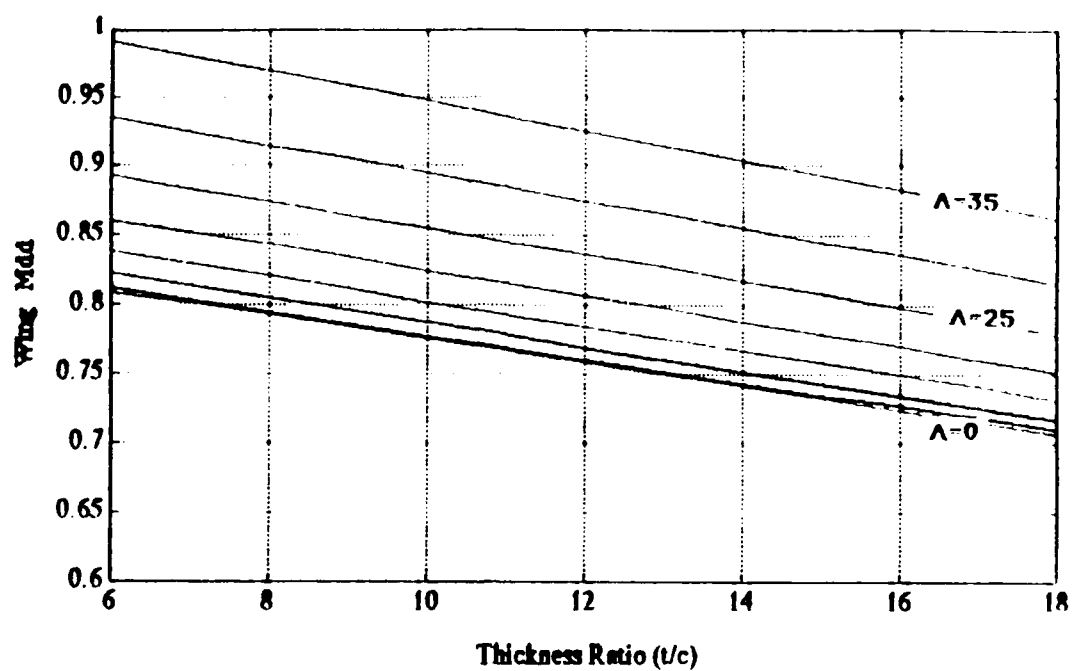
Figure 9.   Wing M_{dd} With Varying Wing Geometry
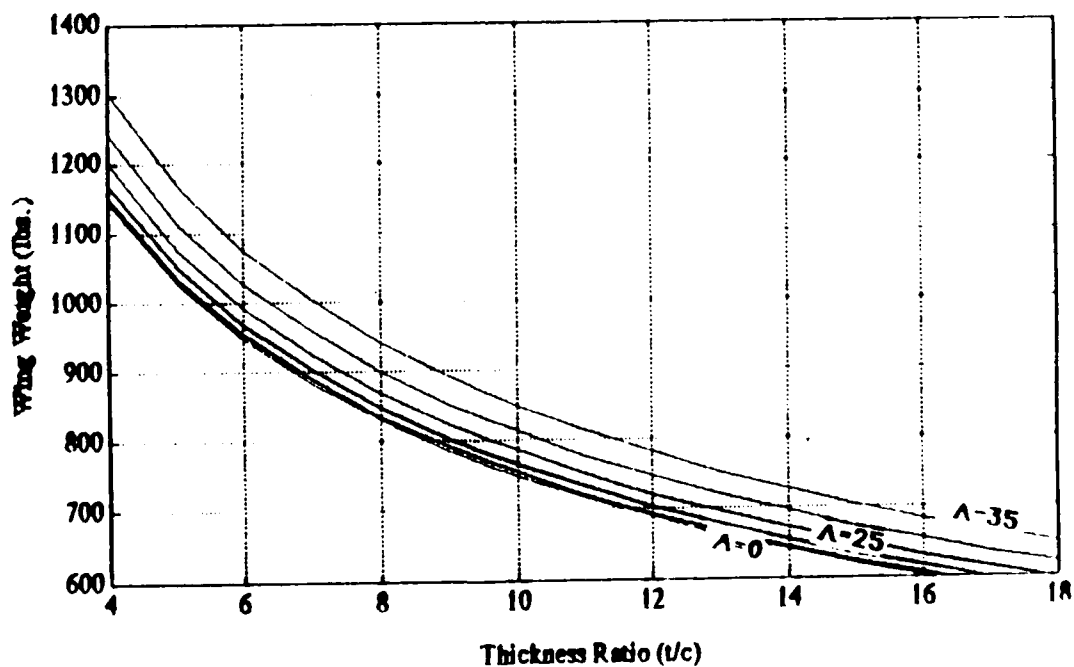
Figure 10.   Wing Weight With Varying Geometry

34

Another consideration in the planform design was aspect ratio. It was clear that in order to satisfy aggressive loiter requirements, a high aspect ratio would be necessary. For a given wing area, this would mean a larger wing span. Too large a wing span causes two problems however. First, it would result in line-up difficulties during carrier landings. Second, the large wing span would result in signal interference with the rotodome antenna, degrading radar performance. The selected wing span of 72 feet results in a aspect ratio of 8.11. The resulting maximum L/D ratio is 16.

C. LIFT CURVE SLOPE

With the selection of the wing planform design, a calculation of the wing's lift curve slope was then possible. Calculations were done in accordance with the procedures set forth in References (1), (2) and (18). The lift curve slopes for three flap settings are shown in Figure 11.

D. HIGH LIFT DEVICES

In order to make landing speeds slow enough to meet the Proposed RFP carrier suitability requirements, a CL_{max} of approximately 3.0 is required. To accomplish this, double slotted flaps are necessary. In accordance with the procedures set forth in Reference (2), ΔCL_{max} and $\Delta \alpha_o$ values were calculated. A maximum ΔCL_{max} was calculated to be 0.98.

Two design characteristics that will help increase CL_{max} with the flaps down should be mentioned. First, engines should be situated on the wing so

that engine exhaust will flow through the slotted flaps. Second, use of a aileron droop system with the flaps will help increase the CL_{max} of the entire wing.
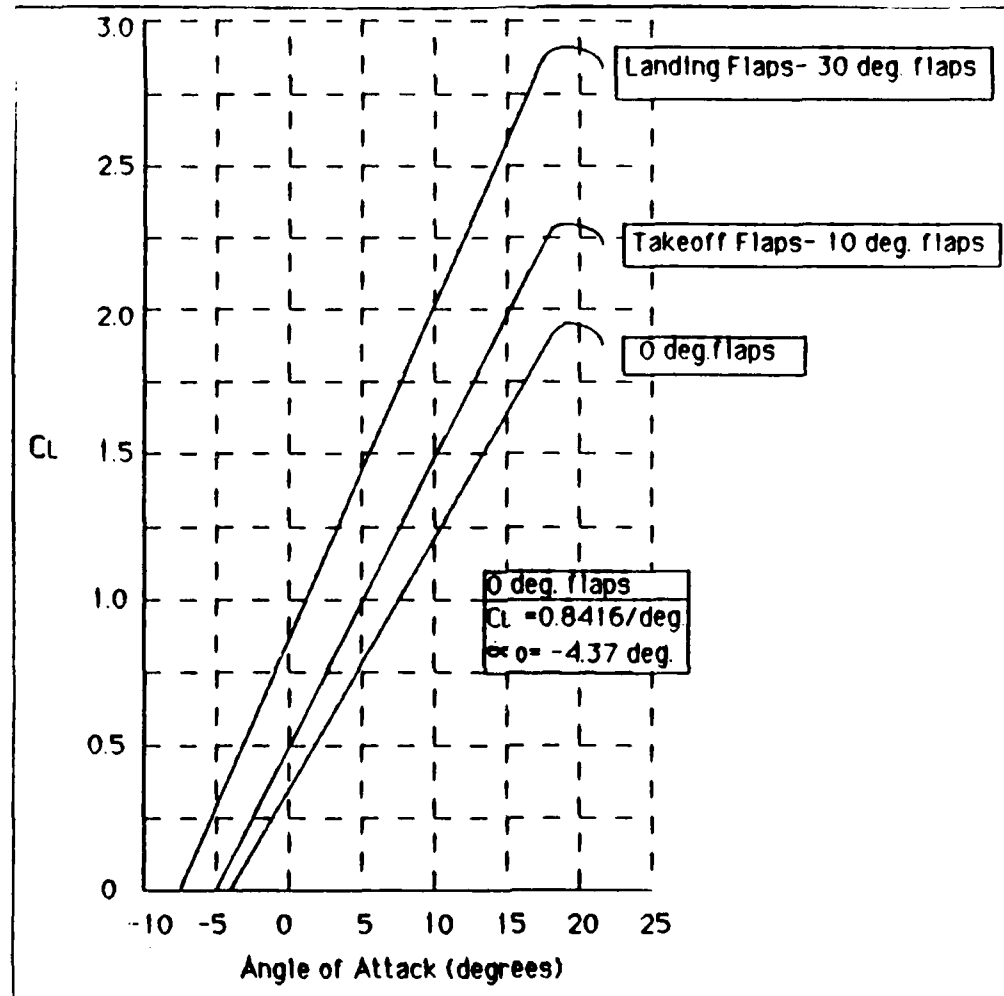
Figure 11. AEW Lift Curve Slope

E. PARASITIC DRAG CALCULATION

Parasitic drag (CDo) calculations were performed in accordance with procedures set forth in Reference (18). A CD_o computer program was written in MATLAB and is presented in Appendix G. A CD_o of approximately 0.0205 was

36

computed by the program. This CD_o value will be used to calculate a drag polar for the AEW Aircraft.

F. DRAG POLAR

The AEW drag polar was computed assuming CD as a parabolic function of CL. A first iteration efficiency factor of 0.8 was assumed. Also, the previously determined aspect ratio of 8.11 and CD_o of 0.0205 were used in the equation. A drag polar for the AEW aircraft in the clean configuration is shown in Figure 12.
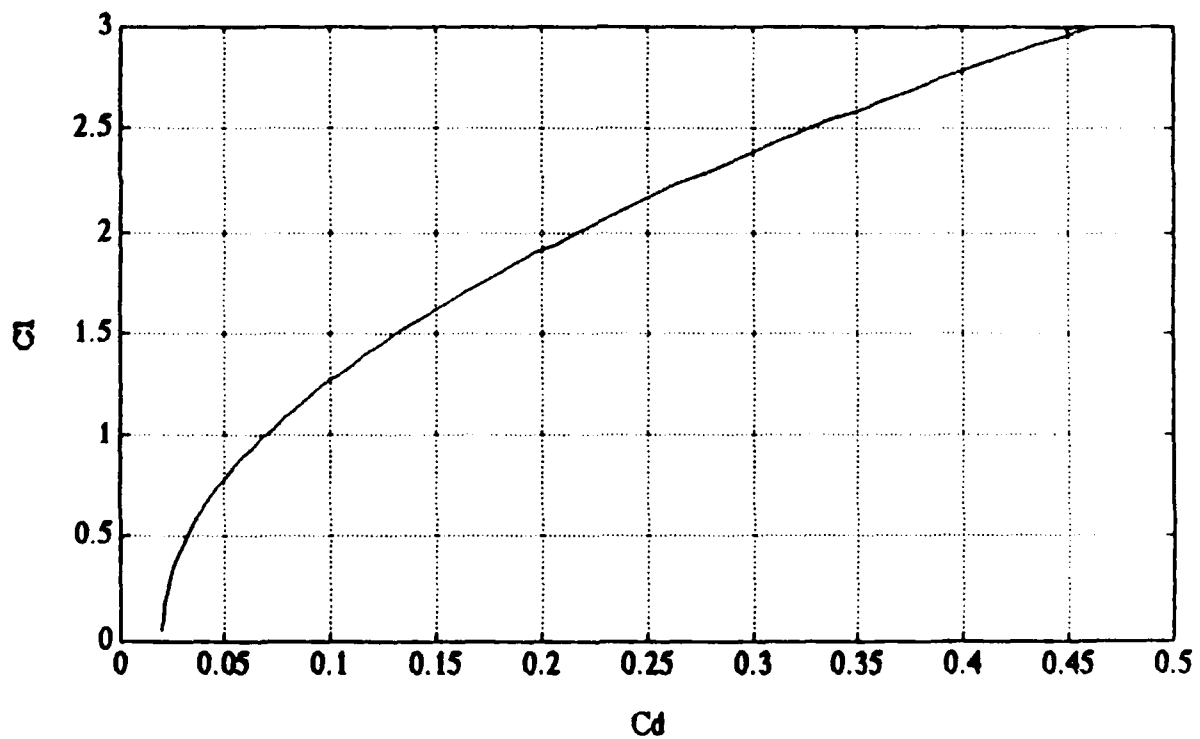
Figure 12. AEW Drag Polar

V. PERFORMANCE

This chapter will present the results of a preliminary performance analysis conducted for the AEW aircraft. This analysis was primarily performed using a computer program written in MATLAB. The program is presented in Appendix H, and also includes some aerodynamic calculations such as Coefficient of Drag (C_D) and Lift-to-Drag ratio (L/D). A Takeoff and Landing computer program is also included in Appendix H. Performance calculations were done in accordance with References (1) and (19). The equations in the programs are denoted with the equation number from the appropriate Reference. For all performance characteristics, it has been assumed standard day unless otherwise noted. Additionally, all results were generated for the clean configuration, with the obvious exceptions being the takeoff and landing phases of flight.

A. Takeoff and Landing

Because of the angle between the aft landing gear, the vertical stabilizers and the ground (see Figure 6), it is necessary to limit aircraft rotation to no more than 18 degrees. This angle of rotation is sufficient however, because the typical rotation on takeoff is approximately 10 degrees. References (1), (2) and (19) provided schematics and distance equations necessary for takeoff and landing. Takeoff and landing schematics are shown in Figures 13 and 14, and

are reproduced from Reference (1). Takeoff and landing distances are shown in Tables 7 and 8.
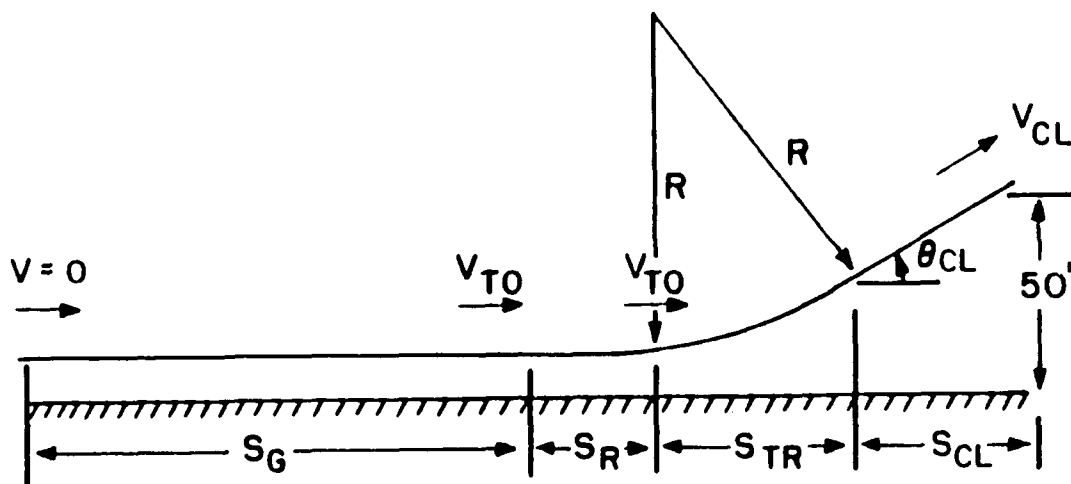
Figure 13.   Takeoff Schematic [Ref. 1]

TABLE 7.   TAKEOFF DISTANCES

Takeoff Distances	Standard Day	Hot Day (90°F)
S_G (ft)	1390	1378
S_R (ft)	555	555
S_{TR} to 50′ (ft)	888	888
$S_{TO\ total}$ (ft)	2833	2821
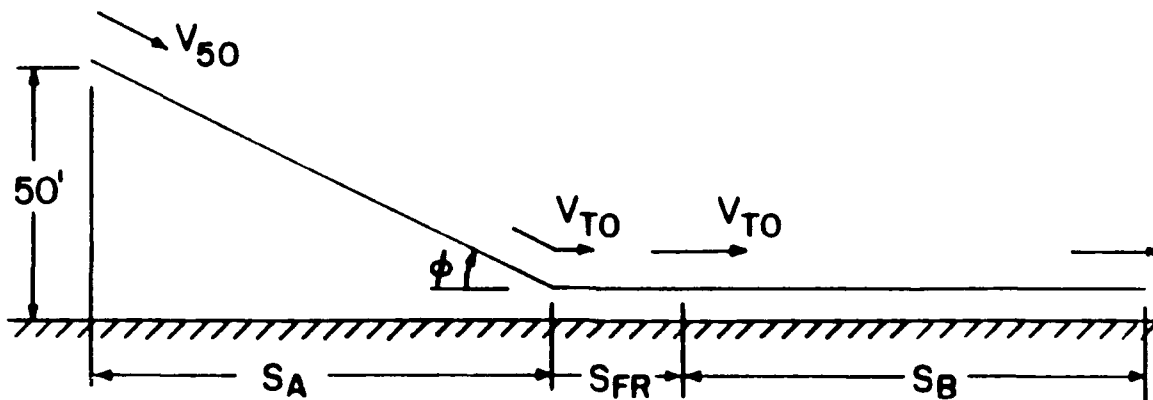
Figure 14.   Landing Schematic [Ref. 1]

TABLE 8.   LANDING DISTANCES

Landing Distances	Standard Day	Hot Day (90°F)
S_A to 50'(ft)	1354	1350
S_{FR} (ft)	155	165
S_B (ft)	1982	2317
$S_{L\,total}$ (ft)	3491	3832

B.   Thrust Required

The thrust required for the AEW aircraft at three altitudes between sea level and 35,000 feet are shown in Figure 15. The calculated thrust required curves were used to generate other performance characteristics such as power required and rate of climb.

40
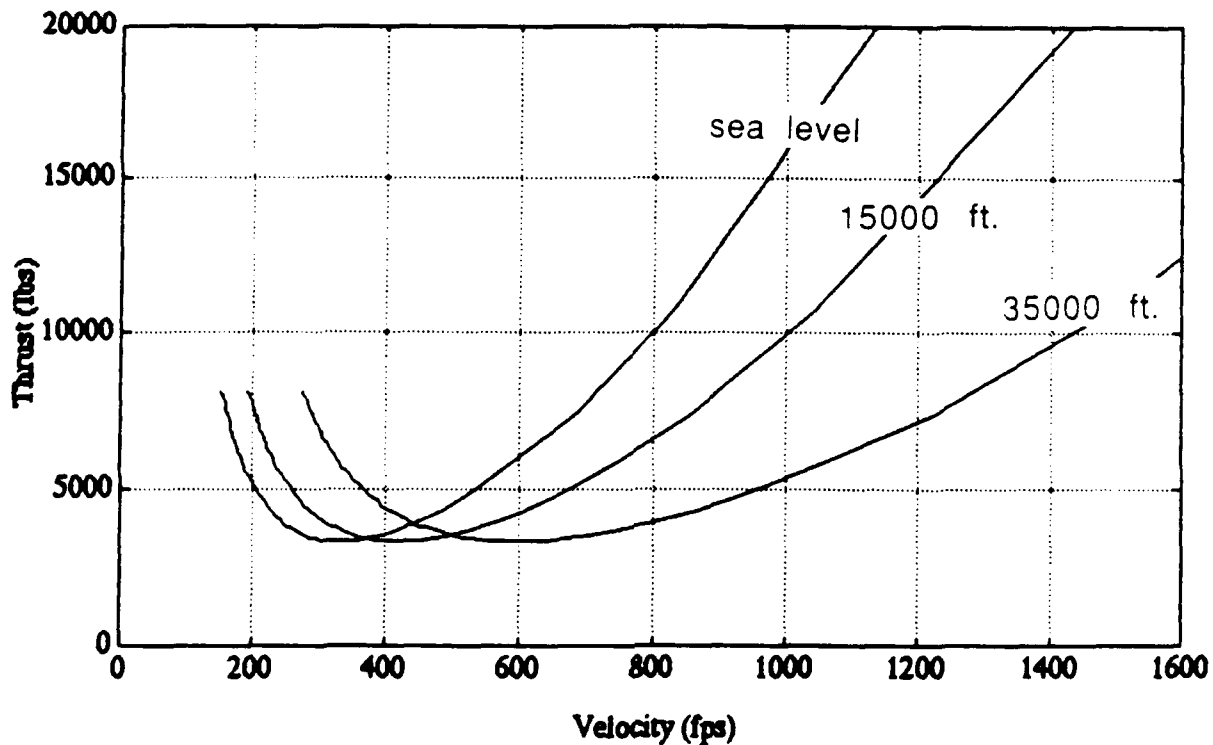
Figure 15. AEW Thrust Required

C.   Power Required and Power Available

AEW Power Required and Power Available Curves at sea level, 15000 ft. and 35000 ft are shown in Figures 16, 17 and 18. Note that two power available lines are shown on each graph. The solid line represents the power available predicted by simple theory. The dashed line is a result of the ONX/OFFX computer program obtained from Reference (7), and is thought to represent a more realistic power available curve. It is clear that the two theoretical predictions agree only until approximately M=0.4. With increase in speed, the difference between simple theory and ONX/OFFX becomes quite

41

significant. This is important because power available directly relates to excess

power which in turn is instrumental in defining other performance characteristics

such as rate of climb and maximum Mach number in level flight. Note also that

the power required due to drag divergence is not included in this analysis.
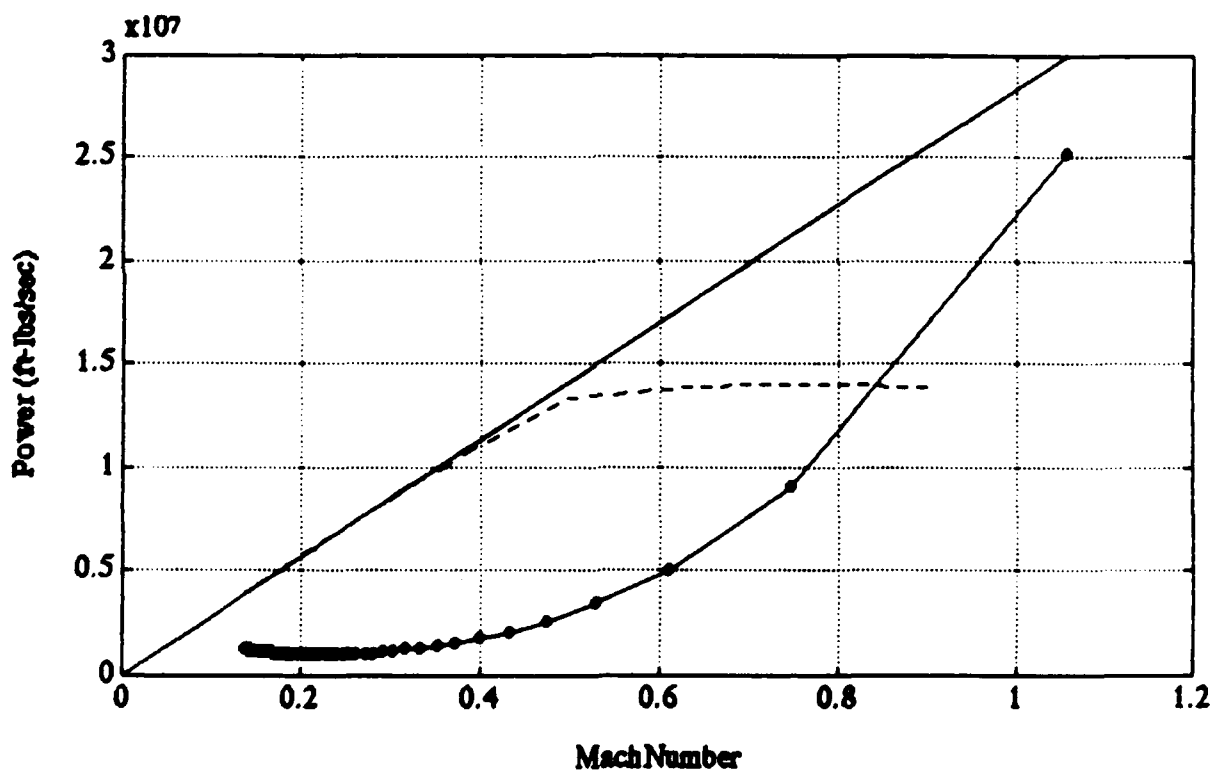
Figure 16.   Power Available and Power Required at Sea Level
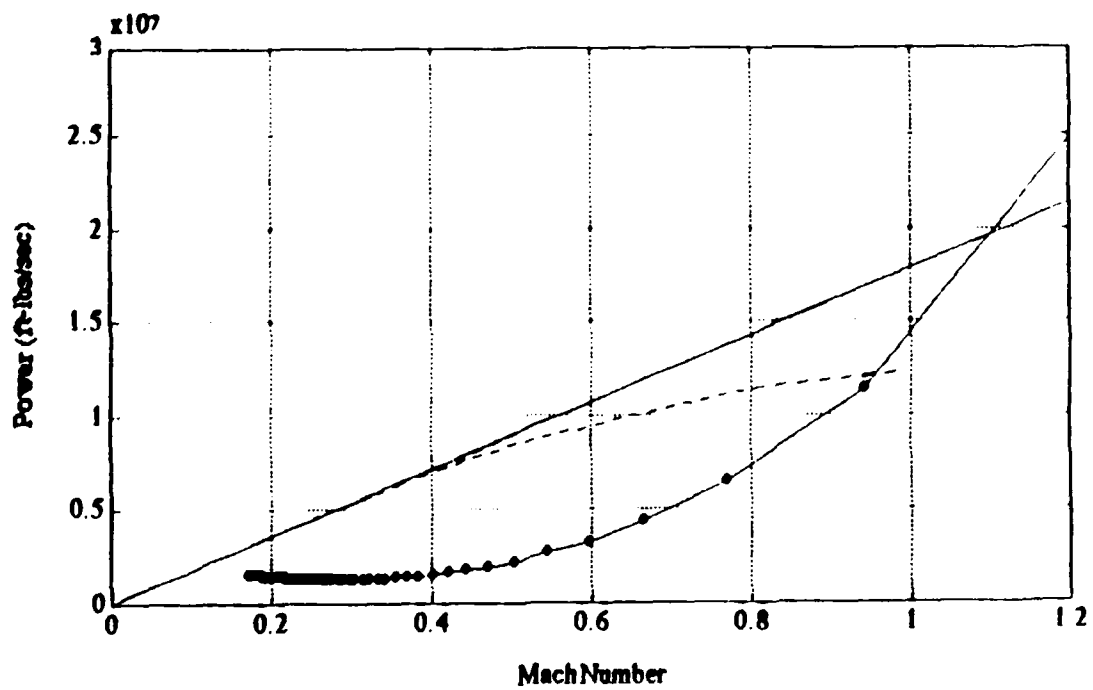
Figure 17. Power Available and Power Required at 15000 Feet
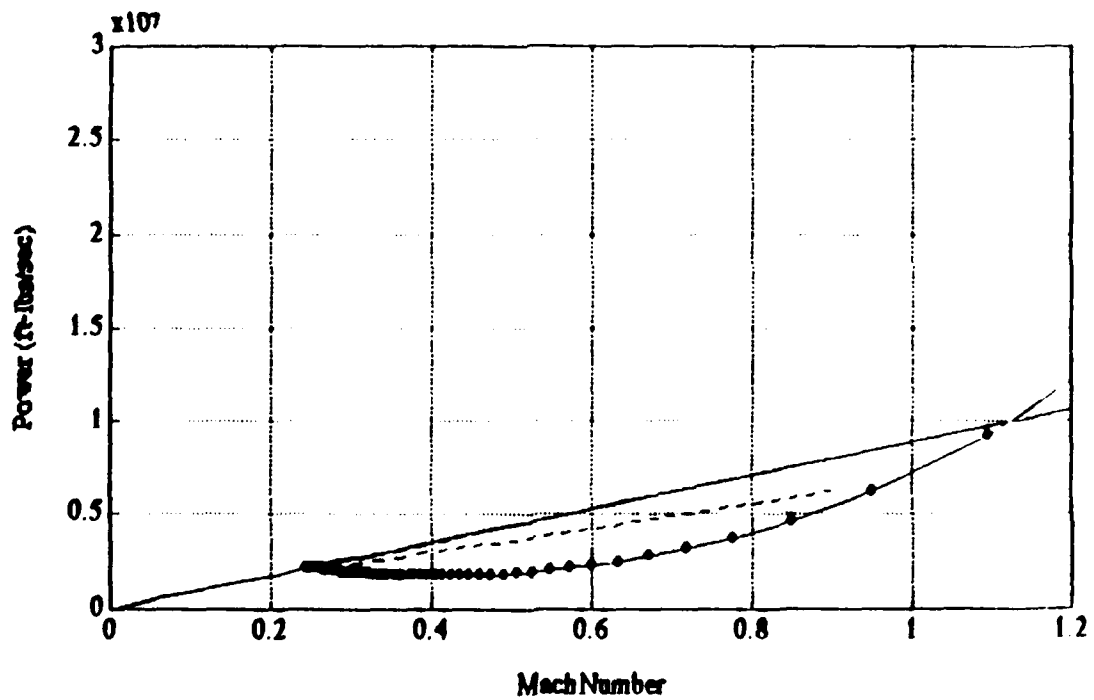
Figure 18. Power Available and Power Required at 35000 Feet

43

D. Climb Performance

AEW Rate of Climb at sea level and 15000 feet is shown in Figure 19. Rate of Climb plots were generated at various altitudes until a service ceiling (rate of climb < 100 fpm) was found. A plot of the climb rates vs. altitude is presented in Figure 20. It was determined the AEW aircraft will have a service ceiling of approximately 38260 ft. Although a service ceiling was not specified in the Proposed RFP, this ceiling is sufficient to perform the AEW mission. It is approximately 1660 feet higher than the service ceiling of the E-2C. Also note that the AEW aircraft has an absolute ceiling of 38600 feet.
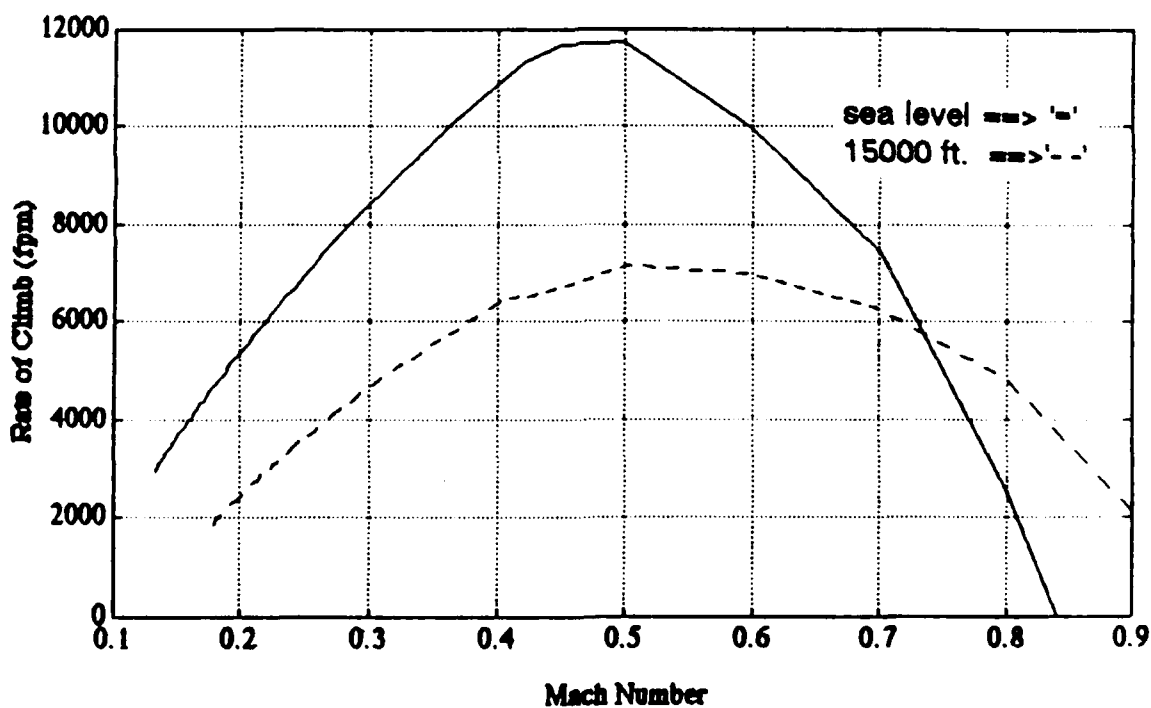
Figure 19. AEW Climb Performance at Sea Level and 15000 Feet
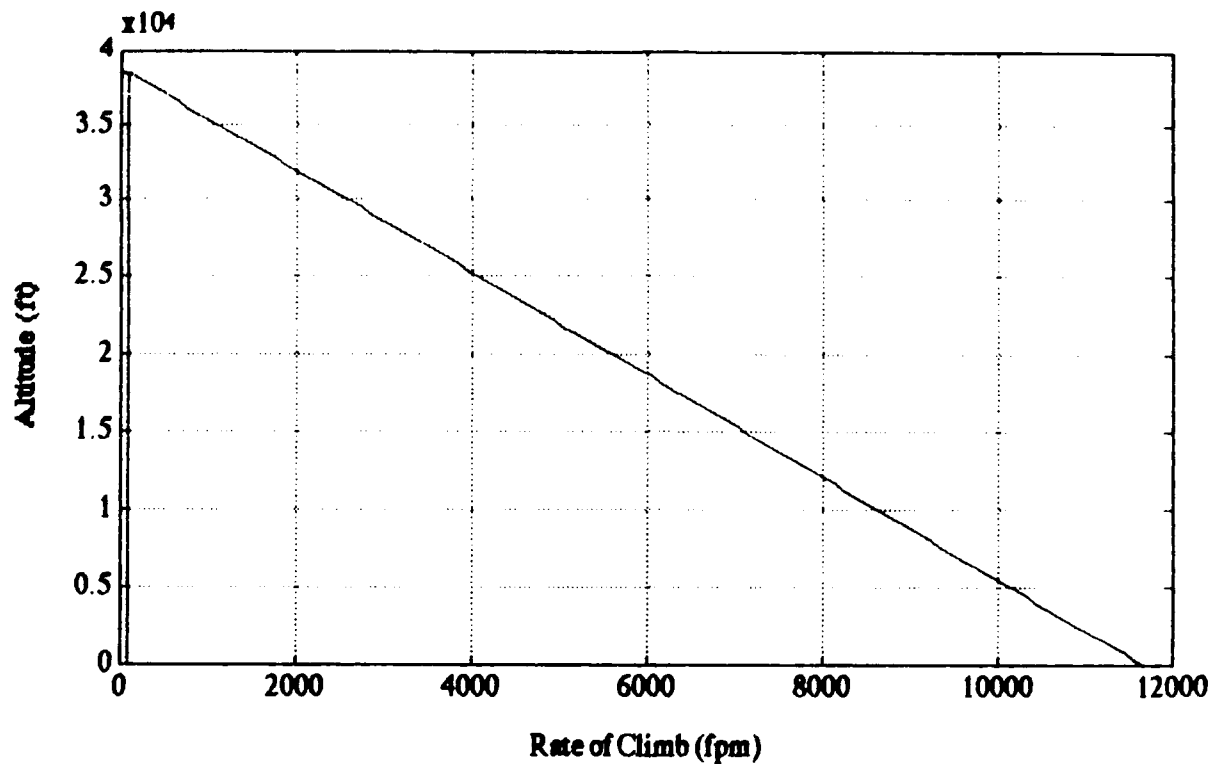
Figure 20. Absolute and Service Ceiling Determination

E. Range and Endurance

Range and Endurance predictions are shown in Figures 21 and 22 respectively. Both predictions are made using the Breguet equations obtained from Reference (19). The Range and Endurance plots are shown with variation in velocity at 35000 ft.

45
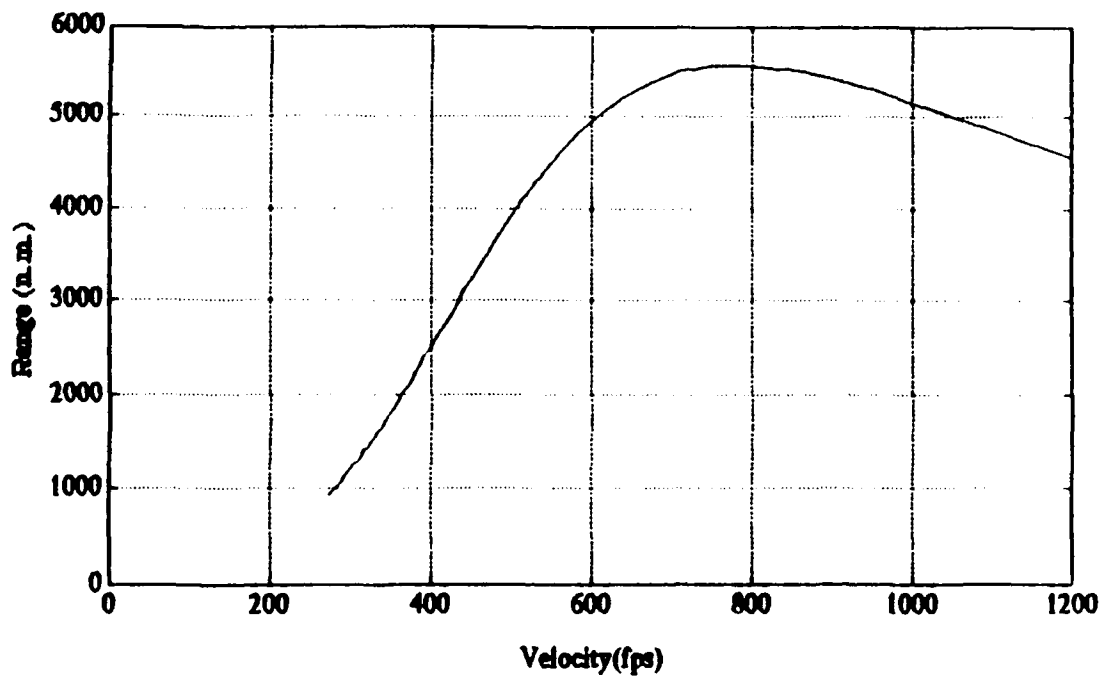
Figure 21.   AEW Range at 35000 Feet
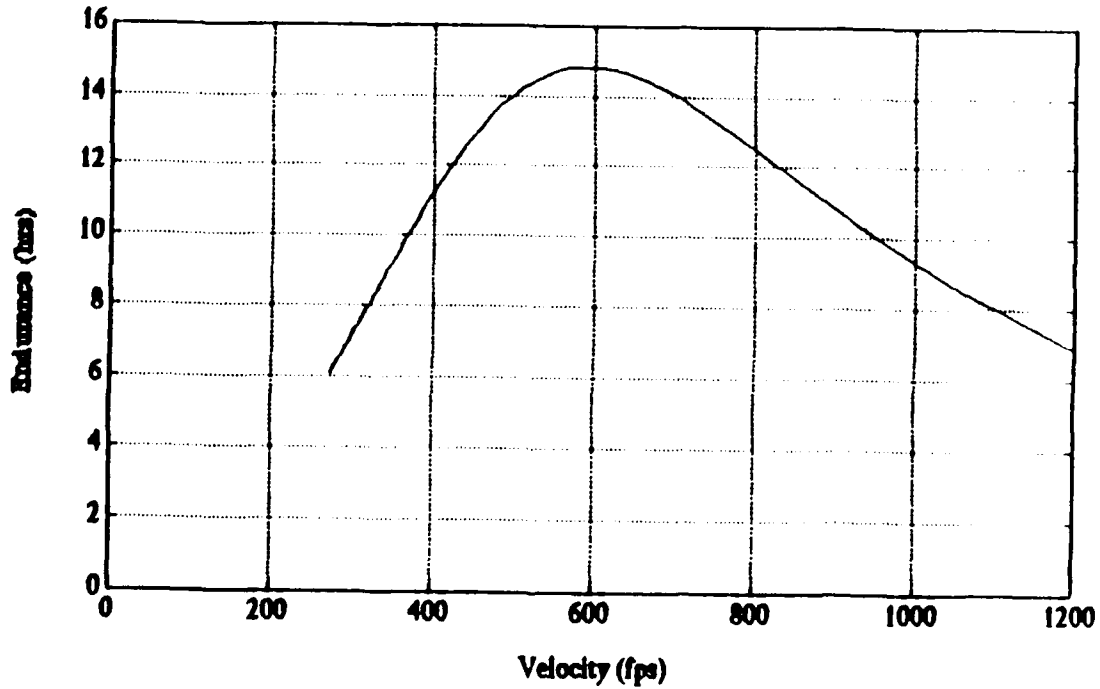
Figure 22.   AEW Endurance at 35000 Feet

46

F. ACCURACY OF PERFORMANCE ANALYSIS

As with any analysis, it is important to examine the results of the performance analysis based on past experience and on historical trends of similar aircraft. In other words, "Are the results of this analysis reasonable?"

Based on historical trends of aircraft performance, it is clear that the climb performance (Figure 19) is far too optimistic. Based on the described design of the AEW aircraft, it is very unlikely that it would be capable of climbing at nearly 12000 fpm at sea level. One possible explanation for this performance is too large a T/W ratio. It is unlikely however, that this is a significant part of the problem. According to this analysis, even if the AEW aircraft's T/W ratio was half the current ratio of 0.46, the aircraft would still climb at sea level at 6000 fpm. This is clearly unreasonable. Two other possible explanations of the optimistic climb performance are immediately apparent. First, the predicted CDo of may be far too optimistic. The CDo analysis does not account for interference drag. As a result, the actual CDo is usually higher than the predicted value. This difference might be significant on the AEW aircraft which probably has substantial interference drag. It should be noted that the CDo of the E-2C is 0.0375 which is far higher than the predicted AEW CDo of 0.0205. Second, the actual lifting efficiency may be lower than the preliminary estimation. A more accurate analysis of the aircraft's aerodynamic characteristics will be possible only after Computational Fluid Dynamics (CFD) analyses, or wind tunnel tests are performed.

The results of the Range and Endurance analyses (Figure 21 and 22) are also unreasonably optimistic. Because both the fuel capacity (14000 lbs.) and the TSFC (0.33) are reasonable, it is likely that the aforementioned explanations would account for the unrealistic range and endurance results.

VI. STABILITY AND CONTROL

In order to understand what the handling qualities of the AEW aircraft might be, a stability and control analysis of the aircraft is necessary. The purpose of this chapter is to provide a conceptual analysis of the stability and control characteristics of the aircraft. It is important to note that this analysis is a very rough approximation. Some of the parameters are the result of design approximations presented in previous chapters. Other parameters are impossible to predict accurately without the use of wind tunnel testing. In these cases, the value of the parameter was selected based on similar existing aircraft and past experience.

The analysis was performed at three mission-relatable flight conditions. The flight conditions are: 1) M= 0.2 at sea level, 2) M = 0.48 at 35000 feet and 3) M = 0.76 at 35000 feet.

A. STABILITY AND CONTROL DERIVATIVES

The stability and control derivative analysis was performed in accordance with References (8), (18) and (20). A stability and control computer program was written in MATLAB and is included as Appendix I. The analysis assumes no aeroelastic effects of the aircraft. All derivatives have the units of rad^{-1}. Finally, any effects of thrust have been neglected in this analysis. The stability

and control derivatives for the AEW aircraft are show.: in Table 9, along with an E-2C comparison at M=0.4 and 30000 feet.

B. DYNAMIC ANALYSIS

The dynamic analysis was performed in accordance with Reference (20). A dynamic modes computer program was written in MATLAB and is included as Appendix J. The analysis assumes small perturbation, linear theory. Results for the Short Period and Phugoid (or Long Period) modes are approximated to second-order systems. Any effects of thrust have been neglected in this analysis. The dynamic modes for the AEW aircraft are shown in Table 10.

The short period natural frequency (Wn) and damping ratio (Z) are approximated in Reference (20) as:

$$Wn = \sqrt{((Z_\alpha {}^* Mq)/u_o) - M_\alpha}) \tag{1}$$

$$Z = -(Mq + M(\alpha \text{ dot}) + Z_\alpha/u_o)/(2^*Wn) \tag{2}$$

A representative example of the dynamic modes is graphically presented in Figure 23. The figure shows the short period mode at the three flight conditions. All three primary modes have similar characteristics. They are all relatively lightly damped with very long periods and small amplitudes.

50

TABLE 9.   AEW STABILITY AND CONTROL DERIVATIVES

DERIVATIVE	M=0.2 at S.L.	M=0.48 at 35K	M=0.76 at 35K	E-2C Comparison
CL_α	4.8220	5.1700	6.2500	6.970
Cm_α	-1.1814	-1.2666	-1.5312	-0.450
$CL(\alpha\ dot)$	1.1172	1.2475	1.6497	6.160
$Cm(\alpha\ dot)$	-2.3556	-2.6304	-3.4785	-8.300
Clq	5.8328	6.6205	9.1761	11.43
Cmq	-7.8521	-8.7682	-11.5949	-21.27
Clß	-0.1279	-0.1307	-0.1273	-0.0915
Cnß	0.0576	0.0571	0.0560	0.0763
Cyß	-0.5877	-0.5877	-0.5877	-0.9680
Cl(ß dot) (1.0e-03*)	-0.4781	0.0553	0.7729	Not Avail.
Cn(ß dot)	-0.0025	0.0002	0.0020	0.0220
Cy(ß dot)	-0.0065	0.0005	0.0056	-.0601
Clp	-2.4765	-2.5993	-2.8140	-0.4200
Cnp	0.1319	0.0764	0.0291	-0.0732
Cyp	0.0023	-0.0235	-0.0406	0.1119
Clr	0.4717	0.3620	0.2667	0.2580
Cnr	-0.0855	-0.0848	-0.0833	-0.1236
Cyr	0.2470	0.2459	0.2437	0.3180
Cl δa	0.5429	0.5361	0.5226	0.0697
Cn δa	-0.0775	-0.0447	-0.0174	-0.00593
Cy δa	0	0	0	Not Avail.
Cl δe	0.2968	0.3314	0.4383	0.644
Cm δe	-0.6258	-0.6988	-0.9241	-1.670
Cl δr	-0.0024	0.0267	0.0609	-0.0381
Cn δr	-0.2509	-0.2789	-0.3655	-0.2202
Cy δr	0.7426	0.8292	1.0965	0.5760

TABLE 10. AEW DYNAMIC CHARACTERISTICS

DYNAMIC MODE	M=0.2 at S.L.	M=0.48 at 35K	M=0.76 at 35K
Short Period			
-Roots	-0.0177± 0.0521i	-0.0061± 0.0304i	-0.0078± 0.0334i
$-Wn_1$	0.0550	0.0310	0.0342
$-Z_2$	0.3221	0.1950	0.2273
$-Wd_3$	0.521	0.0304	0.0334
-Period (sec)	121	206	188
Long Period			
-Roots	-0.0004± 0.0039i	1.0e-03 * -0.0314± 0.7165i	1.0e-03 * -0.0111± 0.2859i
$-Wn_1$	0.0040	0.0007	0.0003
$-Z_2$	0.0930	0.0438	0.0389
$-Wd_3$	0.0039	0.0007	0.0003
-Period (sec)	1595	8770	2198
Dutch Roll			
-Roots	-0.0162± 0.1554i	-0.0062± 0.0890i	-0.0064± 0.0901i
$-Wn_1$	0.1562	0.0892	0.0903
$-Z_2$	0.1035	0.0698	0.0704
$-Wd_3$	0.1554	0.0890	0.0901
-Period (sec)	40	71	70
Roll Response			
-Root	-1.7652	-0.5727	-0.6194
Spiral Mode			
-Root	0.0004	0	0

Notes: 1-Natural Frequency
2-Damping Ratio
3-Damped Frequency
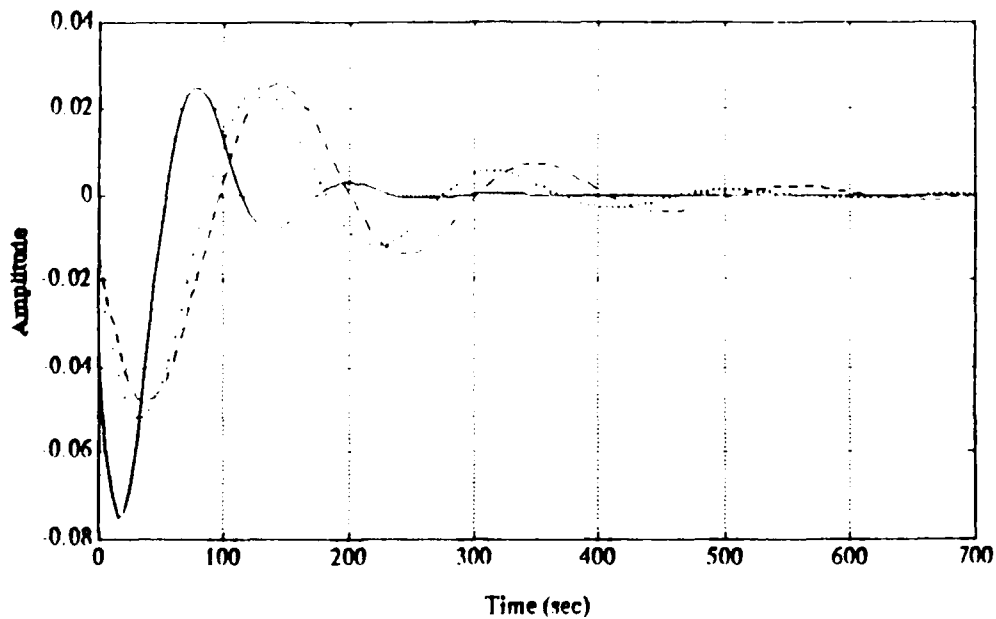
Figure 23. Short Period Response

C. ACCURACY OF STABILITY AND CONTROL ANALYSIS

One of the advantages of the dynamic analysis is that the final results (i.e., damping frequency and period) are directly relatable, and easily understandable, handling characteristics. The accuracy of these characteristics can be qualitatively evaluated based on historical trends and past experience. The accuracy of the dynamic characteristics are directly related to the accuracy of the stability and control derivatives, because the derivatives are used in the dynamic analysis.

The results of the dynamic analysis are clearly unreasonable. The most obvious discrepancy is in the periods of the three primary dynamic modes (short period, long period, and dutch roll). Short period and dutch roll periods for an aircraft of this kind typically range from 2 to 8 seconds. Obviously, values

53

ranging between 40 and 206 seconds are unreasonably large. The long period values between 1595 and 8770 seconds are also unreasonably large. Long period values for an aircraft of this kind are typically about 120 seconds. Also note the very lightly damped frequencies of all three primary dynamic modes. It is unreasonable that these modes would be so lightly damped, and is inconsistent with historical trends.

Many of the stability and control derivatives appear unreasonable as compared with the E-2C. The most unrealistic AEW derivatives include Cm_α, $CL_{(\alpha \; dot)}$, $Cm_{(\alpha \; dot)}$, Cmq, and Clp. This would naturally cause unreasonable dynamic results. The short period approximation equations are shown on page 50. Since Cm_α and Cmq are inaccurate, this will result in an unrealistic natural frequency. Also, since $Cm_{(\alpha \; dot)}$ and natural frequency are inaccurate, this causes an unrealistic damping ratio. Poor initial assumptions are the most likely cause of the unrealistic derivatives. Some inputs were impossible to accurately predict within the scope of this research. Such inputs include the downwash gradient at the horizontal tail, Cmo, and the moments of inertia. One primary conclusion can be drawn from this analysis. Although the method for attaining stability and control derivatives in Reference (18) is extremely detailed, truly accurate stability and control derivatives can only be acquired from wind tunnel tests on a scaled model. Because most of the unrealistic derivatives are longitudinally related, any follow-on research should include a thorough re-examination of the longitudinal analysis.

VII. CONCLUSIONS

A. ACCURACY

Because this thesis presents the results of a conceptual design, the aircraft's characteristics are by their very nature, a first iteration only. Future studies of the AEW aircraft must necessarily include wind tunnel tests of a scaled model. Reasonably accurate values of many of the aircraft's parameters can only be obtained through wind tunnel tests.

One of the genuine benefits of this research was the many computer programs that were generated. As the design process for this (or any other) aircraft continues, these programs can be used to obtain more accurate results through the input of more accurate parameters.

B. EXISTING ROTODOME/AVIONICS

Before the design of this aircraft proceeds beyond the preliminary design stage, consideration must be given to the use of new airborne detection technologies. Based on historical trends, it is likely that the integration of the E-2C's detection system into a new airframe will be difficult. The result would be an increase in both developmental and life cycle costs. Although new detection technologies such as a phased-array radar may be costly to develop, the benefits and the life cycle costs must be investigated.

C. SUPERCRITICAL AIRFOIL

Use of supercritical airfoils on aircraft is a relatively new technology that should be explored further. The airfoil appears to be ideally suited for aircraft that must operate in the transonic regime, and display aggressive endurance characteristics.

D. POSSIBLE PROBLEM AREAS

1. Escape System

Within the scope of this design effort, no satisfactory ejection system could be determined. The obvious hinderance to a viable ejection system is use of the existing rotodome antenna. Difficulties in developing a viable ejection system will most likely occur, regardless of the system, as long as a conventional rotodome antenna is used. A conventional early warning phased-array radar system for example, would be approximately the same size as the current antenna. The difficulties in ejection therefore, would be similar. Ejection of the aircrew would be much more successful with an antenna that is not in the form of a rotodome but within the wings and body of the aircraft. This would necessitate the use of a phased-array radar system, and therefore, would be costlier to develop. Before a formal AEW RFP is developed, a clear decision will have to be made on the aircrew escape system issue, and the resulting impact on the radar system.

2. Divergent Drag Mach Number (M_{dd})

Although the wing M_{dd} of 0.81 is high enough to operate in the required regime, future studies should include an analysis of the drag penalties of other aircraft parts in this transonic range. Emphasis should be placed on the fuselage and the rotodome antenna. The relatively wide fuselage and blunt nose may cause significant drag penalties at the target high-speed dash Mach number of 0.78. With a thickness ratio of 0.3, the rotodome antenna is also likely to have a M_{dd} far below the required operating range. It may, of course, require transonic wind tunnel tests to verify how significant these drag penalties are.

3. Horizontal Tail Effectiveness

It can be seen from Figure 6, that the horizontal tail is directly behind the wing and rotodome support pylon. The aerodynamic disturbance created by the wing and pylon could result in the loss of horizontal tail effectiveness under some flight conditions. This can only be verified however with wind tunnel tests of a scaled model, or by a CFD analysis.

4. Wingfold System

Another area of difficulty could be in the wingfold system. Because a double-wingfold system is new technology, developmental costs may be high. The double-wingfold will be an engineering challenge to both the structures and the flight control design teams. It should be pointed out that if an aircraft design employs a phased-array radar system with a non-conventional antenna

such as the one previously mentioned. the need for a double-wingfold system might be eliminated.

E. RECOMMENDATIONS

Within the scope of this research, the design of an AEW aircraft using the existing rotodome and avionics should be abandoned. Use of the rotodome will negatively affect the aircraft's normal and emergency operations. Considering all factors involved, it is unlikely there will be substantial savings using the existing rotodome and avionics.

Future aircraft designs should include integration of a phased-array radar system. This system offers the flexibility needed for an aircraft required to possess ejection and wingfold systems. Reference (21) provides an example of such a design. The aircraft, called the Boeing EX, is shown in Figure 24. A comparative analysis of the Boeing EX and the AEW aircraft is provided in Table 11. It is clear from the Figure 24, that the phased-array radar system allows for more flexibility in the design process, and eliminates the aforementioned ejection and wingfold problems.

Gross weight = 55.200 lbs
Operating weight = 35.380 lbs
Overall length = 51 ft-2 in
Overall height = 18 ft-6 in
Wing span = 63 ft-4 in (29 ft-1 in folded)
Wing area = 845 sq ft
Spot factor = 1.34 (F-18 reference)
TF34-400 Engines (SLST = 9,275 lbs each)
T700-GE-401 turboshaft engine for radar power
(1690 eshp)
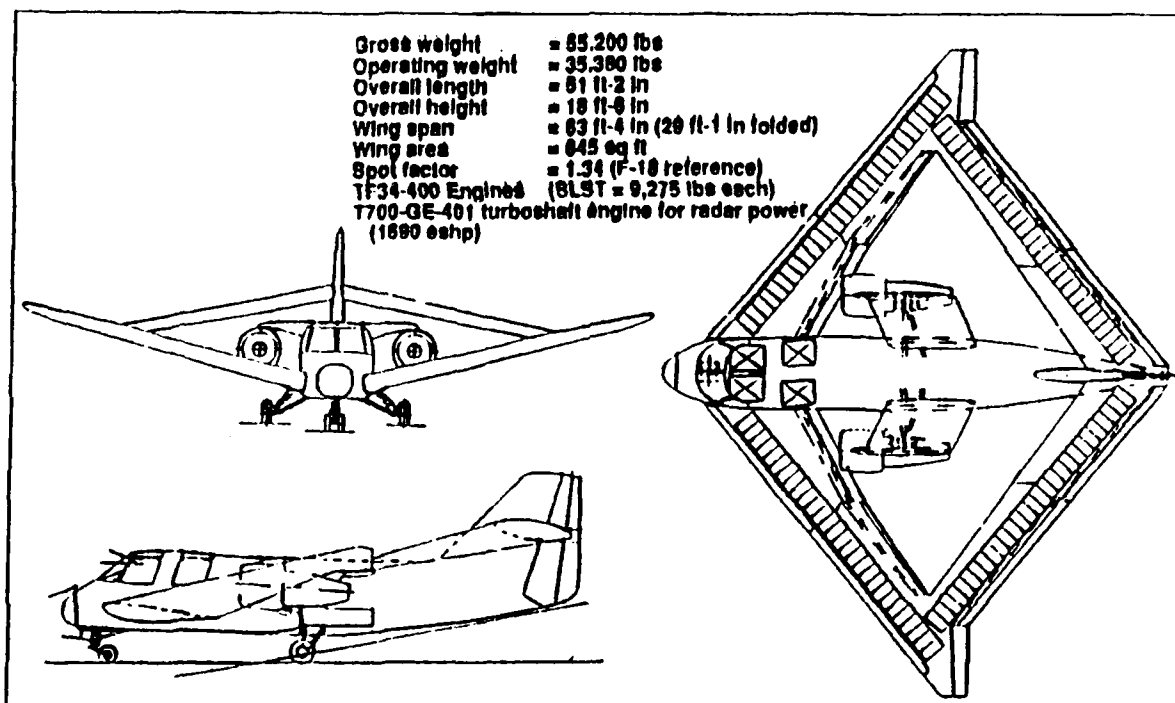
Figure 24.   Boeing EX [Ref. 21]

TABLE 11.   AIRCRAFT COMPARISON

CHARACTERISTIC	BOEING EX	AEW AIRCRAFT
Overall Length	51.2 ft.	55.0 ft.
Wing Span	63.3 ft.	72.0 ft.
Wing Area	845 sq.ft.	639 sq. ft.
Design Mach	0.76	0.78
Takeoff Weight	55200 lbs.	53000 lbs
T/W	0.34	0.46
Antenna	Mounted in Wings	Existing Rotodome
Ejection Capability	Yes	No

59

In conclusion, it must again be emphasized that this analysis was the first iteration on a conceptual design only. Therefore, the scope of the research was limited. A more complete analysis is only possible after an entire design team is assembled.

APPENDIX   A

AEW AIRCRAFT DESIGN
NAVAL POSTGRADUATE SCHOOL   .

PROJECT OBJECTIVES

The object of this design study is to perform the necessary trade
studies required to define the most cost effective, low risk
airframe configuration capable of meeting future airborne early
warning (AEW) requirements in the 21st century. The mission is a
deck-launched high speed dash, low speed loiter at 20,000 to 35,000
feet altitude and return. The goal is to select the greatest high
speed dash Mach number consistent with the maximum range and loiter
requirements that will provide a carrier suitable aircraft. The
aircraft will have ejection capability provisions for all members
of the four to six member aircrew. A fanjet (no turboprops) power-
plant will provide aircraft propulsion. The EX configuration must
exhibit low initial purchase cost and low life-cycle cost.

MISSION DEFINITION

DECK LAUNCHED SURVEILLANCE: The total mission cycle time (quadruple cycle) is desired to be at least 7 hours 30 minutes (with one re-fueling) plus reserves with a minimum acceptable cycle time (triple cycle) of 5 hours 45 minutes (no refueling) plus reserves.

1. For taxi, warmup, takeoff and acceleration to M=0.3; fuel allowance at sea level static thrust is equal to 5 minutes at intermediate thrust (no afterburner).

2. Acceleration: Maximum power acceleration from M=0.3 to best rate of climb speed at sea level.

3. Climb: Best rate of climb to optimum cruise altitude for design cruise Mach number.

4. Cruise: Cruise-out (high speed dash at M=0.7-0.85) at design Mach number at optimum cruise altitude.

5. Turn: 3g sustained desired; 2g sustained minimum at the weight corresponding to the end of cruise-out.

6. Loiter: Conduct surveillance at maximum endurance flight condition for minimum of 4 hours 30 minutes (200 nm station, no refueling).

7. Descent: Descend to best return cruise altitude (no time, distance or fuel used allowances).

8. Cruise-back at optimum altitude and best cruise Mach number.

9. Descent: Descend to sea level (no time, distance or fuel used allowances).

10. Land.

11. Reserves: Fuel allowance equal to 20 minutes loiter at sea level at speed for maximum endurance plus 5% of initial total fuel.

DESIGN CRITERIA

WEIGHT: The maximum takeoff gross weight will be 60,000 lb$_f$.

CREW: The aircraft will have an aircrew of from four to six members, including a single pilot. A weight allowance of 230 lb$_f$ is required for crew members and his/her equipment.

AVIONICS: Design an optimal configuration of flat panel displays for tactical cockpit operation. Nominal display sizes for consideration are 6x8, 8x8, 13x13, 3x5, 6x6 and 4x4. Determine any other feasible sizes. Architecture for the operation of the displays should not be of concern. Recommend (trade study result) the best possible combination of displays based on the need for the pilot to control the aircraft during takeoff, landing and on-station flight; consider also the best display combinations based on viewing and interactions with tactical displays.

Data/graphics displayed on a panel of any given size should be interchangeable with any other panel of the same size. Consideration must be given to supportability (e.g. availability of display sizes in other aircraft communities) and to minimizing clutter. Recommend screen formats for the transfer of as many discrete functions and indicators as possible to flat panel displays. Use the existing 24 foot rotodome.

SELF DEFENSE: Presume that a future missile would be the size of a compressed carriage AIM-7 Sparrow and would weigh 500 lb$_f$. Two missiles are required. A chaff and flare launcher is required. Provide two wet wing stations.

LOAD FACTOR: 3g sustained is desired; 2g sustained minimum at the weight corresponding to the end of cruise-out.

CARRIER SUITABILITY: Compatibility with CVN-68 carriers and subsequent implies the following criteria:

1. MK-7 mod 3 arresting gear.
2. C13-1 catapults.
3. 130,000 lb$_f$ maximum elevator capacity (aircraft plus loading plus GFE).
4. 85x52 foot elevator dimensions.
5. 57 feet 8 inches minimum station "o" to JBD hinge for MK-7 JBD locations.
6. 18 feet 9 inches minimum from tailpipe to JBD hinge.

63

7. Maximum, unfolded span of 82 feet.
8. 22 foot maximum landing gear width.
9. 25 foot maximum hanger deck height except under VAST stations in the forward part of the hanger where the clearance is 17 feet 6 inches. The maximum folded height of the aircraft should not exceed 18.5 feet.

LAUNCH: Launch wind-over-deck (WOD) should not exceed zero knots operational. Operational is minimum plus 15 knots. Assume a 5 knot improvement on the C13-1 catapult.

ARREST: Arresting WOD should not exceed zero knots. Assume a 5 knot improvement on the MK-7 mod 3 arresting gear. Approach speed for WOD calculations is 1.05 times V approved.

WAVE-OFF: For multi-engine aircraft, a minimum wave-off rate of climb of 500 feet per minute, with one engine inoperative, shall be available.

POWER PLANT: Fan jets (perhaps, upgraded TF-34 engines). NO TURBOPROPS.

COCKPIT: High visibility cockpit is required for pattern work at ship.

IN-FLIGHT
REFUELING: The aircraft must have an in-flight refueling capability.

STRUCTURE: The airframe structure must accommodate DIRST.

SELF-DEFENSE
CAPABILITY: The EX aircraft must have a self-defense capability [derived from complete (survivability, vulnerability and susceptibility) studies].

GROWTH: The structure must be capable of considerable weight growth beyond the initial production configuration (at least 4,000 lb$_f$).

COST: Low purchase cost and low life-cycle cost is highly desirable. Assume a total buy of 50 aircraft.

GENERAL: Attention shall be given to quality, maintainability, manufacturability and concurrent engineering issues.

64

APPENDIX B

```
%This is a constraint analysis program which is designed to plot various flight
%conditions as a function of thrust-to-weight ratio (Tsl/Wto) and wing loading
%(Wto/S).This program incorporates  different cases which corresponds to
%different flight conXditions. Each case will be seperated with a dashed line.
%this program is based on the material covered in chapter 2 of Mattingly's (et
%al) aircraft engine design book. All equations are from Mattingly unless
%specifically stated otherwise.
%------------------------------------------------------------------------
%Tsl/Wto will henceforth be known as TW. Wto/S will be known as WS.
%Operative equation.
%TW/WS=(B/a)*((q*S/(B*W))*(K1*(n*B*W/(q*S))^2+K2*(n*B*W/(q*S))+CDo+R/(q*S))+1/V*d
/dtX(h+V^2/(2*go))) (eqn. 2-11)
%A parabolic drag polar is assumed. Therefore K2=0 throughout.
%------------------------------------------------------------------------
%Case 1:Constant Alt./Speed Cruise. High Speed Dash @ M=0.78 & h=30K ft.
%dh/dt=dV/dt=0. Constant altitude & no acceleration.
n1=1;%normal g loading
R1=0;%Additional drag. Assumed zero throughout
K2=0;%Drag Curve constant
B1=0.905;%Weight Fraction
K11=0.06;%Drag Curve constant. Obtained from Nicolai page E-7.
P1=2116*.2360;%Pressure at 35K ft.
M1=0.78;%Mach Number
CDo1=.0345;%Drag coefficient at zero lift (approximate)
q1=(1.4/2)*P1*M1^2;%Dynamic Pressure
RR1=0.3106;%Density ratio at 30K ft.
a1=(0.568+0.25*(1.2-M1)^3)*RR1^0.6;%Installed full throttle thrust lapse for a
high bypass turbofan (eqn. 2-42)
T1=1;%counter
for WS1=20:5:140;%the range of wing loading
WS1M(T1)=WS1;
TW1(T1)=(B1/a1)*(K11*B1*WS1/q1+K2+CDo1/(B1*WS1/q1));%the resulting T/W ratio.
%eqn 2.12
T1=T1+1;%counter
end
WS1o=q1/B1*sqrt(CDo1/K11);%The minimum W/S for case 1.
TW1o=(B1/a1)*(K11*B1*WS1o/q1+K2+CDo1/(B1*WS1o/q1));%The minimum T/W for case 1
%------------------------------------------------------------------------
%Case 1e: Maximum Endurance @ 35K ft.
n1e=1;%normal g loading
B1e=0.8;%Weight Fraction
K11e=0.045;%Drag Curve constant.Obtained from Nicolai page E-7.
M1e=0.45;%Mach Number
q1e=(1.4/2)*P1*M1e^2;%Dynamic Pressure
a1e=(0.568+0.25*(1.2-M1e)^3)*RR1^0.6;%Installed full throttle thrust lapse for a
high bypass turbofan (eqn. 2-42)
T1=1;%counter
```

65

```
for WS1e=20:5:140;%the range of wing loading
WS1eM(T1)=WS1e;
TW1e(T1)=(B1e/a1e)*(K11e*B1e*WS1e/q1e+K2+CDo1/(B1e*WS1e/q1e));%the resulting T/W
ratio. eqn 2.12
T1=T1+1;%counter
end
WS1oe=q1e/B1e*sqrt(CDo1/K11e);%The minimum W/S for case 1e
TW1o=(B1e/a1e)*(K11e*B1e*WS1oe/q1e+K2+CDo1/(B1e*WS1oe/q1e));%The minimum T/W for
case 1e
%---------------------------------------------------------------------------
%Case 2:Constant Speed Climb. This is a "snapshot" of the climb only. Taken at
%an assumed TAS=330 fps, M=0.41, &15K ft. w/ an assumed dh/dt of 4000 fpm.
%dU/dt=0;
n2=1;%normal g loading
R2=0;%Additional drag. Assumed zero throughout
P2=0.5646*2116.2;%Pressure at 15K ft.
U=433;%Velocity
dhdt=67;%Rate of Climb (ft/s)
M2=0.41;%Mach Number
B2=0.975;%Weight Fraction
K12=0.05;%Drag Curve constant.Obtained from Nicolai page E-7.
q2=(1.4/2)*P2*M2^2;%Dynamic Pressure
CDo2=0.0345;%Drag coefficient at zero lift
RR2=0.6295;%Density ratio at 15K ft.
a2=(0.568+0.25*(1.2-M2)^3)*RR2^0.6;%Installed full throttle thrust lapse for a
high bypass turbofan (eqn. 2-42)
T2=1;%counter
for WS2=20:5:140;%the range of wing loading
WS2M(T2)=WS2;
TW2(T2)=(B2/a2)*(K12*B2*WS2/q2+K2+CDo2/(B2*WS2/q2)+1/U*dhdt);%the resulting T/W
ratio. eqn 2.14
T2=T2+1;%counter
end
WS2o=q2/B2*sqrt(CDo2/K12);%The minimum W/S for case 2
TW2o=(B2/a2)*(K12*B2*WS2o/q2+K2+CDo2/(B2*WS2o/q2)+1/U*dhdt);%The minimum T/W for
case 2
%---------------------------------------------------------------------------
%Case 3:Constant Alt./Speed Turn. Sustained g turn.
%dh/dt=dU/dt=0
n3=2;%normal g loading
R3=0;%Additional drag. Assumed zero throughout
P3=0.4599*2116.2;%Pressure at 20K ft.
B3=0.85;%Weight Fraction
K13=0.045;%Drag Curve constant. Obtained from Nicolai page E-7.
K2=0;%Drag Curve constant
M3=0.46;%Mach Number
CDo3=.0345;%Drag coefficient at zero lift
```

66

```
q3=(1.4/2)*P3*M3^2;%Dynamic Pressure
RR3=0.5332;%Density ratio at 20K ft.
a3=(0.568+0.25*(1.2-M3)^3)*RR3^0.6;%Installed full throttle thrust lapse for a
high bypass turbofan (eqn. 2-12)
T3=1;%counter
for WS3=20:5:140;%the range of wing loading
WS3M(T3)=WS3;
TW3(T3)=(B3/a3)*(K13*n3^2*B3*WS3/q3+K2*n3+CDo3/(B3*WS3/q3));%the resulting T/W
ratio. eqn 2.15
T3=T3+1;%counter
end
WS3o=q3/B3*sqrt(CDo3/K13);%The minimum W/S for case 3
TW3o=(B3/a3)*(K13*n3^2*B3*WS3o/q3+K2*n3+CDo3/(B3*WS3o/q3));%The minimum T/W for
case 3
%-----------------------------------------------------------------------
%Case 4:Horizontal Acceleration
%dh/dt=0;constant altitude
n4=1;%normal g loading
R4=0;%Additional drag. Assumed zero throughout
Vi=400;%Initial velocity.
Vf=776;%Final velocity.
dt=300;%Time for acceleration (in seconds)
P4=2116.4*0.2360;%Pressure at 35K ft.
dVdt=(Vf-Vi)/dt;%Acceleration
B4=0.85;%Weight Fraction
K14=.055;%Drag Curve constant. Obtained from Nicolai page E-7.
K2=0;%Drag Curve constant
M4=.58;%Mach Number.A "snapshot" in the middle of the run
CDo4=.0345;%Drag coefficient at zero lift
g=32.17;%Acceleration due to gravity (ft/sec)
q4=(1.4/2)*P4*M4^2;%Dynamic Pressure
RR4=.3106;%Density ratio at 35K ft.
a4=(0.568+0.25*(1.2-M4)^3)*RR4^0.6;%Installed full throttle thrust lapse for a
high bypass turbofan (eqn. 2-12)
Z=1/g*dVdt;
T4=1;%counter
for WS4=20:5:140;%the range of wing loading
WS4M(T4)=WS4;
TW4(T4)=(B4/a4)*(K14*B4*WS4/q4+K2+CDo4/(B4*WS4/q4)+Z);%the resulting T/W ratio.
eqn. 2.18
T4=T4+1;%counter
end
%-----------------------------------------------------------------------
%Case 5: Takeoff Ground Roll
%dh/dt=0;
Sg=3000;%Ground roll takeoff distance
Rh5=.0023769;%Sea level density
```

67

```
Kto=1.2;%stall-to-takeoff velocity ratio
Clm=2.5;%Max lift coefficient for takeoff
B5=1;%Weight Fraction
M5=0;%Mach Number
RR5=1;%Density ratio at sea level
a5=(0.568+0.25*(1.2-M5)^3)*RR5^0.6;%Installed full throttle thrust lapse for a
high bypass turbofan (eqn. 2-42)
g=32.17;%Acceleration due to gravity (ft/sec)
T5=1;%counter
for WS5=20:5:140,%the range of wing loading
WS5M(T5)=WS5;
TW5A(T5)=((20.9*WS5)/(RR5*Clm))/(Sg-87*sqrt(WS5/(RR5*Clm)));%the resulting T/W
ratio. This is from Nicolai (eqn.6-3)!
T5=T5+1;%counter
end
%---------------------------------------------------------------
%Case 7:Landing Roll
%dhdt=0;
Clm=3.0;%Max lift coefficient for landing
Sl=5000;%Landing distance
RR=1;%Density ratio at sea level
TW8=0.2:.1:1.2;
WS8=(Sl-400)*RR*Clm/118;%From Nicolai (eqn. 6-5).Note it is independent of T/W.
for S=1:11,
WS8M(S)=WS8;
end
%---------------------------------------------------------------
%Case 9: Maintainability
MMFH=30;%Maintenance man hours per flight hour
T9=1;%counter
for WS9=20:5:140,%the range of wing loading
WS9M(T9)=WS9;
TW9(T9)=(MMFH/7.25716)-(0.196568/7.25716)*WS9;%the resulting T/W ratio.This is
%Newberry's equation for the fighter aircraft only.
TW9T(T9)=(MMFH/13.6383)-(0.1555/13.6383)*WS9;%the resulting T/W ratio. This is
%Newberry's equation using all25 aircraft. It was used because it is probably
%most realistic.
T9=T9+1;%counter
end
%---------------------------------------------------------------
plot(WS1M,TW1,WS1eM,TW1e,WS2M,TW2,'x',WS3M,TW3,'+',WS4M,TW4,'o',WS5M,TW5A,'*',WS8
M,TW8,'-',WS9M,TW9T,'-.')
```

APPENDIX C

```
%This is an ejection program with expressions from Hoerner's Fluid Dynamic Drag
book, Chapter 13.
%-----------------------------------------------------------------------
W=300;%weight of the seat and crew member
g=32.2;%acceleration due to gravity
M=.2;%Mach number
GAM=1.4;%gamma
P=2116;%*.8321;%pressure
q=(GAM/2)*P*M^2;%dynamic pressure.assumed constant
Dq=9;%drag area (varies between 4 and 9ft^2)
w=60;%approximate average vertical velocity
Q=1;%counter
for Y=0:14,
YM(Q)=Y;
T(Q)=Y/w;%time is equal to velocity divided by distance
T2(Q)=T(Q)^2;%time squared
X1(Q)=8+(g*q*T2(Q)*(Dq/W));%the front seat trajectory. eqn. 26, chap 13
X2(Q)=16+(g*q*T2(Q)*(Dq/W));%the back seat trajectory. eqn. 26, chap 13
Q=Q+1;%counter
end
%plot(X1',YM,'+',X2',YM,'+'),
%-----------------------------------------------------------------------
%this draws the rotodome antenna
Ru=[9.7413 10.929 9.7413];
Rl=[9.7413 9.7413 9.7413];
Rc=[9.7413 8.553 9.7413];
XD=[16 28 40];
plot(XD,Ru,XD,Rl,'-',XD,Rc,'-'),
```

APPENDIX   D

```
%-------------------------------------------------------------
%This weight program has two parts. The first is a subroutine which computes the
%weight of the propulsion and fuel systems. These figures are needed for the
%main program which iterates a takeoff weight.
%-------------------------------------------------------------
%Propulsion Subroutine
%-------------------------------------------------------------
%The below values are inputs that are required for the equations that have been
%obtained from "The Fundamentals of Aircraft Design" by Leland M. Nicolia
(Chapter 20)
AI=pi*2.375^2; %Inlet Area
NI=2; %Number of Inlets
Kgeo=1; %Duct Shape Factor
P2=24; %Max Static Pressure at Engine Compressor Face-psia
Kte=1; %Temperature Correction Factor
Km=1; %Duct Material Factor
Ld=3; %Subsonic Duct Length
Fgw=2154; %Total Wing Fuel In Gallons
Fgf=0; %Total Fuselage Fuel In Gallons
Lf=55; %Fuselage Length
Ne=2; %Number of Engines
B=72; %Wing Span
Weng=2000; %Weight of Engine
%-------------------------------------------------------------
%The equation numbers from Nicolai are included with the appropriate equations.
Wtfd=7.435*NI*(Ld*AI^.5*P2)^.731;%20-15
Wesc=41.6*((Fgw+Fgf)*10^(-2))^.818;%20-16
Wbsc=7.91*((Fgw+Fgf)*10^(-2))^.854;%20-18
Wlfr=13.64*((Fgw+Fgf)*10^(-2))^.392;%20-19
Wdd=7.38*((Fgw+Fgf)*10^(-2))^.458;%20-20
Wtp=28.38*((Fgw+Fgf)*10^(-2))^.442;%20-21
Wec=88.46*((Lf+B)*Ne*10^(-2))^.294;%20-23
Wss=9.33*(Ne*Weng*10^(-3))^1.078;%20-26
Wfs=Wesc+Wbsc+Wdd+Wtp+Wlfr,
Wpp=Wtfd+Wfs+Wec+Wss+(Weng*2),
%-------------------------------------------------------------
%Main Iteration Program
%-------------------------------------------------------------
%This program is designed to find the appropriate takeoff weight(Wto) where the
%equation is a polynomial with fraction exponents.The secant method is used to
%find the desired root.The operative equation (which is so designated below) is
%set up so that %the program will find Wto (a.k.a. X) when Y is equal to
%zero.The many equations that preceed the operative equation are portions of the
%final equation. They are seperate to make the operative equation more
%manageable.
%-------------------------------------------------------------
%The below values are inputs that are required for the equations that have been
```

```
%obtalned from "The Fundamentals of Aircraft Design" by Leland M. Nicolia
(Chapter 20)
N=4.5; %Ultimate Load Factor
toc=0.12; %Maximum Thickness Ratio
Lle=(21*pi/180); %Leading Edge Sweep
Ct=4; %Chord Length at Tip
Cr=13.75; %Chord Length at Root
l=Ct/Cr; %Taper Ratio
A=8.11; %Aspect Ratio
Sw=639; %Wing Area
Sht=180; %Horizontal Tail Planform Area
Bht=24; %Span of Horizontal Tail
tAht=0.86; %Thickness of Horizontal Tail at Root
Cmac=9.77; %MAC of the Wing
Lt=25; %Tail Moment Arm
HtHv=0; %Horizontal Tail Height to Vertical Tail Height Ratio
Svt=45; %Vertical Tail Area
M=.78; %Maximum Mach Number at Sea Level
Sr=22; %Rudder Area
Avt=1.111; %Aspect Ratio of Vertical Tail
lt=0.5; %Taper Ratio of Vertical Tail
Lvt=(30*pi/180); %Sweep of the Vertical Tail
q=800; %Maximum Dynamic Pressure
Lngth=55; %Fuselage Length
H=8; %Maximum Fuselage Heigth
Kinl=1; %Inlet Constant
Npll=2; %Number of Pilots
Ne=2; %Number of Engines
Wtron=10000; %Weight of Avionics
Ncr=4; %Number of Crew
Ksea=149.12; %Ejection Seat Constant
Wrad=3086; %Radome Weight
Wfuel=14000; %Total Fuel Weight
%----------------------------------------------------------------
%The equation numbers from Nicolai are included with the appropriate equations.
%The first loop is used to compute the first two values of Y after the two
%initial guesses for Wto (X) have been made. Two initial guesses are required
%for the secant method.
P=1;
for Wto=40000:10000:50000,%40K & 50K are the two initial guesses.
X(P)=Wto;
Ww=19.29*(1*N*Wto/toc*((tan(Lle)-(2*(1-l))/(A*(1+l)))^2+1)*10^(-6))^.464*((1+l)*A
)^.7*Sw^.58;%20-2
Yh=(Wto*N)^.813*Sht^.584*(Bht/tAht)^.033*(Cmac/Lt)^.28;%20-3a
Wht=.0034*Yh^.915;%20-3a
Yv=(1+HtHv)^.5*(Wto*N)^.363*Svt^1.089*M^.601*Lt^(-.726)*(1+Sr/Svt)^.217*Avt^.337*
(1+lt)^.363*(cos(Lvt))^(-.484);%20-3b
```

71

```
Wvt=2*0.19*Yv^1.014;%20-3b
Wf=11.03*(Klnl^1.23)*(q*10^(-2))^.245*(Wto*10^(-3))^.98*(Lngth/H)^.61;%20-5
Wlg=129.1*(Wto*10^(-3))^.66;%20-7
Whyd=23.77*(Wto*10^(-3))^1.10;%20-35
Wfl=Mpll*(15+.032*Wto*10^(-3));%20-39
Wel=We*(4.80+.006*Wto*10^(-3));%20-40
Wml=.15*(Wto*10^(-3));%20-42
Wes=346.98*((Wfs+Wtron)*10^(-3))^.509;%20-44
Wst=Ksea*Ncr^1.2;%20-50
Wox=16.89*Ncr^1.494;%20-51
Wac=201.66*((Wtron+200*Ncr)*10^(-3))^.735;%20-65
Wfc=1.08*(Wto)^.7;%this equation is from Roskam PartV
%The below equation is the operative equation.
Y(P)=(-Wto)+Ww+Wht+Wvt+Wf+Wlg+Whyd+Wfl+Wel+Wml+Wes+Wst+Wox+Wac+Wrad+Wfuel+Wtron+W
pp+Wfc;
P=P+1;
end
%This concludes the loop that computes the values of Y for the two initial
%guesses.
%-----------------------------------------------------------------------
%The second loop is designed to actually find the root.The loop allows for up to
%18 iterations.
for J=3:12,
X(J)=X(J-1)-Y(J-1)*((X(J-1)-X(J-2))/(Y(J-1)-Y(J-2)));%This is the secant method
%formula! It computes a value of X (Wto) from the previous two X's and their
%respective Y values. The rest of this loop just computes the new value of Y
%from the newly compuXted X. More information on the secant method can be found
%in any numerical methods book.
Wto=X(J);
Ww=19.29*(1*H*Wto/toc*(((tan(Lls)-(2*(1-l))/(A*(1+l)))^2+1)*10^(-6))^.464*((1+l)*A
)^.7*Sw^.58;%20-2
Yh=(Wto*H)^.813*Sht^.584*(Bht/tAht)^.033*(Cmac/Lt)^.28;%20-3a
Wht=.0034*Yh^.915;%20-3a
Yv=(1+HtHv)^.5*(Wto*H)^.363*Svt^1.089*H^.601*Lt^(-.726)*(1+Sr/Svt)^.217*Avt^.337*
(1+lt)^.363*(cos(Lvt))^(-.484);%20-3b
Wvt=2*0.19*Yv^1.014;%20-3b
Wf=11.03*(Klnl^1.23)*(q*10^(-2))^.245*(Wto*10^(-3))^.98*(Lngth/H)^.61;%20-5
Wlg=129.1*(Wto*10^(-3))^.66;%20-7
Whyd=23.77*(Wto*10^(-3))^1.10;%20-35
Wfl=Mpll*(15+.032*Wto*10^(-3));%20-39
Wel=We*(4.80+.006*Wto*10^(-3));%20-40
Wml=.15*(Wto*10^(-3));%20-42
Wes=346.98*((Wfs+Wtron)*10^(-3))^.509;%20-44
Wst=Ksea*Ncr^1.2;%20-50
Wox=16.89*Ncr^1.494;%20-51
Wac=201.66*((Wtron+200*Ncr)*10^(-3))^.735;%20-65
Wfc=1.08*(Wto)^.7;%this equation is from Roskam PartV
```

```
%The below equation is the operative equation whos root we are seeking.
Y(J)=(-Wto)+Ww+Wht+Wvt+Wf+Wlg+Whyd+Wfl+Wel+Wal+Wes+Wst+Wox+Wac+Wrad+Wfuel+Wtron+W
pp+Wfc;
end
disp(Wto),
%Wto= 5.1490e+04 lbs
```

APPENDIX   E

AEW1 XLS

GROUP		MOMENT ARM R
		IN FRONT OF THE
AIRFRAME		
		X̄ Arm
WING (OUT)	2250	34
WING (WET)	3580	30
HORIZONTAL TAIL	445	55.5
NACELLES	969	25.5
FUSELAGE	2757	29
VERT TAIL	269	58
FUEL		
WING	14000	30
BLADDER (M)	513	30
DUMPS AND DRAIN(M)	30	33
CELL BACKING (M)	109	30
TRANSFER PUMPS (M)	110	30
INFLIGHT REFUELING	45	15
ENGINES	4000	25.5
ENGINE CONTROLS	118	20
STARTING SYSTEMS	41	
HYD's		
LANDING GEAR (NOSE)	238	13
LANDING GEAR (MAIN)	1473	39
HYD SYSTEM	1762	30
FLIGHT CONTROL SYS.	2043	30
FLT INST	33	10
ENG INST	10	10
AIR COND	1159	31
OXY SYSTEM	134	15
ELECT SYSTEM	1165	35
MISC INST	7	10
APU	50	25
AVIONICS	10000	41
RADOME	3000	33
CHAFF/FLARE LAUNCH	300	33

74

SEATS	787	19
	=SUM(B5:B58)	
XCG FROM "5" FEET FORWARD OF NOSE		
	=D59/B59	
ZCG FROM "5 FT BELOW FUSELAGE		
	=F59/B59	
Ixx=	=L59	slugs/ft^2
Iyy=	=M59	slugs/ft^2
Izz=	=N59	slugs/ft^2
Ixy=	0	slugs/ft^2
Ixz=	=Q59	slugs/ft^2
Izy=	0	slugs/ft^2

X MOM	Z Arm	Z MOM	Y ARM		
=B5*C5	12	=B5*E5	23		
=B6*C6	12	=B6*E6	7.5		
=B7*C7	15	=B7*E7	4.56		
=B8*C8	10	=B8*E8	9.75		
=B9*C9	9	=B9*E9	0		
=B12*C12	13	=B12*E12	11		
=B16*C16	12	=B16*E16	7.5		
=B19*C19	12	=B19*E19	7.5		
=B21*C21	12	=B21*E21	6		
=B23*C23	12	=B23*E23	7.5		
=B25*C25	12	=B25*E25	7.5		
=B26*C26	10	=B26*E26	3.5		
=B27*C27	10	=B27*E27	9.75		
=B28*C28	10	=B28*E28	4.5		
=B36*C36	2.2	=B36*E36	0		
=B37*C37	2.2	=B37*E37	6		
=B38*C38	8	=B38*E38	0		
=B39*C39	8	=B39*E39	0		
=B41*C41	10	=B41*E41	0		
=B42*C42	10	=B42*E42	0		
=B43*C43	12	=B43*E43	0		
=B44*C44	7	=B44*E44	0		
=B46*C46	9	=B46*E46	0		
=B47*C47	11	=B47*E47	0		
=B48*C48	8	=B48*E48	0		
=B49*C49	10	=B49*E49	0		
=B50*C50	19	=B50*E50	0		
=B51*C51	8	=B51*E51	0		

AEW1.XLS

=B53*C53	9.5	=B53*E53	0	
=SUM(D5:D58)		=SUM(F5:F58)		

(XI-Xcg)^2	(YI-Ycg)^2	(ZI-Zcg)^2	Ixx	Iyy
=(C5-Xcg)^2	=(G5)^2	=(E5-Zcg)^2	=B5*(J5+K5)	=B5*(I5+K5)
=(C6-Xcg)^2	=(G6)^2	=(E6-Zcg)^2	=B6*(J6+K6)	=B6*(I6+K6)
=(C7-Xcg)^2	=(G7)^2	=(E7-Zcg)^2	=B7*(J7+K7)	=B7*(I7+K7)
=(C8-Xcg)^2	=(G8)^2	=(E8-Zcg)^2	=B8*(J8+K8)	=B8*(I8+K8)
=(C9-Xcg)^2	=(G9)^2	=(E9-Zcg)^2	=B9*(J9+K9)	=B9*(I9+K9)
=(C12-Xcg)^2	=(G12)^2	=(E12-Zcg)^2	=B12*(J12+K12)	=B12*(I12+K12)
=(C16-Xcg)^2	=(G16)^2	=(E16-Zcg)^2	=B16*(J16+K16)	=B16*(I16+K16)
=(C19-Xcg)^2	=(G19)^2	=(E19-Zcg)^2	=B19*(J19+K19)	=B19*(I19+K19)
=(C21-Xcg)^2	=(G21)^2	=(E21-Zcg)^2	=B21*(J21+K21)	=B21*(I21+K21)
=(C23-Xcg)^2	=(G23)^2	=(E23-Zcg)^2	=B23*(J23+K23)	=B23*(I23+K23)
=(C25-Xcg)^2	=(G25)^2	=(E25-Zcg)^2	=B25*(J25+K25)	=B25*(I25+K25)
=(C26-Xcg)^2	=(G26)^2	=(E26-Zcg)^2	=B26*(J26+K26)	=B26*(I26+K26)
=(C27-Xcg)^2	=(G27)^2	=(E27-Zcg)^2	=B27*(J27+K27)	=B27*(I27+K27)
=(C28-Xcg)^2	=(G28)^2	=(E28-Zcg)^2	=B28*(J28+K28)	=B28*(I28+K28)
=(C36-Xcg)^2	=(G36)^2	=(E36-Zcg)^2	=B36*(J36+K36)	=B36*(I36+K36)
=(C37-Xcg)^2	=(G37)^2	=(E37-Zcg)^2	=B37*(J37+K37)	=B37*(I37+K37)
=(C38-Xcg)^2	=(G38)^2	=(E38-Zcg)^2	=B38*(J38+K38)	=B38*(I38+K38)
=(C39-Xcg)^2	=(G39)^2	=(E39-Zcg)^2	=B39*(J39+K39)	=B39*(I39+K39)
=(C41-Xcg)^2	=(G41)^2	=(E41-Zcg)^2	=B41*(J41+K41)	=B41*(I41+K41)
=(C42-Xcg)^2	=(G42)^2	=(E42-Zcg)^2	=B42*(J42+K42)	=B42*(I42+K42)
=(C43-Xcg)^2	=(G43)^2	=(E43-Zcg)^2	=B43*(J43+K43)	=B43*(I43+K43)
=(C44-Xcg)^2	=(G44)^2	=(E44-Zcg)^2	=B44*(J44+K44)	=B44*(I44+K44)
=(C46-Xcg)^2	=(G46)^2	=(E46-Zcg)^2	=B46*(J46+K46)	=B46*(I46+K46)
=(C47-Xcg)^2	=(G47)^2	=(E47-Zcg)^2	=B47*(J47+K47)	=B47*(I47+K47)
=(C48-Xcg)^2	=(G48)^2	=(E48-Zcg)^2	=B48*(J48+K48)	=B48*(I48+K48)
=(C49-Xcg)^2	=(G49)^2	=(E49-Zcg)^2	=B49*(J49+K49)	=B49*(I49+K49)
=(C50-Xcg)^2	=(G50)^2	=(E50-Zcg)^2	=B50*(J50+K50)	=B50*(I50+K50)
=(C51-Xcg)^2	=(G51)^2	=(E51-Zcg)^2	=B51*(J51+K51)	=B51*(I51+K51)

AEW1.XLS

=(C53-Xcg)^2	=(G53)^2	=(E53-Zcg)^2	=B53*(J53+K53)	=B53*(I53+K53)
			=SUM(L5:L57)	=SUM(M5:M57)
			=L58/32.174	=M58/32.174

Izz	Ixy	Iyz	Izx
=B5*(I5+J5)	=0	=0	=B5*(C5-Xcg)*(E5-Zcg)
=B6*(I6+J6)	=0	=0	=B6*(C6-Xcg)*(E6-Zcg)
=B7*(I7+J7)	=0	=0	=B7*(C7-Xcg)*(E7-Zcg)
=B8*(I8+J8)	=0	=0	=B8*(C8-Xcg)*(E8-Zcg)
=B9*(I9+J9)	=0	=0	=B9*(C9-Xcg)*(E9-Zcg)
=B12*(I12+J12)	=0	=0	=B12*(C12-Xcg)*(E12-Zcg)
=B16*(I16+J16)	=0	=0	=B16*(C16-Xcg)*(E16-Zcg)
=B19*(I19+J19)	=0	=0	=B19*(C19-Xcg)*(E19-Zcg)
=B21*(I21+J21)	=0	=0	=B21*(C21-Xcg)*(E21-Zcg)
=B23*(I23+J23)	=0	=0	=B23*(C23-Xcg)*(E23-Zcg)
=B25*(I25+J25)	=0	=0	=B25*(C25-Xcg)*(E25-Zcg)
=B26*(I26+J26)	=0	=0	=B26*(C26-Xcg)*(E26-Zcg)
=B27*(I27+J27)	=0	=0	=B27*(C27-Xcg)*(E27-Zcg)
=B28*(I28+J28)	=0	=0	=B28*(C28-Xcg)*(E28-Zcg)
=B36*(I36+J36)	=0	=0	=B36*(C36-Xcg)*(E36-Zcg)
=B37*(I37+J37)	=0	=0	=B37*(C37-Xcg)*(E37-Zcg)
=B38*(I38+J38)	=0	=0	=B38*(C38-Xcg)*(E38-Zcg)
=B39*(I39+J39)	=0	=0	=B39*(C39-Xcg)*(E39-Zcg)
=B41*(I41+J41)	=0	=0	=B41*(C41-Xcg)*(E41-Zcg)
=B42*(I42+J42)	=0	=0	=B42*(C42-Xcg)*(E42-Zcg)
=B43*(I43+J43)	=0	=0	=B43*(C43-Xcg)*(E43-Zcg)
=B44*(I44+J44)	=0	=0	=B44*(C44-Xcg)*(E44-Zcg)
=B46*(I46+J46)	=0	=0	=B46*(C46-Xcg)*(E46-Zcg)
=B47*(I47+J47)	=0	=0	=B47*(C47-Xcg)*(E47-Zcg)
=B48*(I48+J48)	=0	=0	=B48*(C48-Xcg)*(E48-Zcg)
=B49*(I49+J49)	=0	=0	=B49*(C49-Xcg)*(E49-Zcg)
=B50*(I50+J50)	=0	=0	=B50*(C50-Xcg)*(E50-Zcg)
=B51*(I51+J51)	=0	=0	=B51*(C51-Xcg)*(E51-Zcg)

AEW1.XLS

=B53*(I53+J53)	=0	=0	=B53*(C53-Xcg)*(E53-Zcg)
=SUM(N5:N57)	=0	=0	=SUM(Q5:Q57)
=N58/32.174	=O58/32.	=P58/32.	=Q58/32.174

GROUP		MOMENT ARM REFERENCED FROM "5" FEET IN FRONT OF THE NOSE, "5 FEET BELOW THE FUS					
AIRFRAME							
		X Arm	X MOM	Z Arm	Z MOM	Y ARM	(Xi-Xcg)^2
WING (OUT)	2250	34	76500	12	27000	23	2.519329
WING (WET)	3580	30	107400	12	42960	7.5	5.821413
HORIZONTAL TAIL	445	55.5	24697.5	15	6675	4.56	533.0206
NACELLES	969	25.5	24709.5	10	9690	9.75	47.78626
FUSELAGE	2757	29	79953	9	24813	0	11.64693
VERT TAIL	269	58	15602	13	3497	11	654.7068
FUEL							
WING	14000	30	420000	12	168000	7.5	5.821413
BLADDER (M)	513	30	15390	12	6156	7.5	5.821413
DUMPS AND DRAIN(M)	30	33	990	12	360	8	0.34485
CELL BACKING (M)	109	30	3270	12	1308	7.5	5.821413
TRANSFER PUMPS (M)	110	30	3300	12	1320	7.5	5.821413
INFLIGHT REFUELING	45	15	675	10	450	3.5	303.2042
ENGINES	4000	25.5	102000	10	40000	9.75	47.78626
ENGINE CONTROLS	116	20	2320	10	1160	4.5	154.0766
STARTING SYSTEMS	41						
HYD's							
LANDING GEAR (NOSE)	236	13	3068	2.2	519.2	0	376.8553
LANDING GEAR (MAIN)	1473	39	57447	2.2	3240.6	6	43.39172
HYD SYSTEM	1762	30	52860	8	14096	0	5.821413
FLIGHT CONTROL SYS.	2043	30	61290	8	16344	0	5.821413
FLT INST	33	10	330	10	330	0	502.3318
ENG INST	10	10	100	10	100	0	502.3318
AIR COND	1159	31	35929	12	13908	0	1.995892
OXY SYSTEM	134	15	2010	7	938	0	303.2042
ELECT SYSTEM	1165	35	40775	9	10485	0	6.693808
MISC INST	7	10	70	11	77	0	502.3318
APU	50	25	1250	8	400	0	54.94902
AVIONICS	10000	41	410000	10	100000	0	73.74068
RADOME	3000	33	99000	19	57000	0	0.34485
CHAFF/FLARE LAUNCH	300	33	9900	8	2400	0	0.34485

SEATS	787	19	14953	9.5	7476.5	0		179.9021
	51393		1665789		560703			
XCG FROM "5" FEET FORWARD OF NOSE								
	32.41276							
ZCG FROM "5 FT BELOW FUSELAGE								
	10.91011							
Ixx=	100006.3	slugs/ft^2						
Iyy=	74175.85	slugs/ft^2						
Izz=	147693.2	slugs/ft^2						
Ixy=	0	slugs/ft^2						
Ixz=	-14.9335	slugs/ft^2						
Izy=	0	slugs/ft^2						

(Yl-Ycg)^2	(Zl-Zcg)^2	Ixx	Iyy	Izz	Ixy	Iyz	Izx
529	1.18786	1192923	8341.175	1195918	0.00	0.00	3,892.31
56.25	1.18786	205627.5	25093.2	222215.7	0.00	0.00	-9,414.12
20.7936	16.7272	16696.75	244637.8	246447.3	0.00	0.00	42,018.80
95.0625	0.828301	92918.19	47107.51	138420.4	0.00	0.00	6,096.34
0	3.648521	10058.97	42169.57	32110.6	0.00	0.00	17,972.19
121	4.367839	33723.89	177291	208665.1	0.00	0.00	14,384.64
56.25	1.18786	804130	98129.82	868999.8	0.00	0.00	-36,815.00
56.25	1.18786	29465.62	3595.757	31842.63	0.00	0.00	-1,349.01
36	1.18786	1115.636	45.98129	1090.346	0.00	0.00	19.20
56.25	1.18786	6260.727	764.0107	6765.784	0.00	0.00	-286.63
56.25	1.18786	6318.165	771.02	6827.855	0.00	0.00	-289.26
12.25	0.828301	588.5235	13661.46	14195.44	0.00	0.00	713.14
95.0625	0.828301	383563.2	194458.2	571395	0.00	0.00	25,165.50
20.25	0.828301	2445.083	17968.97	20221.89	0.00	0.00	1,310.45
0	75.86602	17904.38	106842.2	88937.84	0.00	0.00	39,904.60
36	75.86602	164778.7	175666.7	116944	0.00	0.00	-84,514.23
0	8.468742	14921.92	25179.25	10257.33	0.00	0.00	12,371.71
0	8.468742	17301.64	29194.79	11893.15	0.00	0.00	14,344.72
0	0.828301	27.33393	16604.28	16576.95	0.00	0.00	673.14
0	0.828301	8.283008	5031.601	5023.318	0.00	0.00	203.98
0	1.18786	1376.729	3689.968	2313.239	0.00	0.00	-1,784.57
0	15.28896	2048.721	42678.09	40629.37	0.00	0.00	9,123.50
0	3.648521	4250.527	12048.81	7798.287	0.00	0.00	-5,757.33
0	0.00808	0.056561	3516.379	3516.323	0.00	0.00	-14.10
0	8.468742	423.4371	3170.888	2747.451	0.00	0.00	1,078.60
0	0.828301	8283.008	745689.8	737406.8	0.00	0.00	-78,153.35
0	65.44831	196338.9	197373.5	1034.551	0.00	0.00	14,252.11
0	8.468742	2540.623	2644.078	103.4551	0.00	0.00	-512.68

AEW1.XLS

0	1.988411	1564.88	143147.9	141583	0.00	0.00	14,884.90
		3217604	2386534	4751882	0.00	0.00	-480.4688632
		100006.3	74175.85	147693.2	0	0	-14.93345133

APPENDIX F

Coordinates of 12 Percent Thick Supercritical Airfoil SC(2)-0712
Designed for 0.7 Lift Coefficient
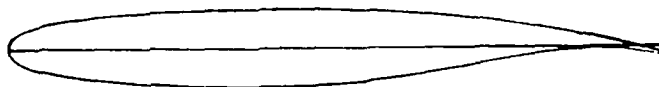
x/c	$(y/c)_u$	$(y/c)_l$	x/c	$(y/c)_u$	$(y/c)_l$
0.000	0.0000	0.0000	.500	.0584	-.0554
.002	.0092	-.0092	.510	.0581	-.0546
.005	.0141	-.0141	.520	.0577	-.0537
.010	.0190	-.0190	.530	.0573	-.0528
.020	.0252	-.0252	.540	.0569	-.0518
.030	.0294	-.0294	.550	.0564	-.0508
.040	.0327	-.0327	.560	.0559	-.0496
.050	.0354	-.0353	.570	.0554	-.0484
.060	.0377	-.0376	.580	.0549	-.0471
.070	.0397	-.0396	.590	.0543	-.0457
.080	.0415	-.0414	.600	.0537	-.0443
.090	.0431	-.0430	.610	.0530	-.0429
.100	.0446	-.0445	.620	.0523	-.0414
.110	.0459	-.0459	.630	.0516	-.0398
.120	.0471	-.0472	.640	.0508	-.0382
.130	.0483	-.0484	.650	.0500	-.0366
.140	.0494	-.0495	.660	.0491	-.0349
.150	.0504	-.0505	.670	.0482	-.0332
.160	.0513	-.0514	.680	.0472	-.0315
.170	.0522	-.0523	.690	.0462	-.0298
.180	.0530	-.0531	.700	.0451	-.0280
.190	.0537	-.0539	.710	.0440	-.0262
.200	.0544	-.0546	.720	.0428	-.0244
.210	.0551	-.0553	.730	.0416	-.0226
.220	.0557	-.0559	.740	.0403	-.0208
.230	.0562	-.0564	.750	.0390	-.0191
.240	.0567	-.0569	.760	.0376	-.0174
.250	.0572	-.0574	.770	.0362	-.0157
.260	.0576	-.0578	.780	.0347	-.0141
.270	.0580	-.0582	.790	.0332	-.0125
.280	.0584	-.0585	.800	.0316	-.0110
.290	.0587	-.0588	.810	.0300	-.0095
.300	.0590	-.0591	.820	.0283	-.0082
.310	.0592	-.0593	.830	.0266	-.0070
.320	.0594	-.0595	.840	.0248	-.0059
.330	.0596	-.0596	.850	.0230	-.0050
.340	.0598	-.0597	.860	.0211	-.0043
.350	.0599	-.0598	.870	.0192	-.0038
.360	.0600	-.0598	.880	.0172	-.0035
.370	.0601	-.0598	.890	.0152	-.0033
.380	.0601	-.0598	.900	.0131	-.0034
.390	.0601	-.0597	.910	.0110	-.0036
.400	.0601	-.0596	.920	.0088	-.0041
.410	.0601	-.0594	.930	.0065	-.0049
.420	.0600	-.0592	.940	.0042	-.0059
.430	.0599	-.0589	.950	.0018	-.0072
.440	.0598	-.0586	.960	-.0007	-.0087
.450	.0596	-.0582	.970	-.0033	-.0105
.460	.0594	-.0578	.980	-.0060	-.0126
.470	.0592	-.0573	.990	-.0088	-.0150
.480	.0590	-.0567	1.000	-.0117	-.0177
.490	.0587	-.0561			

APPENDIX G

```
%Zero lift drag coefficent of entire aircraft. This program will compute
%isolated parts of the aircraft & then sum them. This is from ORTCOM.
%------------------------------------------------------------------------
%Part 1: Isolated Wing
Cr=13.75;%Root Chord (ft)
Ct=4;%Tip Chord (ft)
toc=.12;%Thickness Ratio
Lle=21*pi/180;%Leading Edge Sweep (rads)
B=72;%Wing Span (ft)
NU=1.573*10^(-4);%Viscosity (ft^2/s)
Uinf=820;%Freestream Velocity (ft/s)
l=Ct/Cr;%Taper Ratio
B2=B/2;%Half Wing Span (ft)
TLle=tan(Lle);%Tangent of Leading Edge Sweep (rads)
Ctp=TLle*B2;
Crp=Ct+Ctp-Cr;
Sfp=2*((B2*(Cr+Crp))-(.5*B2*Ctp)-(.5*B2*Crp));%Wing Area (ft^2)
Cb=(2/3)*Cr*((1+l+l^2)/(1+l));%C bar - Mean Aerodynamic Chord
Re=Uinf*Cb/NU;%Reynolds Number
Cbf=0.455*(log10(Re))^(-2.58);%Average Turbulent Skin Friction Coefficient
Cdow=2*Cbf*(1+(2*toc)+(100*toc^4)),%Cdo of the Wing. eqn. 4.1.5.1a
%------------------------------------------------------------------------
%Part 2: Isolated Rotodome (not including Pylon)
Crr=24;%Rotodome Root Chord (ft)
Ctr=0;%Rotodome Tip Chord (ft)
tocr=.135;%Rotodome Thickness Ratio
lr=Ctr/Crr;%Rotodome Taper Ratio
Cbr=(2/3)*Crr*((1+lr+lr^2)/(1+lr));%C bar - Rotodome Mean Aerodynamic Chord
Rer=Uinf*Cbr/NU;%Reynolds Number
Cbfr=0.455*(log10(Rer))^(-2.58);%Rotodome Average Turbulent Skin Friction
%Coefficient
Cdor=2*Cbfr*(1+(2*tocr)+(100*tocr^4));%Cdo of Rotodome prior to multiplication
%of Rotodome-Wing Area Ratio. eqn. 4.1.5.1a
Sr=pi*12^2;%Rotodome Area (ft^2)
Cdorp=Cdor*Sr/Sfp,%Cdo prime of Rotodome
%------------------------------------------------------------------------
%Part 3: Rotodome Pylon (Support)
%The Pylon has been approximated as a wing with the following dimensions.
Crs=13;%Rotodome Pylon Root Chord (ft)
Cts=8;%Rotodome Pylon Tip Chord (ft)
tocs=.3;%Rotodome Pylon Thickness Ratio
ls=Cts/Crs;%Rotodome Pylon Taper Ratio
Cbs=(2/3)*Crs*((1+ls+ls^2)/(1+ls));%C bar-Rotodome Pylon Mean Aerodynamic Chord
Res=Uinf*Cbs/NU;%Reynolds Number
Cbfs=0.455*(log10(Res))^(-2.58);%Rotodome Pylon Average Turbulent Skin Friction
%Coefficient
Cdos=2*Cbfs*(1+(2*tocs)+(100*tocs^4));%Cdo of Rotodome Pylon prior to
```

```
%multiplication of Pylon-Wing Area Ratio. eqn. 4.1.5.1a
Ss=((13+6)/2)*6.4;%Rotodome Pylon Area (ft^2)
Cdosp=Cdos*Ss/Sfp,%Cdo prime of Rotodome Pylon
%----------------------------------------------------------------
%NOTE:The actual Cdo from Parts 2 & 3 was obtained from Grumman and is 0.008.
%----------------------------------------------------------------
%Part 4: Isolated Fuselage (Body)
%This program assumes a ogive shaped body.
Dmax=8;%Max Diameter of Fuselage
Lb=55;%Fuselage Length
FR=Lb/Dmax;%Fineness Ratio
Db=1.0;%Base Diameter
Reb=Uinf*Lb/NU;%Reynolds Number
Cbfb=0.455*(log10(Reb))^(-2.58);%Fuselage Average Turbulent Skin Friction
%Coefficient
SwoSb=18.85;%From USAF S&C DatCom Figure 2.3.3
Sb=pi*4^2;%Frontal Area of Fuselage
Cdof=1.02*Cbf*(1+(1.5/(Lb/Dmax)^1.5)+(7/(Lb/Dmax)^3))*SwoSb;%Cdo-Fuselage Skin
%Friction. First part of eqn. 4.2.3.1a
Cdobb=(0.029*(Db/Dmax)^3)/(sqrt(Cdof));%Base Pressure Cdo. eqn. 4.2.3.1b
Cdob=Cdof+Cdobb;%Cdo of Fuselage prior to multiplication of Fuselage-Wing Area
%Ratio. eqn. 4.2.3.1a
Cdobp=Cdob*Sb/Sfp,%Cdo prime of Fuselage
%----------------------------------------------------------------
%Part 5: Isolated Horizontal Tail
Crh=9;%Horizontal Tail Root Chord (ft)
Cth=6;%Horizontal Tail Tip Chord (ft)
Cthp=3;
toch=.12;%Horizontal Tail Thickness Ratio
Bh2=12;%Horizontal Tail Half Span
lh=Cth/Crh;%Horizontal Tail Taper Ratio
Cbh=(2/3)*Crh*((1+lh+lh^2)/(1+lh));%C bar-Horizontal Tail Mean Aerodynamic Chord
Reh=Uinf*Cbh/NU;%Reynolds Number
Cbfh=0.455*(log10(Reh))^(-2.58);%Horizontal Tail Average Turbulent Skin Friction
%Coefficient
Cdoh=2*Cbfh*(1+(2*toch)+(100*toch^4));%Cdo of Horizontal Tail prior to
%multiplication of Horizontal Tail-Wing Area Ratio. eqn. 4.3.3.1a
Saph=2*(Crh*Bh2-.5*Bh2*Cthp);%Horizontal Tail Area (ft^2)
Cdohp=Cdoh*Saph/Sfp,%Cdo prime of Horizontal Tail
%----------------------------------------------------------------
%Part 6: Isolated Vertical Tail
Crv=6;%Vertical Tail Root Chord (ft)
Ctv=3;%Vertical Tail Tip Chord (ft)
Cthp=3;
tocv=.12;%Vertical Tail Thickness Ratio
lv=Ctv/Crv;%Vertical Tail Taper Ratio
Cbv=(2/3)*Crv*((1+lv+lv^2)/(1+lv));%C bar-Vertical Tail Mean Aerodynamic Chord
```

88

```
Rev=VInf*Cbv/NU;%Reynolds Number
Cbfv=0.455*(log10(Rev))^(-2.58);%Vertical Tail Average Turbulent Skin Friction
%Coefficient
Cdov=2*Cbfv*(1+(2*tocv)+(100*tocv^4));%Cdo of Vertical Tail prior to
%multiplication of Vertical Tail-Wing Area Ratio. eqn. 4.4.3.1a
Sapv=90;%Vertical Tail Area (ft^2)
Cdovp=Cdov*Sapv/Sfp,%Cdo prime of Vertical Tail
%------------------------------------------------------------------------
%Total
Cdo=Cdow+Cdorp+Cdosp+Cdobp+Cdohp+Cdovp,%Total Aircraft Cdo. eqn.4.5.3.1b
Cdoa=Cdow+.008+Cdobp+Cdohp+Cdovp,%Total Aircraft Cdo using actual rotodome drag
Information.
%------------------------------------------------------------------------
%Cdo =0.0177
%Cdoa=0.0205
```

APPENDIX H

```
%This program Is designed to calculate the Coefficient of Drag, Lift-to-Drag
%Ratio, Thrust Required, Power Required, Power Available, Excess Power, Rate
%of Climb, Endurance and Range. The equations are found In any Intrductory
%aircraft book. This analXysis was performed using Anderson's "Introduction to
%Flight, Chapter 6.
%--------------------------------------------------------------------------
Cdo=0.0205;%Aircraft Coefficient of Drag
AR=8.11;%Aspect Ratio
e=0.8;%Efficiency
W=53000;%Aircraft Weight
Wfuel=14000;%Fuel Weight
We=53000-14000;%Empty Weight
RO=.0023769*1;%Density (sl/ft^3)
SIG=RO/.0023769;%Density Ratio
Thr=25400*(SIG);%Thrust
SFC=0.33/3600;%Specific Fuel Consumption
S=639;%Wing Area (ft^2)
K=1/(pi*AR*e);
T=1;%counter
for A=.05:.05:3,%This Is the range of Cl chosen.
 Cl(T)=A;%Coefficient of Lift Matrix
 Clsq(T)=A^2;%Cl squared
 Cd(T)=Cdo+K*A^2;%Computed Cd Matrix. eqn. 6.1c
 LoD(T)=Cl(T)/Cd(T);%Lift-to-Drag Ratio (max L/D=16)
 TR(T)=W/LoD(T);%Thrust Required for Level, Unaccelerated Flight. eqn. 6.15
 V(T)=sqrt(2*W/(RO*S*Cl(T)));%Velocity calculated from Cl. eqn. 6.16
 PTR(T)=.5*RO*V(T)^2*S*Cdo;%Parasitic Thrust Required for Level, Unaccelerated
%Flight. eqn. 6.17 (1st part)
 ITR(T)=.5*RO*V(T)^2*S*K*A^2;%Induced Thrust Required for Level, Unaccelerated
%Flight. eqn. 6.17 (2nd part)
 PR(T)=TR(T)*V(T);%Power Required for Level, Unaccelerated Flight. eqn. 6.23
 PRp(T)=sqrt(2*W^3*Cd(T)^2/(RO*S*Cl(T)^3));%Power Required for Level,
%Unaccelerated Flight (double check). eqn. 6.26
 PPR(T)=PTR(T)*V(T);%Parasitic Power Required for Level, Unaccelerated Flight
 IPR(T)=ITR(T)*V(T);%Induced Power Required for Level, Unaccelerated Flight
 PAp(T)=Thr*V(T);%Power Available (the slope of this line Is the thrust)
 EDR(T)=(1/SFC)*LoD(T)*log(W/We);%Endurance. eqn.(6.63)
 RNG(T)=2*sqrt(2/(RO*S))*(1/SFC)*(sqrt(Cl(T))/Cd(T))*(sqrt(W)-sqrt(We));%Range-
%eqn.(6.68)
 Gang(T)=atan(1/LoD(T))*(180/pi);%Glide angle (In degrees). eqn. 6.47
 %Grng(T)=H*LoD(T);%Glide Range. figure 6.30
 T=T+1;%counter
end
X=1;%counter
for VA=0:35.7:999.6, %0 to 1000 fps
 VAM(X)=VA;%Velocity Matrix
 PA(X)=Thr*VA;%Power Available Matrix (Thr Is the slope of this line)
```

90

```
  X=X+1;%counter
  end
PS=PAp-PA;%Excess Power Matrix. eqn. 6.42
RoC=PS/W;%Rate of Climb. eqn. 6.43
Thet=asin(RoC./V).*(180/pi);%climb angle. eqn. 6.41
%disp(LoD),                                              ,
%disp(PS),
%disp(RoC.*60),
%plot(Cd,Cl),
%plot(Cd,Clsq),
%plot(V,TR),
%plot(V,TR,V,PTR,'--',V,ITR,'--'),
%plot(V,PR,V,PPR,'--',V,IPR,'--',V,PAp,'x',VAM,PA,'-'),
%plot(V,EDR./3600),
%plot(V,RNG./6000),
%plot(V,RoC*60),
%----------------------------------------------------------------
%this is a result of actual thrust/power obtained from ONX/OFFX
PAsl=[8347933 11130578 13378120 13693171 14048422 13970359 13852273];%actual PA
Matrix at sea level
PA15 =1.0e+07*[0.5347 0.70064 0.8346 1.13623 1.2283];%Power Available at 15K
PA35 =1.0e+06*[2.2604 3.0139 3.6222 5.5050 6.2335];%Power Available at 35K
Msl=[.3 .4 .5 .6 .7 .8 .9];
M=V./(1116);
Mam=VAM./(1116);
M15=[.3 .4 .5 .8 .99];
M35=[.3 .4 .5 .8 .9];
%plot(M,PA,'o',M,PAp,'-',Mam,PA,'-',M,PA,'-',M35,PA35,'--'),
PSR1=1.0e+07*[0 .2195122 .6585366 .8780488 1.0341463 1.03 .9993 .9405 .8893
.8443 .8046 .7692 .7374 .7087 .6825 .6586 .6365 .6161 .5972 .5796 .5631 .5477
.5332 .5194 .5065 .4942 .4825 .4714 .4609 .4508 .4411 .4318 .4230 .4144 .4062
.3983 zeros(1,25)];
PSR2=1.0e+07*[zeros(1,36) .3907 .3834 .3763 .3694 .3628 .3563 .3501 .3441 .3382
.3325 .3269 .3215 .3163 .311 .3062 .3013 .2966 .2920 .2874 .2830 .2787 .2745
.2703 .2663 .2623];
PSR=PSR1+PSR2;%actual PS (excess power) matrix at Sea Level
MR1=[.84 .8 .7 .6 .5 .45 .4198 .3886 .3635 .3427 .3252 .3100 .2968 .2852 .2748
.2655 .2571 .2494 .2424 .2359 .2299 .2244 .2192 .2144 .2099 .2056 .2017 .1979
.1943 .1909 .1877 .1847 .1818 .1790 .1763 .1738 .1714 .1690 .1668 .1647 .1626
zeros(1,20)];
MR2=[zeros(1,41) .1606 .1587 .1568 .1550 .1533 .1516 .1500 .1484 .1469 .1454
.1440 .1426 .1412 .1399 .1386 .1374 .1362 .1350 .1339 .1327];
MR=MR1+MR2;
RoCR=(PSR./W)*60;%actual RoC Matrix
%plot(MR,RoCR),
PSR15l=1.0e+06*[0 1.852 4.259 5.556 6.204 6.296 5.926 5.6713 5.4431 5.2319
5.0362 4.8543 4.6846 4.5260 4.3771 4.2371 4.1051 3.9804 3.8621 3.7499 3.6431
```

```
3.5413 3.4441 3.3511 3.2620 3.1766 3.0944 3.0154 2.9394 2.8660 2.7951
zeros(1,26)];
PSR152=1.0e+06*[zeros(1,31) 2.7267 2.6605 2.5963 2.5342 2.4739 2.4154 2.3585
2.3032 2.2494 2.1970 2.1460 2.0962 2.0477 2.0003 1.9541 1.9089 1.8647 1.8215
1.7792 1.7378 1.6973 1.6575 1.6186 1.5804 1.5430 1.5062];
PSR15=PSR151+PSR152;%actual PS (excess power) matrix at 15K
MR151=[.957 .9 .8 .7 .6 .5 .45 0.4023 0.3852 0.3701 0.3566 0.3445 0.3336 0.3236
0.3145 0.3061 0.2984 0.2912 0.2845 0.2782 0.2724 0.2669 0.2617 0.2568 0.2522
0.2478 0.2436 0.2396 0.2359 0.2323 0.2288 0.2255 0.2224 0.2194 0.2165
zeros(1,22)];
MR152=[zeros(1,35) 0.2137 0.2110 0.2084 0.2059 0.2035 0.2012 0.1989 0.1967
0.1946 0.1926 0.1906 0.1887 0.1868 0.1850 0.1833 0.1816 0.1799 0.1783 0.1767
0.1752 0.1737 0.1723];
MR15=MR151+MR152;
RoCR15=(PSR15./W)*60;%actual RoC Matrix
%plot(MR15,RoCR15,'--'),
```

```
%this program computes the takeoff and landing distances for the NEW aircraft.
It is based on the analysis presented in chapter 10 of Nicolai.
%-------------------------------------------------------------------
Vlo=185;%velocity at lift off
T=25400;%thrust
g=32.17;%acceleration due to gravity
W=53000;%weight
Cdo=.02;%parasitic drag
S=639;%total wing area
RO=.0023769;%density (90 deg. day-->.002241)
Cl=2.04;%coefficient of lift
b=72;%wing span
h=11.4;%height of wing above ground
Ph=((16*h/b)^2)/(1+((16*h/b)^2));
AR=8.11;%aspect ratio
e=.8;%efficiency
K=1/(pi*e*AR);
L=.5*RO*Vlo^2*S*Cl;%lift
Cd=Cdo+(Ph*Cl^2*K);%coefficient of drag
D=.5*RO*Vlo^2*S*Cd;%drag
fr=.04;%friction
Slo=(Vlo^2*(W/g))/(2*(T-(D+fr*(W-L)))),%distance to takeoff
Sro=3*Vlo,%distance to rotate
Rf=Vlo^2/(g*(1.152-1));%radius of rotation
Scl=Rf*sin(.16978),
Htof=Rf*(1-cos(.16978)),
Sobs=(50-Htof)/tan(.16978),
Stot=Slo+Sro+Scl+Sobs,
Sloo=1.44*W^2/(g*RO*S*3*(T-(D+fr*(W-L)))),
%-------------------------------------------------------------------
Wl=47000;
Clm=3;
Vs=sqrt(2*Wl/(Clm*RO*S));
Vl=1.2*Vs;
Vlf=1.235*Vs;
Clf=2*Wl/(RO*Vlf^2*S);
Cd=Cdo+(Ph*Clm^2*K);%coefficient of drag
D=.5*RO*Vl^2*S*Cd;%drag
frl=.5;
Rlf=Vlf^2/(g*(1.22-1)),
Sgl=(50-(Rlf*(1-cos(2*pi/180))))/tan(2*pi/180),
Slf=Rlf*sin(2*pi/180),
Sl=1.69*W^2/(g*RO*S*Clm*(T-(D+frl*(W-L)))),%landing rollout
Slft=Sgl+Slf+Sl,
%-------------------------------------------------------------------
```

APPENDIX I

```
%This program will compute the stability derivatives for three flight
conditions. The conditions will be at M=0.2, 0.16, 0.76. Corresponding altitudes
will be h=sl, 30K, and 30K respectively. These conditions will be denoted by a
1, 2, and 3 respectively. %When parameters have defined with little more than an
educated guess, It will be denoted with a * symbol. Calculations are done IAW
Roskam Part VI.
%------------------------------------------------------------------------
W=47000;%mid range weight
S=639;%wing reference area
Lc4=17.5*pi/180;%sweep at quarter chord
K=1/(pi*.8*8.11);
Cdo=0.02;%parasitic drag coefficient
Cmowf=-.1542;%Roskam Part VI,Chap 8
dCmdCl=-.245;%(dCm/dCl)average of DatCom & Roskam results
Q=1;%counter
for M=.2:.28:.77,
 if M<0.3,
  P=2116.2;%pressure @ sea level
 else
  P=2116.2*.2975;%pressure @ 30K
 end
 MM(Q)=M;
 CL(Q)=W*2/(1.4*P*M^2*S);%coefficient of lift
 Cm(Q)=Cmowf+CL(Q)*dCmdCl;%linear moment coefficient
 CD(Q)=Cdo+K*CL(Q)^2;%drag coefficient
 CDu(Q)=(-4)*K*CL(Q)^2;%eqn(10.10)
 CLu(Q)=(M^2*cos(Lc4)^2*CL(Q))/(1-M^2*cos(Lc4)^2);%eqn(10.11)
 Q=Q+1;%counter
end
%------------------------------------------------------------------------
CLa=[4.822 5.17 6.25];%computed in the Lift Curve Slope program.
Cma=dCmdCl.*CLa;%eqn(10.19)
%------------------------------------------------------------------------
Sh=160;%horizontal tail surface area
Xbach=(25.7/9.77);%defined in chapter 10, Page 380
Xbcg=(5.1/9.77);%defined in chapter 10, Page 380
ada=.95;%*horizontal-to-freestream dynamic pressure (qh/q)
deda=0.33;%*downwash gradient at horizontal tail (page 272)
CLah=[3.00 3.35 4.43];%*lift curve slopes of the horizontal &vertical tails
Ubh=(Xbach-Xbcg)*(Sh/S);%horizontal tail volume coefficient
CLad=2*ada*deda*Ubh.*CLah;%Cl alpha dot
Cmad=(-2)*ada*deda*Ubh*(Xbach-Xbcg).*CLah;%Cm alpha dot
%------------------------------------------------------------------------
%This concludes the longitudinal calculations FOR NOW and begins Lat-Dir
%calculations.
%------------------------------------------------------------------------
%1) CuB-sideforce-due-to-sideslip (10.2.4.1.1)
```

```
Dih=2;%dihedral (in degrees)
Ki=1.75;%from figure 10.8 (2x=-3.5 & df/2=4)
Ro=3.5;%radius of fuselage where the flow ceases to be a potential (fig10.10,11)
So=pi*Ro^2;%area at that point
Bv=10;%total span of the vertical tail
Sv=45;%area of one of the vertical tails
Av=Bv^2/Sv;%vertical tail aspect ratio
Avratio=1.028;%from figure 10.19
Aveff=Av*Avratio;%effective Av
CyBveff=3;%from figure 10.18
Cyratio=0.865;% from figure 10.17
CyBw=-.00573*Dih;%CyB of the wing
CyBf=(-2)*Ki*(So/S);%CyB of the fuselage
CyBv=(-2)*Cyratio*CyBveff*(Sv/S);%CyB of the vertical tail
CyB=CyBw+CyBf+CyBv;%the grand total
%----------------------------------------------------------------------------
%2) ClB-rolling moment-due-to-sideslip (10.2.4.1.2)
ClBCl=-.001;%from figure 10.20. Iterating between taper ratio of 0 & .5
KmL=[1.01 1.125 1.3];%figure 10.21 using M=.2,.48,.76 & c/2=15 degrees
Kf=0.97;%figure 10.22
ClBClA=.0002;%figure 10.23
ClBDih=-.00022;%figure 10.24. Iterating between taper ratio of 0 & .5
B=72;%wing span
AR=8.11;%aspect ratio
Dfave=((pi*3.75^2)/.7854)^.5;
dClBDih=(-.0005)*AR*(Dfave/B)^2;
KmDih=[1.01 1.07 1.2];%figure 10.25 using M=.2,.48,.76 & c/2=15 degrees
Zw=-3.5;%see figure 10.9
dClBzw=.042*AR^.5*(Zw/B)*(Dfave/B);
etan=0.94;%*tan(17.5)times wing twist of (-3) degrees. see page 397
dClBet=-.000031;%figure 10.26
for Q=1:3,
ClBwf(Q)=57.3*(CL(Q)*(ClBCl*KmL(Q)*Kf+ClBClA)+Dih*(ClBDih*KmDih(Q)+dClBDih)+dClBz
w+etan*dClBet);%ClB of the wing-fuselage combination
end
Bh=24;%horizontal tail span
ClBhf=.65.*ClBwf;%*ClB of the tail-fuselage combination
ClBh=(Sh*Bh/(S*B)).*ClBhf;%ClB of the horizontal tail
Zv=4;%see figure 10.27
Lv=24;%see figure 10.27
alf=pi/180*[10 4 0];%estimated A.O.A from the respective Cl's
ClBv=CyB*((Zv.*cos(alf)-Lv.*sin(alf))/B);%ClB of the vertical tail
ClB=ClBwf+ClBh+ClBv;%the grand total
%----------------------------------------------------------------------------
%3) CnB-yawing moment-due-to-sideslip (10.2.4.1.3)
CnBw=0;%approximate
Kn=.00165;%figure 10.28
```

95

```
Kri=1.55;%*figure 10.29
Sfs=376;%approximate fuselage side area
Lf=55;%fuselage length
CnBf=(-57.3)*Kn*Kri*(Sfs*Lf/(S*B));%CnB of the fuselage
CnBv=(-CyBv)*((Lv.*cos(alf)+Zv.*sin(alf))/B);%CnB of the vertical tail
CnB=CnBw+CnBf+CnBv;%the grand total
%----------------------------------------------------------------
%4) CyBd-sideforce-due-to-rate of-sideslip (10.2.5.1)
Sigba=[-.023 -.025 -.028];%figure 10.30
Sigbd=[.84.87.90];%figure 10.31
Sigbet=[-.02 .022 -.024];%figure 10.32
Sigbwf=[.14 .145 .15];%figure 10.33
et=(-3);%*wing twist in degrees
Lp=26;%quarter chord of wing to quarter chord of vertical tail
Zp=10;%from bottom of fuselage to quarter chord of the vertical tail
for Q=1:3,
dSigdB(Q)=Sigba(Q)*alf(Q)*180/pi+Sigbd(Q)*(Dih/57.3)-Sigbet(Q)*et+Sigbwf(Q);%eqn.
 10.47
CyBd(Q)=2*dSigdB(Q)*(Sv/S)*((Lp*cos(alf(Q))+Zp*sin(alf(Q)))/B);%eqn. 10.16
%----------------------------------------------------------------
%5) ClBd-rolling moment-due-to-rate of-sideslip (10.2.5.2)
ClBd(Q)=CyBd(Q)*((Zp*cos(alf(Q))-Lp*sin(alf(Q)))/B);%eqn. 10.48
%----------------------------------------------------------------
%6) CnBd-yawing moment-due-to-rate of-sideslip (10.2.5.3)
CnBd(Q)=CyBd(Q)*((Lp*cos(alf(Q))+Zp*sin(alf(Q)))/B);%eqn. 10.49
%----------------------------------------------------------------
%7) Cyp- sideforce-due-to-roll rate (10.2.6.1)
Cyp(Q)=2*CyBv*((Zv*cos(alf(Q))-Lv*sin(alf(Q)))/B);%eqn. 10.50
end
%----------------------------------------------------------------
%8) Clp- rolling moment-due-to-roll rate (10.2.6.2)
for Q=1:3,
BMa(Q)=(1-MM(Q)^2)^.5;%eqn. 10.53
KMa(Q)=(CLa(Q)*BMa(Q))/(2*pi);%eqn.10.54
end
CLaratio=1;%lift coefficient ratio
BClpk=[-.49 -.48 -.43];%figure 10.35
Clpdr=1-4*Zw/(B*sin(2*pi/180))+12*(Zw/B)^2*(sin(2*pi/180))^2;%eqn. 10.55
ClpDCLr=-.0015;%figure 10.36
CDow=.0059;%from the CDo program
Clph=0;%approximate from eqn. 10.59
Clpv=CyBv*2*(Zv/B)^2;%eqn 10.60
for Q=1:3,
Clpdrag(Q)=ClpDCLr*CL(Q)^2-.125*CDow;%eqn. 10.56
Clpw(Q)=BClpk(Q)*(KMa(Q)/BMa(Q))*CLaratio*Clpdr+Clpdrag(Q);%eqn. 10.52
end
Clp=Clph+Clpv+Clpw;%the grand total (line100)
```

96

```
X  --------------------------------------------------------------
X9) Cnp- yawing moment-due-to-roll rate (10.2.6.3)
Cbar=9.77;XM.A.C.
Xbar=0;Xdistance from the c.g. to the a.c. (positve for a.c. aft of c.g.)
Cnpet=.0004;Xfigure 10.37
CO=cos(Lc4);CO2=(cos(Lc4))^2;TA=tan(Lc4);TA2=tan(Lc4)^2;
CnpClOO=(-1/6)*(AR+6*(AR+CO)*((Xbar/Cbar)*TA/AR+TA2/12))/(AR+4*CO);Xeqn. 10.65
for Q=1:3,
Bnp(Q)=(1-MM(Q)^2*CO2)^.5;Xeqn. 10.64
CnpClOM(Q)=((AR+4*CO)/(AR*Bnp(Q)+4*CO))*((AR*Bnp(Q)+.5*(AR*Bnp(Q)+CO)*TA2)/(AR+.5
*(AR+CO)*TA2))*CnpClOO;Xeqn. 10.63
Cnpw(Q)=(-CnpClOM(Q))*CL(Q)+Cnpet*et;Xeqn. 10.62
Cnpv(Q)=(-(2/(B^2)))*CyBv*(Lv*cos(alf(Q))+Zv*sin(alf(Q)))*(Zv*cos(alf(Q))-Lv*sin(
alf(Q))-Zv);Xeqn. 10.67
end
Cnp=Cnpw+Cnpv,Xthe grand total
X--------------------------------------------------------------
Xback to the longitudinal derivatives briefly
X--------------------------------------------------------------
X9) Clq- lift-due-to-pitch rate (10.2.7.2)
Xw=0;Xfigure 10.39
for Q=1:3,
ClqwHO(Q)=(.5+2*Xw/Cbar)*CLa(Q);Xeqn. 10.71
Clqw(Q)=((AR+2*CO)/(AR*Bnp(Q)+2*CO))*ClqwHO(Q);Xeqn. 10.70
Clqh(Q)=2*CLah(Q)*Vbh*ada;Xeqn. 10.72
end
Clq=Clqw+Clqh,Xthe grand total
X--------------------------------------------------------------
X10) Cmq- pitching moment-due-to-pitch rate (10.2.7.3)
for Q=1:3,
Cmq(Q)=1.1*(-2)*CLah(Q)*ada*Vbh*(Xbach-Xbcg);Xeqn. 10.78 times 1.1 to account
Xfor the wing-body component.This is from Roskam's "Airplane Flight Dynamics and
XAutomatic Flight Controls" book Part 1, page 188.
end
X--------------------------------------------------------------
Xback to the lat-der derivatives briefly
X--------------------------------------------------------------
X11) Cyr- sideforce-due-to-yaw rate (10.2.8.1)
for Q=1:3,
Cyr(Q)=(-2)*CyBv*(Lv*cos(alf(Q))+Zv*sin(alf(Q)))/B;Xeqn. 10.80
end
X--------------------------------------------------------------
X12) Clr- rolling moment-due-to-yaw rate (10.2.8.2)
ClrCLOO=.257;Xfigure 10.41
dClrdlh=.083*pi*AR*sin(Lc4)/(AR+4*CO);Xeqn. 10.84
dClret=(-.014);Xfigure 10.42
for Q=1:3,
```

```
NUI=1+((AR*(1-Bnp(Q)^2))/(2*Bnp(Q)*(AR*Bnp(Q)+2*CO)))+((AR*Bnp(Q)+2*CO)/(AR*Bnp(Q
)+4*CO))*TA2/8;%numerator of eqn. 10.83
DEI=1+((AR+2*CO)/(AR+4*CO))*TA2/8;%denominator of eqn. 10.83
ClrCLOM(Q)=(NUI/DEI)*ClrCLOO;%eqn. 10.83
Clrw(Q)=CL(Q)*ClrCLOM(Q)+ACIrdlh*Olh+ACIret*et;%eqn. 10.82
Clrv(Q)=(-(2/(B^2)))*CyBv*(Lv*cos(alf(Q))+Zv*sin(alf(Q)))*(Zv*cos(alf(Q))-Lv*sin(
alf(Q)));%eqn. 10.87
end
Clr=Clrw+Clrv;%the grand total
%----------------------------------------------------------------------
%13) Cnr- yawing moment-due-to-yaw rate (10.2.8.3)
CnrCLr=0;%figure 10.44
CnrCDo=(-.35);%figure 10.45
for Q=1:3,
Cnrw(Q)=CnrCLr*CL(Q)^2+CnrCDo*CDow;%eqn. 10.87
Cnrv(Q)=(2/(B^2))*CyBv*(Lv*cos(alf(Q))+Zv*sin(alf(Q)))^2;%eqn. 10.88
end
Cnr=Cnrw+Cnrv;%the grand total
%----------------------------------------------------------------------
%Elevator control derivatives (10.3.2)
%----------------------------------------------------------------------
Kb=.47;%figure 8.52
CldCldt=.82;%*figure 8.15. Note:the elevator-to-hor. tall chord ratio & the
%alleron-to-chord ratio are about the same. This is important for section 17).
Cldt=5.2;%figure 8.14
Kprime=1;%approximate (figure 8.13)
AdCLAdcl=1.02;%figure 8.53
Alfde=Kb*CldCldt*Cldt*AdCLAdcl*(Kprime/(2*pi*.88));%*eqn. 10.94
%----------------------------------------------------------------------
%14) CLAe- lift-due-to-elevator (10.3.2.2)
for Q=1:3,
CLlh(Q)=ada*(Sh/S)*CLah(Q);%eqn. 10.91
ClAe(Q)=Alfde*CLlh(Q);%eqn. 10.95
end
%----------------------------------------------------------------------
%15) CmAe- pitching moment-due-to-elevator (10.3.2.3)
for Q=1:3,
Cmlh(Q)=ada*Vbh*(-CLah(Q));%eqn. 10.91
CmAe(Q)=Alfde*Cmlh(Q);%eqn. 10.95
end
%----------------------------------------------------------------------
%Alleron control derivatives (10.3.5)
%----------------------------------------------------------------------
%16) CyAa- sideforce-due-to-alleron (10.3.5.1)
CyAa=0;%eqn. 10.105
%----------------------------------------------------------------------
%17) ClAa- rolling moment-due-to-alleron (10.3.5.1)
```

```
bCplak=[.4 .395 .385];%figure 10.46b
for Q=1:3,
Cpla(Q)=(KMa(Q)/BMa(Q))*bCplak(Q);%eqn. 10.107
Alfdela(Q)=(CldCldt*Cldt)/CLa(Q);%eqn. 10.109.
Cla(Q)=Alfdela(Q)*Cpla(Q);%eqn. 10.108
end
Claa=2*Cla;%eqn. 10.113
%---------------------------------------------------------------------
%18) Cnaa- yawing moment-due-to-aileron (10.3.5.1)
Ka=-.115;%figure 10.48
for Q=1:3,
Cnaa(Q)=Ka*CL(Q)*Claa(Q);%eqn. 10.114
end
%---------------------------------------------------------------------
%19) Cyar- sideforce-due-to-aileron (10.3.8.1)
Sv2=90;%total vertical tail area
Kp2=.8;%figure 8.13
CldCldt2=.82;%*figure 8.15
Cldt2=5.7;%figure 8.14
for Q=1:3,
Cyar(Q)=CLah(Q)*Kp2*Kb*CldCldt2*Cldt2*(Sv2/S);%eqn. 10.123
end
%---------------------------------------------------------------------
%20) Clar- rolling moment-due-to-aileron (10.3.8.2)
for Q=1:3,
Clar(Q)=Cyar(Q)*((Zv*cos(alf(Q))-Lv*sin(alf(Q)))/B);%eqn. 10.124
end
%---------------------------------------------------------------------
%21) Cnar- yawing moment-due-to-aileron (10.3.8.3)
for Q=1:3,
Cnar(Q)=(-Cyar(Q))*((Lv*cos(alf(Q))+Zv*sin(alf(Q)))/B);%eqn. 10.125
end
%---------------------------------------------------------------------
```

APPENDIX   J

```
%This program will calculate the dynamic characteristics of the NEW aircraft.
The programming is based on the dynamic approximations presented in Etkin's
book, First edition, @1959, Chapters 6 & 7. Stability Derivatives are acquired
from the Stability Derivative program.
%-----------------------------------------------------------------------
%longitudinal modes
%-----------------------------------------------------------------------
Mass=53000/32.2;%mass in slugs
Cbar=9.77;%mean aerodynamic chord
S=639;%wing reference area
L1=Cbar/2;%page 192 (longitudinal only)
RO1=.0023769;%density at sea level
RO2=.0023769*.3106;%density at 35000 ft.
MU1=Mass/(RO1*S*L1);%page 192
MU2=Mass/(RO2*S*L1);%page 192
CL=[1.2413    0.7244    0.2890];%reference CL. From Stab. Der. program
CD=[0.0956    0.0457    0.0241];%reference CD. From Stab. Der. program
CLa=[4.8220   5.1700    6.2500];%reference CLa. From Stab. Der. program
CDu=[-0.3024  -0.1030   -0.0164];%reference CDu. From Stab. Der. program
alf=pi/180*[10 4 0];%estimated A.O.A from the respective Cl's
%-----------------------------------------------------------------------
%phugoid modes
Wnp(1)=CL(1)/(sqrt(2)*MU1);%eqn.(6.7,4) assuming negligible Czu and Czq
Wnp(2)=CL(2)/(sqrt(2)*MU2);%eqn.(6.7,4) assuming negligible Czu and Czq
Wnp(3)=CL(3)/(sqrt(2)*MU2);%eqn.(6.7,4) assuming negligible Czu and Czq
for Q=1:3,
Cxu(Q)=(-2)*(CD(Q)+CL(Q)*tan(alf(Q)))-CDu(Q);%page 150 (11)
Zep(Q)=(-Cxu(Q))/(2*sqrt(2)*CL(Q));%eqn.(6.7,4) assuming negligible Czu and Czq
Wdp(Q)=sqrt(1-Zep(Q)^2)*Wnp(Q);%damping frequency
Tp(Q)=(2*pi)/Wdp(Q);%period
end
Char1=[1 (2*Zep(1)*Wnp(1)) Wnp(1)^2];%characteristic equation
Char2=[1 (2*Zep(2)*Wnp(2)) Wnp(2)^2];%characteristic equation
Char3=[1 (2*Zep(3)*Wnp(3)) Wnp(3)^2];%characteristic equation
R1=roots(Char1);%the roots
R2=roots(Char2);%the roots
R3=roots(Char3);%the roots
%-----------------------------------------------------------------------
%short period modes
Iyy=74176;%moment of inertia from the CG program
Ib1=Iyy/(RO1*S*L1^3);%non-dimensional moment of inertia. Page 192.
Ib2=Iyy/(RO2*S*L1^3);%non-dimensional moment of inertia. Page 192.
Cza=(-1)*(CLa+CD);%eqn.(5.2,3)
Cma=[-1.1814   -1.2666   -1.5312];%from stability derivative program
Cmq=[-7.8521   -8.7682   -11.5949];%from stability derivative program
Cmad=[-2.3556  -2.6304   -3.4785];%from stability derivative program
Wns(1)=sqrt((Cza(1)*Cma(1)-2*MU1*Cma(1))/(2*MU1*Ib1));%eqn.(6.7.7) assuming
```

100

```
negligible Czadot and Czq
for Q=2:3;
Uns(Q)=sqrt((Cza(Q)*Cmq(Q)-2*MU2*Cma(Q))/(2*MU2*Ib2));%eqn.(6.7,7) assuming
negligible Czadot and Czq
end
Zes(1)=(-1)*((2*MU1*Cmq(1)+Ib1*Cza(1)+2*MU1*Cmad(1))/(2*(2*MU1*Ib1*(Cza(1)*Cmq(1)
-2*MU1*Cma(1)))^.5));%eqn.(6.7,7) assuming negligible Czadot and Czq
for Q=2:3,
Zes(Q)=(-1)*((2*MU2*Cmq(Q)+Ib2*Cza(Q)+2*MU2*Cmad(Q))/(2*(2*MU2*Ib2*(Cza(Q)*Cmq(Q)
-2*MU2*Cma(Q)))^.5));%eqn.(6.7,7) assuming negligible Czadot bnd Czq
end
for Q=1:3,
Wds(Q)=sqrt(1-Zes(Q)^2)*Uns(Q);%damping frequency
Ts(Q)=(2*pi)/Wds(Q);%period
end
Char1s=[1 (2*Zes(1)*Uns(1)) Uns(1)^2];%characteristic equation
Char2s=[1 (2*Zes(2)*Uns(2)) Uns(2)^2];%characteristic equation
Char3s=[1 (2*Zes(3)*Uns(3)) Uns(3)^2];%characteristic equation
R1s=roots(Char1s);%the roots
R2s=roots(Char2s);%the roots
R3s=roots(Char3s);%the roots
%----------------------------------------------------------------------
%Lateral-Directional modes
%----------------------------------------------------------------------
B=72;%wing span
L2=B/2;%page 226
Ixx=100006;%moment of inertia from the CG program
Izz=147693;%moment of inertia from the CG program
Ixz=-14.9335;%moment of inertia from the CG program
Ia1=Ixx/(RO1*S*L2^3);%non-dimensional moment of inertia. Page 192.
Ia2=Ixx/(RO2*S*L2^3);%non-dimensional moment of inertia. Page 192.
Ic1=Izz/(RO1*S*L2^3);%non-dimensional moment of inertia. Page 192.
Ic2=Izz/(RO2*S*L2^3);%non-dimensional moment of inertia. Page 192.
Ie1=Ixz/(RO1*S*L2^3);%non-dimensional moment of inertia. Page 192.
Ie2=Ixz/(RO2*S*L2^3);%non-dimensional moment of inertia. Page 192.
Cyß=-0.5877;%from stability derivative program
Cyr=0.2437;%from stability derivative program
Clp=[-2.4765    -2.5993    -2.8140];%from stability derivative program
Clr=[0.4717     0.3620     0.2667];%from stability derivative program
Cnp=[0.1319     0.0764     0.0291];%from stability derivative program
Cnr=[-0.0855    -0.0848    -0.0833];%from stability derivative program
Clß=[-0.1279    -0.1307    -0.1273];%from stability derivative program
Cyp=[0.0023     -0.0235    -0.0406];%from stability derivative program
Cnß=[0.0576     0.0571     0.0560];%from stability derivative program
%----------------------------------------------------------------------
A(1)=2*MU1*(Ia1*Ic1-Ie1^2);%polynomial coefficient. eqn.(7.1,3)
A(2)=2*MU2*(Ia2*Ic2-Ie2^2);%polynomial coefficient. eqn.(7.1,3)
```

```
A(3)=A(2);
B(1)=CyB*(le1^2-la1*lc1)-2*MU1*(lc1*Clp(1)+la1*Cnr(1)+le1*(Clr(1)+Cnp(1)));%polyn
omial coefficlent. eqn.(7.1,3)
for Q=2:3,
B(Q)=CyB*(le2^2-la2*lc2)-2*MU2*(lc2*Clp(Q)+la2*Cnr(Q)+le2*(Clr(Q)+Cnp(Q)));%polyn
omial coefficlent. eqn.(7.1,3)
end
C(1)=2*MU1*(Cnr(1)*Clp(1)-Cnp(1)*Clr(1)+la1*CnB(1)+le1*ClB(1))+la1*(CyB*Cnr(1)-Cn
B(1)*Cyr)+lc1*(CyB*Clp(1)-ClB(1)*Cyp(1))+le1*(CyB*Cnp(1)-CnB(1)*Cyp(1)+Clr(1)*CyB
-Cyr*ClB(1));%polynomial coefficlent. eqn.(7.1,3)
for Q=2:3,
C(Q)=2*MU2*(Cnr(Q)*Clp(Q)-Cnp(Q)*Clr(Q)+la2*CnB(Q)+le2*ClB(Q))+la2*(CyB*Cnr(Q)-Cn
B(Q)*Cyr)+lc2*(CyB*Clp(Q)-ClB(Q)*Cyp(Q))+le2*(CyB*Cnp(Q)-CnB(Q)*Cyp(Q)+Clr(Q)*CyB
-Cyr*ClB(Q));%polynomial coefficlent. eqn.(7.1,3)
end
D(1)=CyB*(Clr(1)*Cnp(1)-Cnr(1)*Clp(1))+Cyp(1)*(ClB(1)*Cnr(1)-CnB(1)*Clr(1))+(2*MU
1-Cyr)*(ClB(1)*Cnp(1)-CnB(1)*Clp(1))-CL(1)*(lc1*ClB(1)+le1*CnB(1));%polynomial
coefficlent. eqn.(7.1,3)
for Q=2:3,
D(Q)=CyB*(Clr(Q)*Cnp(Q)-Cnr(Q)*Clp(Q))+Cyp(Q)*(ClB(Q)*Cnr(Q)-CnB(Q)*Clr(Q))+(2*MU
2-Cyr)*(ClB(Q)*Cnp(Q)-CnB(Q)*Clp(Q))-CL(Q)*(lc2*ClB(Q)+le2*CnB(Q));%polynomial
coefficlent. eqn.(7.1,3)
end
E(1)=CL(1)*(ClB(1)*Cnr(1)-CnB(1)*Clr(1));%polynomial coefficlent. eqn.(7.1,3)
for Q=2:3,
E(Q)=CL(Q)*(ClB(Q)*Cnr(Q)-CnB(Q)*Clr(Q));%polynomial coefficlent. eqn.(7.1,3)
end
%-------------------------------------------------------------------
CharLD1=[A(1) B(1) C(1) D(1) E(1)];%characterlstlc equation
CharLD2=[A(2) B(2) C(2) D(2) E(2)];%characterlstlc equation
CharLD3=[A(3) B(3) C(3) D(3) E(3)];%characterlstlc equation
RLD1=roots(CharLD1);%the roots
RLD2=roots(CharLD2);%the roots
RLD3=roots(CharLD3);%the roots
[WnL1,ZeL1] = DAMP(CharLD1);%natural frequency and damping ratio
[WnL2,ZeL2] = DAMP(CharLD2);%natural frequency and damping ratio
[WnL3,ZeL3] = DAMP(CharLD3);%natural frequency and damping ratio
WdL1=sqrt(1-ZeL1.^2).*WnL1;%damping frequency
TL1=(2*pi)/WdL1;%period
WdL2=sqrt(1-ZeL2.^2).*WnL2;%damping frequency
TL2=(2*pi)/WdL2;%period
WdL3=sqrt(1-ZeL3.^2).*WnL3;%damping frequency
TL3=(2*pi)/WdL3;%period
%-------------------------------------------------------------------
```

REFERENCES

1. Nicolai, Leland M., *Fundamentals of Aircraft Design*. San Jose. CA, 1984

2. Raymer, Daniel P., *Aircraft Design: A Conceptual Approach*. American Institute of Aeronautics and Astronautics. Washington, D.C., 1989.

3. School of Aerospace Engineering, Georgia Institute of Technology, *The Impact of Total Quality Management (TQM) and Concurrent Engineering On the Aircraft Design Process*. by D.P Schrage, p.1.

4. Taguchi, G., "The Evaluation of Quality", *Special Information Package on Taguchi Methods*, American Supplier Institute, Inc.

5. Hauser, John R., Clausing, D., "The House of Quality", *Harvard Business Review*, pp. 63-73, May-June 1988.

6. Akao, Yoji, *QFD: Integrating Customer Requirements Into Production Design*, Productivity Press, Cambridge, Mass.,1990

7. Mattingly, Jack D., Heiser, William H. and Dailey, Daniel H., *Aircraft Engine Design*, American Institute of Aeonautics and Astronautics, New York, 1987.

8. Roskam, Jan, *Airplane Design*, Parts I-VIII, Roskam Aviation and Engineering Corporation, Ottawa, Kansas, 1985.

9. U.S. and Gas Turbine Engine Specifications, *Aviation Week and Space Technology*, pp. 90 & 109, March 16, 1992.

10. Hoerner, S.F., *Fluid-Dynamic Drag*, published by the author, Midland Park, New Jersey, 1965.

11. Interview between P.J. Reister, LCDR, USN, and the author. October 1992.

12. Bertin, John J., & Smith, Michael L., *Aerodynamics For Engineers*. Second Edition, Prentice Hall, Englewood Cliffs, N.J. 1989.

13. Shevell, R.S., *Fundamentals Of Flight*, Second Edition, Prentice Hall, Englewood Cliffs, N.J. 1989.

14. NASA Technical Paper 2969, *NASA Supercritical Airfoils*, by C.D. Harris, March 1990.

15. Abbott, Ira H. and von Doenhoff, Albert E., *Theory of Wing Sections, Including a Summary of Airfoil Data*, Dover Publications, Inc., New York 1949.

16. Telephone conversation between Harris, C.D., NASA Langley, and the author, Oct 1992.

17. NASA Technical Memorandum 86370, *Pressure Distribution From High Reynolds Number Tests of a NASA SC(3)-0712(B) Airfoil in the Langley 0.3- meter Transonic Cryogenic Tunnel*, by W.G. Johnson, Jr., A.S. Hill and O. Eichmann

18. McDonnell Douglas Flight Control Division, *USAF Stability and Control DATCOM*, St. Louis, 1976.

19. Anderson, John D., Jr., *Introduction to Flight*, 3rd ed., McGraw-Hill Book Co., 1978.

20. Etkin, Bernard, *Dynamics of Flight, Stability and Control*, Second Edition, John Wiley and Sons, Inc., New York, 1959.

21. Henderson, Breck W., "Boeing Pursues Innovative Concept For Future Navy EX", *Aviation Week and Space Technology*, pp. 62-63. March 16, 1992.

INITIAL DISTRIBUTION LIST

1. Defense Technical Information Center   2
   Cameron Station
   Alexandria, VA 22304-6145

2. Library, Code 52   2
   Naval Postgraduate School
   Monterey, CA 93940-5002

3. Professor Conrad F. Newberry   1
   Code AA/NE
   Naval Postgraduate School
   Monterey, CA 93940-5002

4. Professor Richard M. Howard   1
   Code AA/HO
   Naval Postgraduate School
   Monterey, CA 93940-5002

5. Mr. Russ Perkins   1
   Naval Air Systems Command
   AIR-05C
   Washington, D.C. 20361-5000

6. Mr. Thomas Momiyama   1
   Naval Air Systems Command
   AIR-530T
   Washington D.C. 20361-5300

7. Mr. Frank O'Brimski   1
   Advanced Design Branch
   Naval Air Systems Command
   AIR-5223
   Washington D.C. 20361-5220

8. LCDR Michael J. Wagner   1
   c/o 835 E Ave. #G
   Coronado, CA 92118